



Norwegian University  
of Life Sciences

**Master's Thesis 2021 30 ECTS**  
Faculty of Science and Technology

# **Simulation and Analysis of the Energy Demands for Roof-Mounted Photovoltaic Snow Mitigation Systems**

Louise Viketun Skjøndal  
Structural Engineering and Architecture



## **Preface**

This master thesis marks the end of a master's degree in Structural Engineering and Architecture at the Faculty of Science and Technology at the Norwegian University of Life Sciences. The work with this thesis has been challenging, educational, and exciting.

I want to thank my supervisor, Thomas K. Thiis, and co-supervisor, Iver Frimannslund, for guidance and detailed insight on this field of research. You have shown support, been motivational during the process, and provided me with thorough feedback. It has been refreshing to work with such passionate people.

Finally, I would like to thank my closest friends and family for the support and motivation to complete my master's thesis.

Louise Viketun Skjøndal

December 2021

## Abstract

The use of solar panels, or photovoltaic (PV) systems, has been available for some decades, and solar technology is improving by the day. In addition, to facilitate solar energy production, the technology has evolved, and some PV systems provide a heating mode that can mitigate snow loads on roofs. The requirements for building structures were less strict in the past decades and some areas are predicted to experience more intense and heavy snow weather due to global warming. A consequence of these two factors is that existing building stock is not necessarily designed to tolerate the load from heavier snowfall and extra dead load from the solar panels.

This thesis used The Energy Balance Snow Cover Integrated Model (ESCIMO) to simulate the snow water equivalent (SWE) with an added heat source. A validation case was conducted using observed snow load data from a melting scenario with PV mitigation systems on a building in Porsgrunn, Norway, to compare the melt rate using the ESCIMO model for simulation. Different strategies for snow load reduction were investigated on target levels for initiating melting. The melting energy, temperature restrictions, and a snow load buffer were tested over 39 years with modelled weather data on six sites with various climate conditions. A simulation program for heat transfer through building components, WUFI, was used to investigate the energy efficiency of a PV panel.

The results showed that using  $300 \text{ W/m}^2$  of melting energy was the most effective to reduce the snow load. The model provided results comparable with registered snow load reduction from an actual melting case which is used as validation data for the research in this thesis. With temperature restriction and  $300 \text{ W/m}^2$  of melting energy, the average energy demand for 39-years was between  $3\text{-}11 \text{ kWh/m}^2$  depending on the site's climate characteristic and the number of years that required melting. The energy efficiency was highly affected by the snow depth and local climatic conditions. As snow could accumulate faster than the heating system could melt it with temperature restriction in some cases, a snow load buffer based on the target level and amount of overload showed the most reduction.

Photovoltaic snow mitigation systems show results of reduced snow load on roofs in the simulation and analysis. Further studies should investigate observed weather data in the model and field research of PV systems with varied climate conditions and snow depth to investigate the optimal melting strategy and the melting capacity of the system on the local site.

## Sammendrag

Bruken av solcellepanel, eller solcelleanlegg, har eksistert i flere tiår, og solenergiteknologien blir både bedre for hver dag og mer tilgjengelig for publikum. I tillegg til å utnytte solenergi, har teknologien utviklet seg og noen solcelleanlegg har en smeltemodus for å redusere snølast på tak. Kravene til bygningskonstruksjoner har vært lavere de siste tiårene og i noen områder forventes det større og mer intenst snøvær. Eksisterende bygningsmasse er ikke nødvendigvis designet for å tåle belastningen fra høy snølast og den ekstra vekten av solcellepanelene.

I denne oppgaven er *The Energy Balance Snow Cover Integrated Model* (ESCIMO) brukt for å simulere snøvannekvivalenten (SVE) med en tilføyd varmekilde. En validering ble utført ved å bruke observerte snølastdata fra et smeltescenario med solcelleanlegg fra en bygning i Porsgrunn, Norge, til å sammenligne smeltehastigheten ved et smeltescenario i ESCIMO-modellen. Ulike strategier for snølastreduksjonen ble undersøkt. Mengde energi som kreves, temperaturbegrensning og en snølastbuffer ble testet i 39 år med modellerte værdata på seks steder med ulike klimaforhold. Et simuleringsprogram for varmeoverføring gjennom bygningskomponenter, WUFI, ble brukt for å undersøke energieffektiviteten til et solcellepanel.

Resultatene viste at bruk av  $300 \text{ W/m}^2$  med smelteenergi var mest tilstrekkelig i å redusere snølasten. Modellen ga resultater sammenlignbare med registrert snølastreduksjon fra smeltetilfellet i Porsgrunn og danner derfor valideringsgrunnlaget for forskningen i denne oppgaven.

Smeltestrategiene med temperaturbegrensning og bruk av  $300 \text{ W/m}^2$  smelteenergi, lå gjennomsnittlig energibehov i 39 år mellom  $3\text{-}11 \text{ kWh/m}^2$ , avhengig av stedets klimakarakteristikk og antall år med behov for smelting. Energieffektiviteten ble funnet å være sterkt påvirket av snødybden og lokale klimatiske forhold. Etersom snø kan akkumulere raskere enn smeltesystemer kan smelte, spesielt ved temperaturbegrensninger, er bruk av en snølastbuffer basert på smeltegrenser og mengde overbelastning den strategien med mest reduksjon av snølast.

Avslutningsvis viser resultatene at solcelleanlegget reduserer snølast, videre studier bør utføres ved å bruke observerte værdata i modellen og feltundersøkelser av solcelleanlegg med varierte klimaforhold og snødybde for å avgjøre optimal smeltestrategi og smeltekapasiteten til solcelleanlegget.

# Content

Preface .....	2
Abstract .....	3
Sammendrag .....	4
1 Introduction.....	8
1.1 Background.....	8
1.2 Problem.....	9
1.3 Limitations.....	9
1.4 Structure of the thesis .....	10
2 Theory .....	11
2.1 Photovoltaic systems .....	11
2.1.1 Principle, function, and configuration.....	11
2.1.2 PV systems and snow .....	13
2.1.3 PV systems with heating .....	13
2.1.4 Research of using the PV heating systems.....	14
2.2 Snow theory .....	15
2.2.1 Snow as a material.....	15
2.2.2 Phase changes.....	15
2.2.3 Enthalpy .....	16
2.2.4 Properties of snow .....	18
2.3 EN 1991-1-3:2003 The snow load standard .....	22
2.3.1 Determination of the snow load .....	22
2.3.2 Climatic regions .....	25
2.4 Climate and the determination of extreme values .....	26
2.4.1 The Köppen climate classification .....	26
2.4.2 Snow weather changes and predictions in the future .....	28
2.4.3 Measuring snow .....	29
2.4.4 Observed weather data from weather stations.....	29
2.4.5 Modelled weather data - ERA5 .....	29
2.4.6 Calculation and estimation of extreme values.....	30
2.5 Reliability of existing buildings .....	31
2.5.1 Vulnerability of existing structures .....	31
2.5.2 Development of the snow load.....	31
2.6 Snow load control.....	33

2.6.1	Manually by shovelling .....	33
2.6.2	Chemicals .....	33
2.6.3	Thermal de-icing system .....	33
2.6.4	Snow load control in the snow load standard.....	34
2.7	Snow load control at “Down Town” .....	35
2.8	Simulation of surface heat transfer through building components.....	37
2.8.1	Terms in building physics .....	37
2.8.2	WUFI.....	38
2.8.3	WUFI: Transportation mechanisms .....	38
2.8.4	WUFI: Material input.....	40
2.9	Simulation of the snowpack .....	41
2.9.1	The Energy Balance Snow Cover Integrated Model (ESCIMO).....	41
3	Method.....	45
3.1	Validation of the simulation model .....	45
3.1.1	Approach of the validation .....	45
3.1.2	Site characteristic and collection of weather data .....	45
3.1.3	Adjusted temperature data.....	47
3.2	Simulation of the energy efficiency.....	49
3.2.1	Simulation of heat transfer .....	49
3.2.2	Structure and procedure .....	50
3.2.3	Input materials and settings.....	51
3.2.4	Material definitions .....	54
3.3	Simulation of the energy demand.....	56
3.3.1	Site characteristics.....	56
3.3.2	Procedure using the snow cover integrated model.....	59
3.3.3	Extreme values .....	59
3.3.4	Melting strategies .....	59
4	Results.....	62
4.1	Validation .....	62
4.2	Efficiency.....	64
4.3	Extreme value analysis of snow load .....	66
4.4	Snow load simulation – long term.....	68
4.4.1	Results .....	68
4.4.2	Summary of average values .....	88
4.4.3	Extreme values analysis of the snow load.....	90

4.5	Snow load simulation - yearly .....	94
5	Discussion .....	100
5.1	Validation .....	100
	Limitations .....	102
5.2	Energy efficiency .....	103
	Limitations .....	105
5.3	Melting strategies and energy demands .....	106
	Limitations .....	109
5.4	Further studies .....	110
6	Conclusion .....	111
	References .....	112
	Appendix .....	115



# 1 Introduction

## 1.1 Background

A part of the solution for reducing the predicted outcomes of global warming and climate changes is to implement a renewable and sustainable energy supply system. Solar energy is highly relevant as it is an available and versatile energy source.

The demand for renewable and green energy is already present, and this demand is expected to increase significantly in the years to come. The use of solar panels, or photovoltaic systems, has been available for some decades, and the technology is improving by the day. Many producers in the solar energy market have already started the green change, but there is still a long way to go. As there are a large number of existing building stocks with unutilized roofs, the industry has identified a big potential for installing photovoltaic systems to facilitate solar energy production.

Roofs are especially suitable for having photovoltaic systems in urban environments due to their large flat surfaces with high solar irradiation, favourable wind conditions, and accessibility for maintenance. Roof surfaces are often free and unutilized, even in densely populated areas.

Due to climate change the weather conditions are changing. Some geographical areas expect less snowfalls than before. Some regions are already experiencing this development. While other regions, are expected to have, or are already experiencing, more and heavier snowfalls than in the past. Some producers have found that this latter development can be solved utilizing the increasing demand for solar panels. The idea is to use the photovoltaic systems to heat or melt the snow and thus reducing the load on the building. Removing, or at least reducing, the snow load from the system, will also raise the energy production from solar energy. The existing building stock in areas where it is predicted more and heavier snowfalls in the future, are not necessarily designed to tolerate the increased load combined with the extra weight of the solar panels. Buildings built 50-70 years ago may not have the required capacity for today's snow loads, and the snow loads to come. The requirements for building structures were lower in the past decades, and the characteristic snow load was low. A collapse of roof structures due to extreme snow loads can have catastrophic consequences. Reinforcement of under-designed building structures may be the solution to avoid danger for

people and the building structures. Installing photovoltaic heating systems on roofs to reduce the snow load by melting, might another promising alternative. In fact, it may be a more cost-effective way of solving the challenges for existing building stock caused by climate change. Use of PV heating systems for reducing snow load on building structures, especially for flat roofs, has been applied for a number of years. Still, few or none of the data gathering and systematic analyses provide reliable answers on which melting strategy would be optimal for the respective local climate in question, the expectation of energy demand for the client, or what energy efficiency to expect.

## **1.2 Problem**

This thesis aims to answer the main problem:

Energy demand for photovoltaic snow mitigation systems to reduce roof snow load on building structures.

Supported by three sub-problems:

1. Validation of simulation method using measured data from an observed melting scenario using photovoltaic heating systems.
2. Estimation of the energy efficiency of photovoltaic heating systems by simulation.
3. Simulation of the energy demands of photovoltaic snow mitigation systems in varying climatic conditions, and the optimal melting strategy to minimize energy loss.

## **1.3 Limitations**

This thesis is limited to the snow load reduction in civil engineering. Modelling, calculations, and simulations are based on data from Norway and selected countries in Europe. The facts and analyses in this thesis will not necessarily apply to the conditions of other countries. The modelled data will not necessarily provide complete results compared to real-life collected data.

## **1.4 Structure of the thesis**

The thesis consists of six chapters and an additional annex at the end:

### Chapter 1 – Introduction

The introduction chapter introduces the problem of the thesis and the context of this research.

### Chapter 2 – Theory

The theory chapter explain the fundamental concepts and background theory used in this thesis.

### Chapter 3 – Method

The method chapter explains and elaborates the research methodology and procedure of the simulations performed in the thesis.

### Chapter 4 – Results

The results chapter presents the results from the simulations and validation.

### Chapter 5 – Discussion

The discussion chapter aims to discuss the results and answer the problem stated in the thesis.

### Chapter 6 – Conclusion

The conclusion chapter summarizes the findings of the research in this thesis.

### Annex A

This chapter is a supplementary chapter for the results presented earlier in the thesis with more descriptive results and details.

## 2 Theory

This chapter covers the theoretical background and principles of snow loads, the physical properties and the energy balance of snow, alternatives for reducing the snow loads on roofs, and simulation of the snowpack with heating systems used further in the thesis.

### 2.1 Photovoltaic systems

#### 2.1.1 Principle, function, and configuration

Photovoltaic (PV) systems utilize sunlight as a source of energy. A solar cell, or a photovoltaic cell, turns the energy radiated from the sun into electricity. When sunlight, in the form of photons, reaches a photovoltaic cell, the photons excite electrons. Then, the electrical charge is separated with one negative charge in the front layer of the cell and one positive charge in the layer behind the cell. The separation occurs in the layer of a semiconductor material (a material with electrical conductivity between a conductor and an isolator), such as doped silicon. A junction between the layers keeps the electrical charges separated. An electric potential is created between the front and back of the module, due to the separation of electrical charges. The separation results in an induced current in the metal strips placed in the front of the cell. A PV module consists of several PV cells arranged in a series or parallel, or both, electrical configuration with additional components, as listed in table 1 and illustrated in figure 1.

*Table 1. The composition of a PV module (Smets , et al., 2016)*

---

The composition of a PV module
Front glass layer
Encapsulant in front and back layer
Solar cells
Protective layer at the back
Aluminium frame
Junction box

---

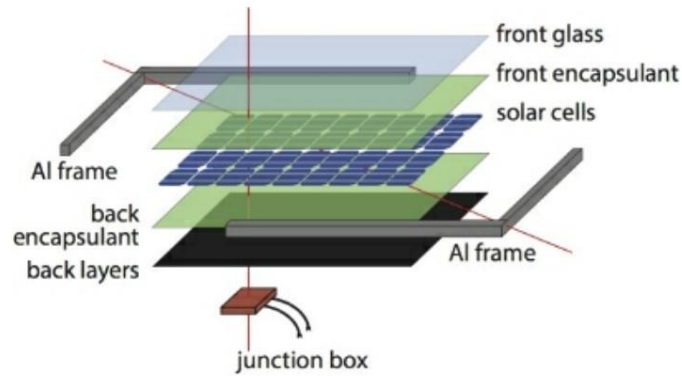


Figure 1. The composition of a PV module (Smets , et al., 2016).

The size of a PV module may vary from the different manufacturers, but a typical size is 1.6 m x 1.0 m. Several modules electrically connected on one supporting structure make up a solar panel. A PV array consists of several connected solar panels (Smets , et al., 2016).

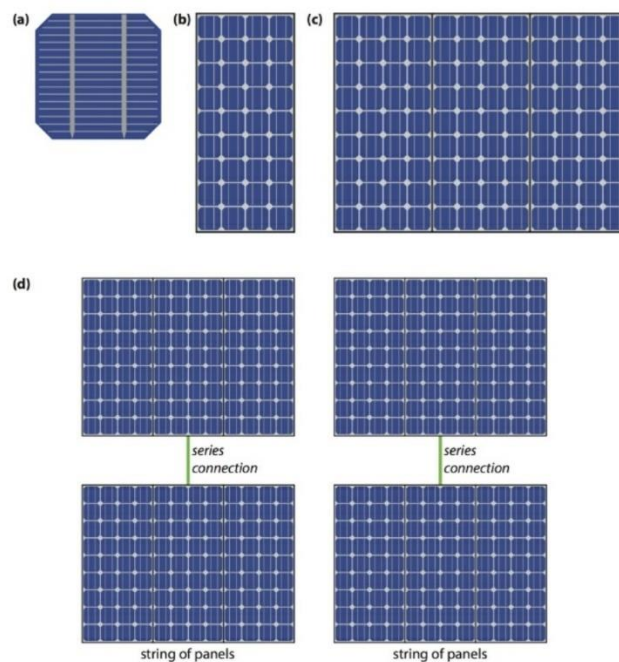


Figure 2. The composition of a PV system. (a) is a solar cell, (b) is a PV module, (c) is a solar panel and (d) is a PV array (Smets , et al., 2016).

A typical set-up is a string of series-connected cells connected in parallels. The number of cells varies, but a standard configuration may consist of 10-30 cells per string, with 2-6 strings of panels. The module's connections may differ by the individual manufacturer and client needs.

The lowest current in a series configuration sets the limit for all the currents in that serie. If a single cell is producing low current, then it will limit the generated power for the whole string. The low current of a cell may be caused by shading, dirt or snow coverage, or it could be dysfunctional. If the cell is non-functioning, it determines the power output and might induce reverse current internally in the string. A reversed current dissipate energy instead of producing energy. This event is called "reverse bias" and causes "hot spots" on the modules. Hot spots are areas with an abnormally high temperature causing material cracks, increased degradation, and junction breakdowns (Smets , et al., 2016).

To prevent the reversed current, bypass diodes are used. The typical connection of the bypass diodes is a connection on each string of cells in a module. In addition to preventing the reverse currents, the diode stops the power production for the whole string. For a module with series-configurated cells, then one cell with low or no electric potential, will prevent the power production for all the cells connected in that string.

### **2.1.2 PV systems and snow**

In colder climates where snowfalls occur, potential damage to PV systems and loss in energy production is at risk. Snow loads on PV systems may damage the PV module's glass and frame and increase the PV systems' mean degradation rate (Köntges, 2018). The snow cover on a PV module may prevent it from generating power caused by the snow's ability to absorb and reflect the solar radiation, depending on the depth of the snow. A full snow cover may give an electrical response similar to an inverter breakdown (Schill, et al., 2015). A partial snow cover may lead to a partial shading that could result in electrical losses similar to serious PV module failures (Tsanakas, et al., 2016). Snow covering on PV systems disadvantages the techniques of PV systems, the energy production, and possibly the snow load capacity of the structure, a solution is to remove the snow.

### **2.1.3 PV systems with heating**

Removing the snow from the PV systems benefits both energy production and minimizing damage to the panels. Because the PV modules generate electricity, which produces heat, a solution to the problem is using the PV panels to melt the snow load. Sending the current back into the PV modules will produce heat at the module's surface, melting and removing snow loads.

PV modules produce DC current and have inverters that convert DC to AC current allowing the current to be re-applied onto the grid. PV heating systems are installed the same way as standard PV systems, besides supplying a rectifying product to change the current from AC to DC (Frimannslund, 2017). In today's market, there are products to optimize energy storage that combine inverters and rectifiers in one unit.

Companies have different solutions to the cause - the Innos "Weight Watcher" markets this system for under-designed flat roofs unable to handle the snow load (Innos, 2021). The Weight Watcher system intends to compensate for the weight of the modules by reducing the snow load when required, enabling under-designed roofs to install PV systems. The Weight Watcher system's design is to reduce the load by melting and sublimation, and not necessarily to clear the module surface from snow. The Weight Watcher system has load sensors installed at several of the module frames to measure the load on module. When the snow load reaches a specific limit, then the system is activated, melting the snow until the load is within satisfying levels. This is the PV system that provided the snow load data for the validation analysis in this thesis.

#### **2.1.4 Research of using the PV heating systems**

A previous study concluded that using PV systems to reduce the snow load on roofs is possible, but it is highly dependent on the climatic conditions during system operations (Frimannslund & Thiis, 2019). The results showed that refreezing of meltwater is a problem when melting is performed with air temperature below 0°C. Freezing meltwater prevents sufficient load reduction, and possibly results in unfavourable load distribution.

There is little to no documentation of the efficiency of a PV heating system. Manufacturers advertise an expected time for a specific amount of snow to be melted, but the documentation in this matter is scarcely available. Regarding the energy demand, it is essential to know the efficiency. The efficiency measures from 0 to 1, or 0 % to 100 %, and knowing the percentage in a melting scenario may have a significant difference in calculating and estimating the energy demand. This study aims to find the expected efficiency for a PV panel in a standardized environment to calculate the energy demand.

## **2.2 Snow theory**

Snow is a natural form of precipitation. In Norway, one-third of all precipitation is snow (NVE, 2020). As part of the global climate system, snow is a complex material, natural hazard in some cases, and an economic resource. When researching a snow melting system, it is essential to understand how snow as a material behaves, how heat affects the energy balance, and the transition between solid, liquid, and vapor phases.

### **2.2.1 Snow as a material**

Snow is a solid form of water, and it occurs in clouds when cooled water droplets solidify to ice crystals and water vapor deposits and freeze in the crystal. Snowflakes are snow crystals alone or in groups. Snow crystals are all unique and can have infinitely many shapes, but all are hexagonal, following the molecular structure of water.

Crystals accumulate on the ground during snowfall, forming a complex material. In the beginning, this is usually soft and loose, but within a time, the ice crystals merge at their points of contact in a process known as “sintering”. It results in a coherent porous structure. As the structure changes, the material properties of the snow also change, such as its density. Snow in natural form is a complex mass and can contain various layers with different properties and is not necessarily a homogenous pack (SLF, 2021).

### **2.2.2 Phase changes**

Materials can be solid, liquid, or gas, depending on the temperature and pressure. The phase diagram provides an overview of where the material's phase will change due to temperature and pressure and not change if it is in an equilibrium state (Tipler & Mosca, 2008). As shown in the phase diagram for water in figure 3, the curves separate the areas of where there is a phase change. Curve O-B is the melting curve, and curve A-O is the sublimation curve.



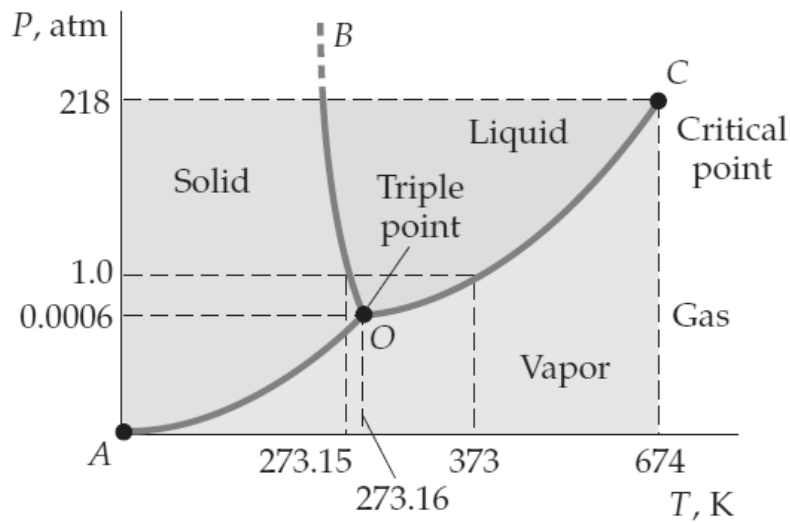


Figure 3. Phase diagram for water from Tipler & Mosca, 2008.

The most relevant phase changes for melting of snow in this thesis occurs when the pressure is of 1 atmosphere (1 atm). Melting occurs at normal atmospheric pressure and temperatures.

### 2.2.3 Enthalpy

Enthalpy describes the amount of heat in a system. Enthalpy is a thermodynamic state function with the symbol  $H$  and is defined as

$$H = U + PV \quad (1)$$

where

$U$  is the system's internal energy

$PV$  is the pressure and volume of the system

When calculating processes with constant pressures, such as the enthalpy function, during a phase transition (melting, freezing, evaporation, condensation) or a chemical reaction, is often used to find the heat in the system. The change in enthalpy,  $\Delta H$ , in a phase transition, is equal to the heat of fusion or possibly the heat of evaporation (Store Norske Leksikon, 2019).

Heat capacity is a constant that measures the proportion of heat (energy) that must be applied to a specific material to raise the temperature in the material in a closed system. It's expressed as

$$C = \frac{q}{\Delta T} \quad (2)$$

where

$C$  is the heat capacity [J/K]

$q$  is the added heat [J]

$\Delta T$  is the increase of temperature [K]

Specific heat capacity,  $c$ , is the heat capacity per unit mass of a specific material. Specific heat capacity often varies with temperature and is different for each state of matter (Store Norske Leksikon, 2019). If the constant is low, even a significant temperature increase will result in low induced heat - and vice versa. The unit is joule per kelvin and per kilogram, J/(K· kg) in the SI-system. Table 4, in subchapter 2.2.4, show the specific heat capacity for snow.

Using the constant of specific heat capacity calculation of the energy required for a material to change in temperature can be expressed as

$$Q_{sensible\ heat} = mc\Delta T \quad (3)$$

where  $Q$  is the energy used [kJ]

$m$  is the mass of the material [kg]

$\Delta T$  is change in temperature [K]

Latent heat is the heat required per unit mass for inducing a phase change in the material. A material may have different latent heat constants based on the in-state phase, atmospheric pressure, and the phase it becomes over time with the applied heat.

Multiplying the latent heat constant with the mass material from the formula below gives the energy required for a phase change.

$$Q_{Latent\ heat} = mL_{phase} \quad (4)$$

$Q_{latent\ heat}$  is the energy required to induce the phase change [kJ]

$m$  is the mass of the material [kg]

$L_{phase}$  is the latent heat constant for the material at the phase change [kJ/kg]

Table 2 shows the latent heat of water. Both vaporization and sublimation of 2257 kJ/kg and 2830 kJ/kg are significantly higher than the melting limit of 333,5 kJ/kg and require more than six times more energy ( (Tipler & Mosca, 2008) and (Oke, 1987) cited by (Frimannslund & Thiis, 2019) p. 84).

*Table 2. Latent heat constants for water.*

Phase change	Latent Heat constant [kJ/kg]
Fusion (273.15 K)	333,5
Vaporization (373.15 K)	2257
Sublimation (273.15 K)	2830

Sublimation is the instant transition from solid to vapor. It naturally occurs when there is a higher partial pressure of water vapor in the snowpack than in the air in the snow. A gradient in specific humidity is created due to the difference, resulting in a mass transportation from the snowpack to the atmosphere (Frimannslund & Thiis, 2019).

#### **2.2.4 Properties of snow**

As snow is a changing material, the properties depend on the snow's microstructure. If the water content in the snow increases, then the hardness of the snow will decrease. When dry snow absorbs water, the total bond area and the number of ice grains are reduced, decreasing the snow hardness (Nuijiten & Høyland, 2016). The main properties of snow used in this thesis are density, specific heat capacity, thermal conductivity, porosity, and vapor diffusion.

*Density ( $\rho$ ) – mass per unit volume [kN/m<sup>3</sup>]*

The density of snow varies greatly. Dry snow tends to have low density and, wet snow has high density. Generally, when melting snow, the density will increase rapidly and finally reach the density of water (999.8 kg/m<sup>3</sup>). Table 3 shows the mean bulk weight density on different types of snow used in EN 1991-1-3:2003 - The snow load standard (Standard Norge, 2008).

*Table 3. Bulk weight density of diverse types of snow. Re-produced from Standard Norge, 2008.*

Type of snow	Bulk weight density [kN/m <sup>3</sup> ]
Fresh	1.0
Settled (several hours or days after its fall)	2.0
Old (several weeks or months after its fall)	2.5-3.5
Wet	4.0

A previous study on a melting snow layer shows that the average density of snow changes over time. The density affected what time the snow layer would start to melt. Figure 5 shows the research results of change in density from both uncompressed, (a), and compressed snow, (b) (Nuijten & Høyland, 2017). As this thesis revolves around snow melting, the determination of the snow density is based on the results depicted in figure 5.

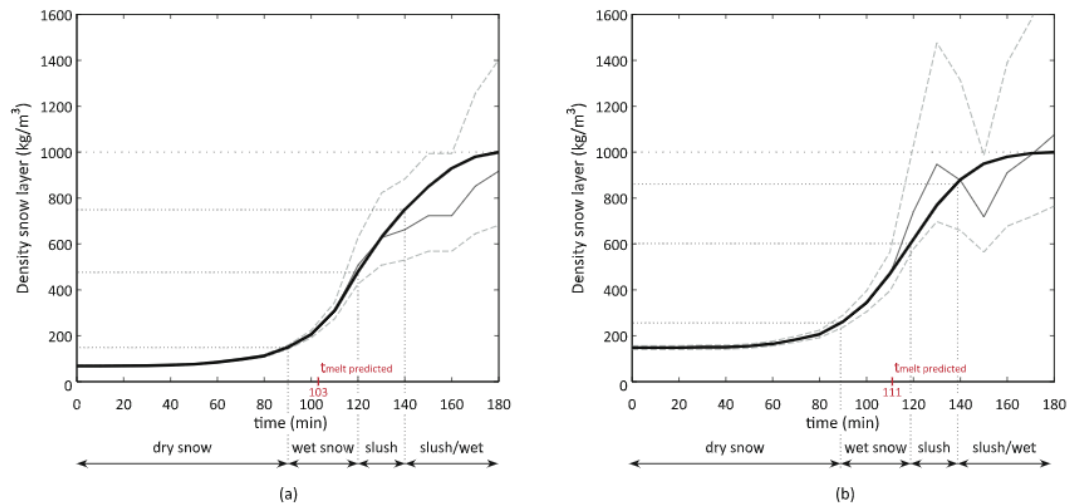


Figure 4. Average change in density of the snow layer during the research (Nuijten & Høyland, 2017). Average  $\pm$  measuring error (dotted line) and an adjusted curve that ends at the density of water (continuous thick line) for uncompressed (a) and compressed snow (b).

*Specific heat capacity (c)- heat capacity per unit mass [kJ/kg K]*

The specific heat capacity for water and snow is listed in table 4. Elaboration on specific heat capacity is found in chapter 2.2.4.

Table 4. Specific heat capacity for water and snow.

Material	Specific heat capacity [kJ/kgK]
Water	4,18
Snow	2,09

*Thermal conductivity (k) – watt per meter kelvin [W/mK]*

Thermal conductivity is a material's ability to conduct heat. Freshly fallen snow has a relatively low thermal conductivity and acts as a good insulator. But the thermal properties can vary significantly during the melting process. The thermal conductivity varies mainly with the density and depends on the snow microstructure. The thermal conductivity of a composite material such as snow is a function of the conductivity of the varied materials, their relative fractions, and the microstructure (Nuijten & Høyland, 2017). Reported values of the

effective thermal conductivity range from 0.025 W/mK to 0.56 W/mK for densities from 10 to 550 kg/m<sup>3</sup> (Cote et al, 2012) cited by (Nuijten & Høyland, 2017).

*Porosity – measure of void spaces [%]*

Porosity or void fraction is a measure of the void spaces in the material, measured in percent or between 0 to 1. The porosity for wet snow is a complex porous medium. The three phases of water are present, and liquid interacts with the solid structure. The porosity is measured usually as 50% (Coléou & Lesaffre , 1998). Figure 6 show results from the study of a melting snow layer comparing volume fraction of compressed and uncompressed snow.

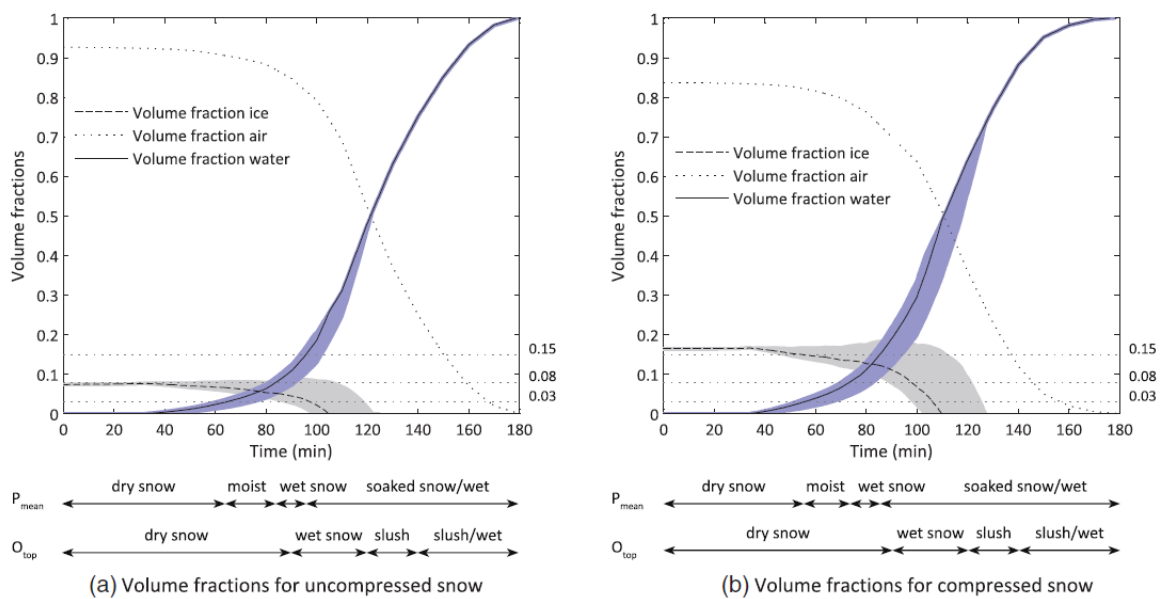


Figure 5. Results on volume fraction for (a) uncompressed and (b) compressed snow (Nuijten & Høyland, 2017).

*Water vapor diffusion resistance – [-]*

Vapor diffusion is a materials relative reluctance to let water vapor pass through and is measured into the properties of air. It is calculated from air’s vapor permeability divided with the vapor permeability of the material (SINTEF Byggforsk, 2014). For this thesis, the water vapor diffusion resistance for snow is set with the value of 1.

## 2.3 EN 1991-1-3:2003 The snow load standard

For structural design in the European Union, the European standard for actions on structures is Eurocode 1. Part 1-3 in Eurocode 1 contains general loads with snow loads, named the snow load standard NS-EN-1991-1-3 (Standard Norge, 2003). This document meets the requirements from the Technical Regulations to the Planning and Building Act. The snow load standard provides a National Annex with specific requirements for each nation (Standard Norge, 2008).

### 2.3.1 Determination of the snow load

According to the current snow load standard, the snow load on roofs is determined for persistent or transient design situations using this formula:

$$S = \mu_i C_e C_t S_k \quad (5)$$

$S$  is the design snow load [kN/m<sup>2</sup>]

$\mu_i$  is the snow load shape coefficient

$C_e$  is the exposure coefficient

$C_t$  is the thermal coefficient

$S_k$  is the characteristic snow load on the ground [kN/m<sup>2</sup>]

From the formula, the design load  $S$  is the product of the three coefficients and the characteristic snow load on the ground. The snow load shape coefficient ( $\mu_i$ ) is determined in chapter 5.3 and the main principle is how the snow load is distributed, drifted or un-drifted, on the roof. The shape, angles, and pitches of the roof affect how the load is arranged, the coefficient takes this into consideration and therefore adjusts on the diverse types of roof design. The coefficient varies from 0 to 1.6.

The exposure coefficient  $C_e$  is determined by the type of topography on the site and if the building is categorized as exposed or sheltered from wind.

Table 5. The exposure coefficient based on the topography on the site. Re-produced from Standard Norge, 2003.

Topography	C <sub>e</sub>
Exposed for wind	0.8
Normal	1.0
Sheltered from wind	1.2

*Exposed topography:* flat siting areas without obstacles, which provide exposure on all sides, completely without or with little terrain protection, taller buildings, or trees.

*Normal topography:* siting areas where the wind does not, in significantly matter, remove snow from the structures as a result from the terrain, other buildings or trees.

*Sheltered topography:* siting areas where the structure is significantly lower than the surrounding terrain or is surrounded by tall trees and/or by higher buildings.

The thermal coefficient  $C_t$  is used, as other values than 1, if the roof have a high heat transfer ( $> 1 \text{ W/m}^2\text{K}$ ) where the snow load is reduced due to melting caused by the heat flux. The coefficient is mainly used for glass roofs, but it is stated in the snow load standard that it may be used for other materials and roof constructions. From the national annex the thermal coefficient is calculated, where it is relevant to consider reduction due to heat transfer, by these formulas:

$$C_t = \left[ 1 - 0,054 \left( \frac{S_k}{3,5} \right)^{0.25} f(U_0, \theta) \right] \cos(2\alpha) \text{ for } 0 \leq \alpha \leq 45^\circ \quad (6)$$

where

$$f(U_0, \theta) = \begin{cases} 0 & U_0 < 1,0 \\ (\theta - 5)[\sin(0,4U_0 - 0,1)]^{0,75} & 0 \leq U_0 \leq 4,5 \text{ and } 5 \leq \theta \leq 18 \\ \theta - 5 & U_0 > 4,5 \text{ and } 5 \leq \theta \leq 18 \end{cases} \quad (7)$$

where

$U_0$  is the heat transfer coefficient for external thermal transition resistance equal to zero [W/m]:

$\alpha$  is the roof angle.



$s_k$  is the characteristic snow load on the ground [kN/m<sup>2</sup>].

$\theta$  is the lowest expected indoor temperature in the winter season.

The  $U_0$  is the given transparent surface, if  $U$  is determined by another value of external thermal transition resistance,  $R_e > 0$ , calculation of  $U$  by this formula is used

$$U_0 = \frac{U}{1 - UR_e} \quad (8)$$

where

$U$  is the thermal transmission of the roof [W/m<sup>2</sup>K]

$R_e$  is the external thermal transition resistance for  $U$  [m<sup>2</sup>K/W]

The standard then elaborates that an examination on the drainage of the melting water, to check that it is efficient and with no dangers of re-icing, is particularly necessary.

The characteristic snow load on the ground  $S_k$  varies depending on the location of the building. The characteristic snow load on the ground is based on a probability of 0.02, or 2 %, not being exceeded in a single year, with no exceptional snow included. This is referred to as the 50-year return period (YRP), and this is specified for each of the municipalities in Norway. The characteristic snow load on the ground provides the minimum limit of snow load that a building must withstand. For areas where the height above sea level ( $H$ ) is less or equal to the height limit ( $H_g$ ), the characteristic snow load ( $S_k$ ) is equal to the fundamental value of characteristic snow load ( $S_{k,0}$ ). If the height is above sea level,  $H > H_g$ , the load is found by

$$s_k = s_{k0} + n\Delta s_k \quad (9)$$

where

$\Delta s_k$  for the municipality is given in the national annex

$n = (H - H_g)/100$  where  $n$  is rounded up to the next integer

### 2.3.2 Climatic regions

Annex C in the snow load standard contains snow maps of Europe divided into nine regions. For this thesis, six locations were chosen for simulations, three in Norway and three in different countries in Europa. “The Norway region”, Bergen, Oslo, and Tromsø were selected from Norway. These three Norwegian cities have great distances and unlike climate categorizations. Three cities from different regions were chosen outside Norway, Copenhagen in Denmark, Cortina d’Ampezzo in Italy, and Grenoble in France. Copenhagen is in the Central East region, Cortina d’Ampezzo is in the Alpine region, and Grenoble is in the Central West region.

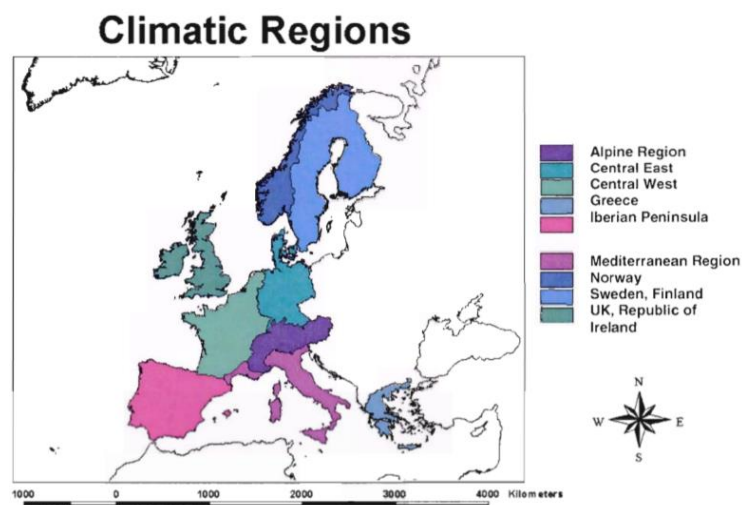


Figure 6. Climatic Regions from the snow load standard

## **2.4 Climate and the determination of extreme values**

The definition of climate is the long-term average of weather. Latitude, terrain, altitude, and nearby water, such as rivers, lakes, and oceans, affect local climates. The most common meteorological variables are temperature, humidity, atmospheric pressure, wind, and precipitation (Wikipedia, 2021). As the climate changes worldwide, the average global temperature increases, and the weather become more extreme. It is predicted that some areas will experience less snow than before, and other areas to experience heavier and more intense snowfalls.

Several classifications systems have been made to classify the climate in different areas; the most popular is the Köppen climate classification scheme.

### **2.4.1 The Köppen climate classification**

Climatologist Wladimir Köppen created the climate classification system in 1884. The system has had several modifications from the original, especially from Rudolf Geiger, and is also referred to as the Köppen -Geiger climate classification system (Wikipedia, 2021).

The system divides climates into five main climate groups, A (tropical), B (dry), C (temperate), D (continental), and E (polar). All groups have several subgroups that are represented as a letter. Table 6 shows the main groups with the associated subgroups. The system bases on the empirical relationship between climate and vegetation, where the climate conditions are defined by temperature and precipitation.

Table 66. The Köppen -Geiger climate classification system with the main groups and subgroups.

Köppen -Geiger climate classification system		
1 <sup>st</sup>	2 <sup>nd</sup>	3 <sup>rd</sup>
A (Tropical)	f (Rainforest) m (Monsoon) w (Savanna, Dry winter) s (Savanna, Dry summer)	
B (Arid)	w(Desert) s(Steppe)	h (Hot) k (Cold)
C (Temperate)	w (Dry winter) f (No dry season) s (Dry summer)	a (Hot summer) b (Warm summer) c (Cold summer)
D (Continental)	w (Dry winter) f (No dry season) s (Dry summer)	a (Hot summer) b (Warm summer) c (Cold summer) d (Very cold winter)
E (Polar)	T (Tundra) F (Eternal frost (ice cap))	

## 2.4.2 Snow weather changes and predictions in the future

As a consequence of global warming, the climate is changing. Some areas expect less snowfalls than before or are already experiencing them. While other areas, it's expected, or already experiencing, more and heavier snowfalls than before.

In 2013, SINTEF Byggforsk conducted an analysis concerning climate and vulnerability of the building stock in Norway. The report recommended measures regarding the characteristic snow load. The report included a map of Norway with colour codes, depicted in figure 7. The blue area represents parts of the country where the study recommends a possible reduction in the future, the green areas where the amount of load should be unchanged and the red areas where the study recommended to increase the load. A total of 34 municipalities were recommended to increase the characteristic snow load on the ground (Kvande, et al., 2013).

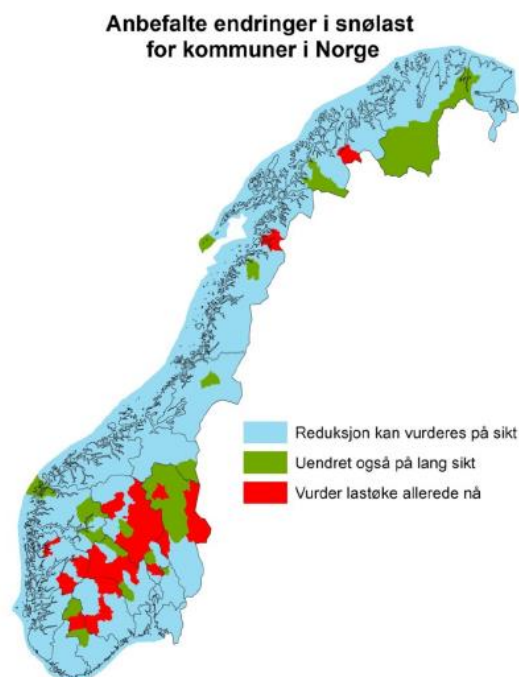


Figure 7. Recommended changes in the characteristic snow load on the ground in Norway (Kvande, et al., 2013).

Results from research in 2018 on the snow load in Europe and climate change showed a significant increase of the snow loads for the period 1951-2010 in many regions in the north and east Italy compared with the reference period (Croce, et al., 2018).

### **2.4.3 Measuring snow**

The amount of snow can be measured by how much water (in m or mm) the snow will melt into in the phase shift, called the snow water equivalent or SWE. SWE is a function of the depth and density of the snow. Only a few weather stations in Norway measure the SWE, making it demanding as a base for analysis. There are accessible websites that provide both modelled and real-time data on other weather parameters that can be used to investigate snow load (NVE, 2020).

### **2.4.4 Observed weather data from weather stations**

To access observations and measurements from all the weather stations available throughout Norway, Norwegian Centre for Climate Services has developed a website called "seKlima". The Norwegian Centre for Climate is a collaboration between the Norwegian Meteorological Institute, the Norwegian Water Resources and Energy Directorate, NORCE, and the Bjerknes Center. There are also weather statistics such as average values and deviations from regular. The stations available in search, list, and map depend on the selected choices in the menus for time resolution, weather element, and period. The weather stations have various equipment and measuring devices and does not necessarily offer the parameter in question (seKlima, 2021).

### **2.4.5 Modelled weather data - ERA5**

ERA5 is produced by the Copernicus Climate Change Service (C3S) at ECMWF (European Centre for Medium-Range Weather Forecasts). The ERA5 provides hourly estimates of a large number of climate variables. The prognoses are calculated with an advanced modelling and data assimilation system utilizing historical observations (ECMWF, 2021). For this thesis, a website that provides variables relevant to energy modelling was used. The ERA5 data was stored in a format optimized for fast time series access on a regular latitude and longitude, on a regular grid between -56 and 71 degrees of latitude with spatial resolution of 0.25 in both longitudinal and latitudinal direction. The data is only provided for non-ocean grid points.

#### 2.4.6 Calculation and estimation of extreme values

A theoretical return period is defined as the inversion of the average frequency of an occurrence. The theoretical return period does not indicate which year the occurrence will happen, but the probability of occurring in one of the years in the given period. In example, maximum snow load per year for a 5-year has a  $1/5 = 0.2$  or 20% chance of being exceeded in any one year. The same applies to the 50-year return period,  $1/50 = 0.02$  or 2% chance of being exceeded in any one year.

The European Committee for Standardization, CEN, have stated in prEN-1991-1-3, 2020 the recommended approach on determining the snow load on the ground (CEN/TC 250, 2020).

It is stated that a sequence of maximum yearly snow loads should be used to determine the snow load on the ground  $S_k$ .

For areas experiencing snow every year, a minimum of 20 years of recording data should be used in the calculation, where snow water equivalent is the preferred record.

Annual maximum snow loads may be considered as the appropriate basis for extreme value analysis in climates that experience snow cover over the complete winter season every year.

For climates that experience several independent periods of snow covers in the winter, the statistical stability of the estimated parameters may be increased by using peaks over a specific threshold. Climates that do not experience snowfall every year should fit the data with non-zero snow load amplitudes. The probabilistic distribution should contain the probability of a year with zero ground snow load.

The different probabilistic distributions should be compared to identify an appropriate distribution on the annual maximum snow load on the ground, where a Gumbel distribution or a lognormal distribution are suitable models from general experience. In this thesis, the lognormal distribution is used. The lognormal distribution is a probability distribution that have a logarithm with a normal distribution. As  $\log(x)$  exists only when  $x$  is positive, it is useful when the quantity of interest must be positive (MathWorks, 2021).

## **2.5 Reliability of existing buildings**

Building reliability is calculated to satisfy a predefined reliability level in the design standard, corresponding to the consequence of building failure. The variables used for dimensioning the structural components (e.g., resistance variables, permanent actions and climatic loads) have a certain statistical probability for occurring.

### **2.5.1 Vulnerability of existing structures**

Investigations presented in Meløysunds's Ph.D. from 2010 showed that existing buildings that are considered vulnerable to the occurrence of large snow loads primarily apply to building structures with a long span made with light structural materials. It was also stated that large variations in snow loads on roofs are observed within short distances due to extreme differences in local climate and topography. The local variations are not considered in the standards, raising questions on the estimation of roof snow loads on many buildings. These results show that the structure either needs an upgrade of the structural elements in the building or performing snow load control to preserve the safety of the building (Meløysund, 2010).

### **2.5.2 Development of the snow load**

The characteristic snow load on the ground in the snow load standard has changed during the last 70 years. In Norway, the characteristic snow load on the ground has gone from applying common national values to local values for each municipality.

Table 7 shows that the characteristic snow load has increased, and coefficients, explained in chapter 2.3, have been added throughout the last 70 years. For buildings designed 70-50 years ago, there is a high probability that they are under-designed, and with the local variations of snow load, structures built in the last 50 years may be under-designed in certain areas.



Table 7. Development of the snow load in standards. Reproduced from Iver Frimannslund's M.Sc. from 2017 that were based on the presentation of the development of the snow load in Vivan Meløysund's Ph.D. from 2010 (Meløysund, 2010) (Frimannslund, 2017).

Standard	-	NS 3052	NS 3479	NS 3479 3 <sup>rd</sup>	NS 3490	NS 3491-3
Year	1949	1970	1979	1990	1999	2001
General load/ Characteristic load	1.5	1.5	1.5-3.5	1.5-3.5	-	1.5-9.0
Changes	-	Snow maps introduced	S <sub>k</sub> with 5 YRP	C <sub>t</sub> introduced	S <sub>k</sub> with 50 YRP	C <sub>e</sub> introduced S <sub>k</sub> altered

## **2.6 Snow load control**

Heavy snowfalls are a problem for many nations. With some regions already having increasing snowfalls and more predicted for the future, snow load control is important to prevent people and material damages.

### **2.6.1 Manually by shovelling**

The most common way to remove snow loads on roof is shovelling the snow. Several tools can be used such as shovels, rakes, or some techniques with ropes is also common. Shovelling is effective in removing most of the snow, but it is highly time consuming and dangerous. Each year there are casualties in several countries worldwide.

### **2.6.2 Chemicals**

Chemicals might be used for de-icing of ice and snow to melt at a lower temperature. The chemicals can be types of salt or chemicals. Mostly used on pavements today. It might be a HSE issue which in any case needs to be handled with care and caution not to harm both nature, people, and materials.

### **2.6.3 Thermal de-icing system**

A typical snow melting system contains of the following components: an energy source, some heat exchanging elements, sensors for measuring actual weather conditions, e.g. snowfall, outdoor temperature and air moist content, and a system control (Mensah, et al., 2016).

There are several ways of controlling snow loads on roofs with heating systems. This thesis focuses on roof mounted PV snow mitigation systems. It has become more widespread to have roof mounted solar PV panels on buildings through the last decade. Manually removing the snow from the panel might be time-consuming and dangerous. A solution is to utilize PV panels in a “reversed” mode, using the electric power to generate heat, so the snow starts to melt, and the water drains off the roof or sublimates. Depending on the location, PV panels can produce solar energy throughout the year, and by removing the snow, the energy production can continue.

#### 2.6.4 Snow load control in the snow load standard

Snow load distribution and intensity on roofs can be described as functions of climate, topography, building shape, roof surface material, heat transportation through the roof, and time.

ISO 4335 is an international standard that specify methods for the determination of snow loads on roofs. Annex F in the standard concerns snow loads on roof with snow control. A sufficiently reliable control device for snow load can reduce the snow load on roofs.

Snow load on the roof with snow control is calculated with the equation

$$s = \mu_b s_n - s_c \quad (10)$$

$\mu_b$  is the slope reduction coefficient

$s_n$  is the snow load on the ground with accumulation for n days [kN/m<sup>2</sup>]

$s_c$  is the controlled snow load [kN/m<sup>2</sup>]

The snow load on the ground with accumulation is calculated with the equation

$$s_n = C_e d_n \rho_n g \quad (11)$$

$C_e$  is the exposure coefficient which consider local topography

$d_n$  is the representative snow depth on the ground when the snow load on the roof is controlled [m]

$\rho_n$  is the equivalent density for ground snow with roof snow control

$g$  is the acceleration of gravity

The definition of representative snow depth on the ground,  $d_n$ , is the annual maximum value of snow accumulation for n days with a return period of years (e.g., 5-, 50-, or 100 years). It is estimated from observed meteorological data of the ground snow depth. n days typically correspond with the duration of snowfall events on the site. Determination of the controlled snow load,  $s_c$ , on a site is set based on field experiments that investigate the capacity of the melting device in question. The controlled snow load is the differential between the initial snow load and the capacity of the snow control device during a heavy snowfall - guaranteeing the reduction.

## 2.7 Snow load control at “Down Town”

In Porsgrunn, Norway, the Citycon “Down Town” shopping centre use PV heating systems for snow load control. The construction of the shopping centre is under-designed for high snow loads, and the owner decided to install a PV heating system from Innos, “The Weight Watcher”, in 2019. Previous snow load control was manually shovelling, which demanded many workers, hours, and safety regulations, shown in Figures 8 and 9.

The roof area is approximately 10 000 m<sup>2</sup>, with about 6000 m<sup>2</sup> covered with PV panels with melting possibilities. Down Town has four zones for melting so that they can melt one zone or more, as desired. Weights that register the snow load are installed in three places in each zone. Each panel has a size of 1.65 m<sup>2</sup>, with a melting energy of 500W per panel. The melting process is initiated when the snow load reaches 75 kg/m<sup>2</sup>.

The property owners and the melting system producer have both stated that the new snow load control is functioning as planned and have successfully reduced the loads on the mall from heavy snowfalls.

In between March the 10<sup>th</sup> and 12<sup>th</sup> in 2021, there was a heavy snowfall in Porsgrunn. The snow weights installed on the panels registered up to 80 kg/m<sup>2</sup> of snow load. Snow melting was initiated on March the 11<sup>th</sup>, and the snow load was substantially reduced. Results shown in figures 10-13.

This thesis used the registered snow load data from Down Town to validate the snowpack simulation with heat from PV panels.



*Figure 9. Snow load control at Down Town shopping center before installing PV heating system, manually shoveling the snow. (FUSen, 2021)*



*Figure 8. PV heating system installed at Down Town shopping center. A total of 6000 m<sup>2</sup> of PV panels with heating systems for melting are installed on the flat roof. (FUSen, 2021)*

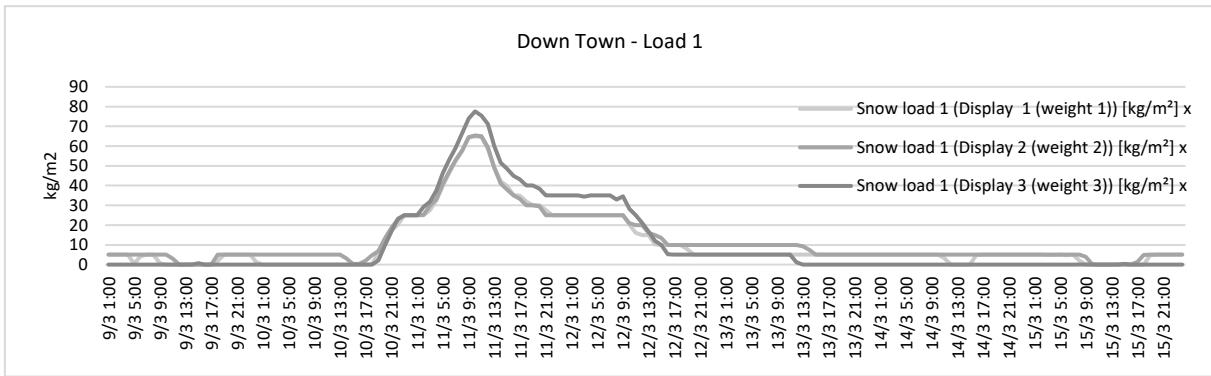


Figure 10. Snow load 1 at Down Town 09-15th of March 2021.

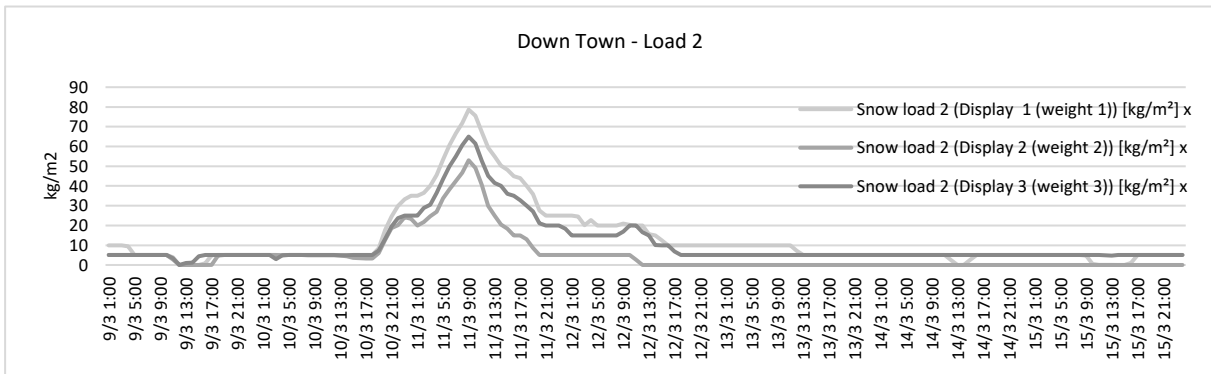


Figure 11. Snow load 2 at Down Town 9-15th of March 2021.

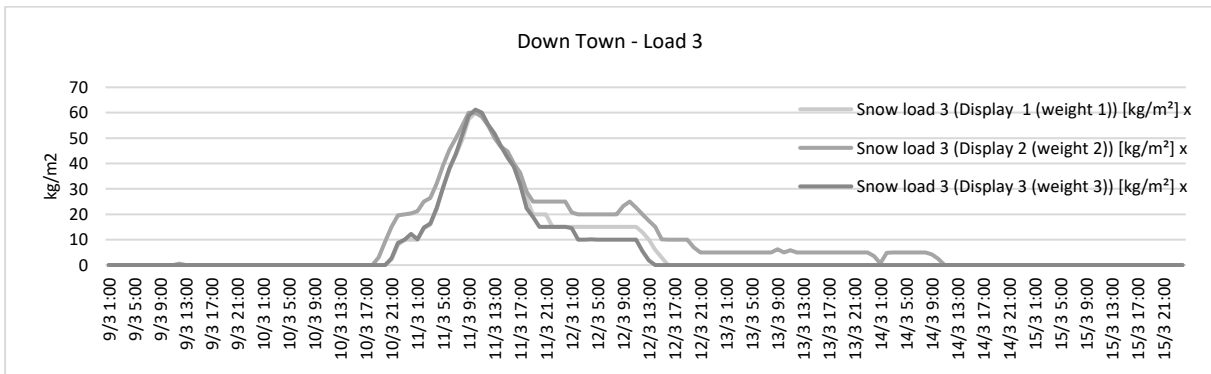


Figure 12. Snow load 3 at Down Town 9-15th of March 2021.

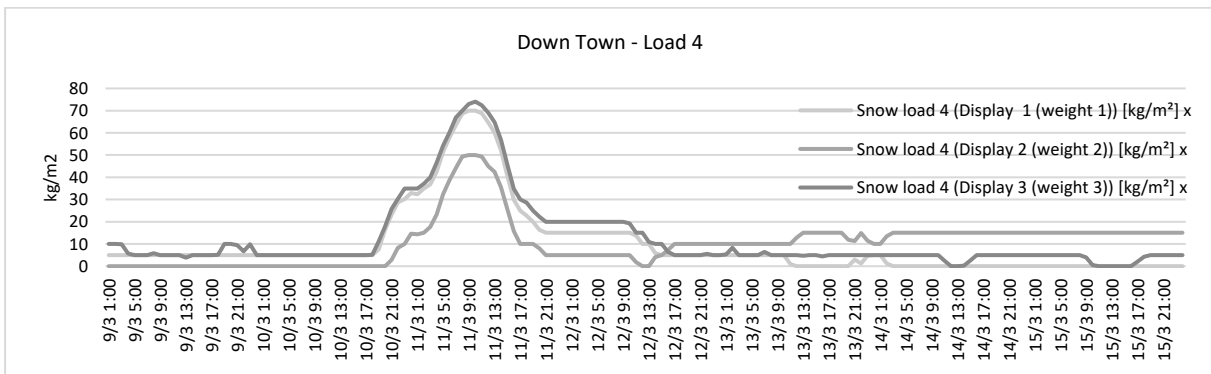


Figure 13. Snow load 4 at Down Town 9-15th of March 2021.

## 2.8 Simulation of surface heat transfer through building components

This thesis is limited to civil engineering. Thus the estimation of the PV panel's efficiency was found by studying the heat transfer through building components.

### 2.8.1 Terms in building physics

Explanation of some key concepts regarding heat transfer is necessary when using a simulation tool that simulates the heat transfer through building components.

*R-value [m<sup>2</sup>K/W]*

Thermal resistance is a measure of the heat flux through a building construction. It relies on the material's thermal conductivity and thickness of the layers. The formula for a homogenous material layer in the construction is

$$R = \frac{d}{\lambda_d} \quad (12)$$

where

$R$  is the thermal resistance of a layer [m<sup>2</sup>K/W].

$d$  is the thickness of the layer [m].

$\lambda_d$  is the thermal conductivity of the material [W/mK].

The total thermal resistance for a construction is the sum of the thermal resistance on each layer in the construction.  $R$  is the inverse of the U-value.

*U-value [W/m<sup>2</sup>K]*

Thermal transmittance is the rate of transfer of heat through a structure, also known as U-value. U-value is the inverse of the total thermal resistance of a building construction

$$U = \frac{1}{R_T} \quad (13)$$

where

$U$  is the thermal transmittance of the construction [W/m<sup>2</sup>K]

$R_T$  is the total thermal resistance of the construction layer [ $\text{m}^2\text{K}/\text{W}$ ]

*Relative humidity [%]*

Relative humidity measures the humidity in the air, from 0 to 1 or 0% to 100%. The air moisture content and water content are expressed as a percentage of the saturation content at the current temperature

$$RH = \frac{v}{v_{SAT}} \cdot 100\% \quad (14)$$

where

RH is the relative humidity [%]

$v$  is the water content [ $\text{g}/\text{m}^3$ ]

$v_{SAT}$  is the saturation content [ $\text{g}/\text{m}^3$ ]

## 2.8.2 WUFI

The WUFI (Wärme und Feuchte instationär) simulation program can calculate moisture and heat transport over time in each construction layer. This simulation program was developed in Germany by Fraunhofer-Institut für Bauphysik (Institute of Building Physics) in 1995. They have been further developing the program since then by creating several programs for different applications and continuously updated software versions (WUFI, 2021).

## 2.8.3 WUFI: Transportation mechanisms

WUFI simulates with an advanced hygrothermal model tailored to the needs of architects and building designers. The software is an easy-to-use and menu-driven program for use on a personal computer to provide customized solutions to moisture engineering and to address damage assessment problems for various building envelope systems.

The transient calculation procedure of the model is outlined by the flow chart in figure 4, reproduced from Karagiozis et al., 2021. Based on the specific building construction with settings from the user, the program calculates moisture and heat transport.

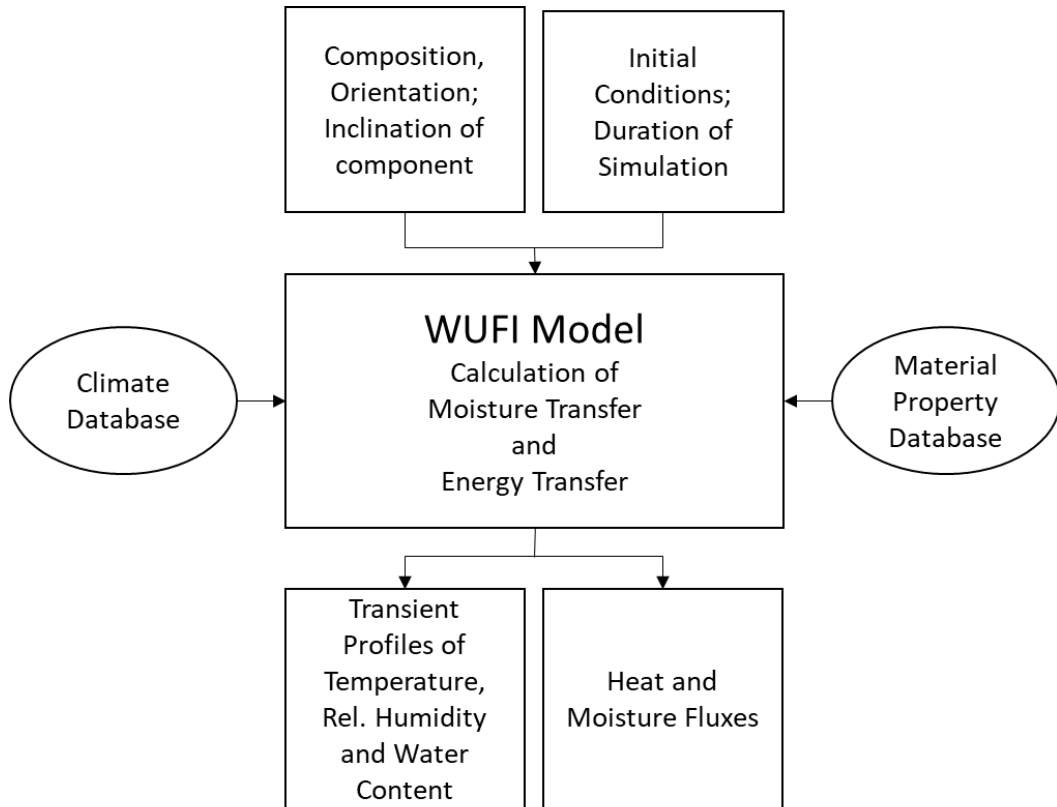


Figure 14. Reproduced model of the transient calculation procedure in WUFI (Karagiozis, et al., 2001)

For the numerical simulations in WUFI the following transport equations is applied:

Heat transport

$$\frac{\partial w}{\partial \phi} \cdot \frac{\partial \phi}{\partial t} = \nabla \cdot (D_{\phi} \nabla \phi + \delta_p \nabla (\phi p_{sat})) \quad (15)$$

Moisture transport

$$\frac{\partial H}{\partial T} \cdot \frac{\partial T}{\partial t} = \nabla \cdot (k \nabla T) + h_v \nabla \cdot (\delta_p \nabla (\phi p_{sat})) \quad (16)$$

where

$c$ : specific heat, J/kgK

$D_{\phi}$ : liquid conduction coefficient, kg/ms

$H$ : total enthalpy, J/m<sup>3</sup>

$h_v$ : latent heat of phase change, J/kg



$k$  : thermal conductivity, W/(mK)

$p_{sat}$ : saturation vapor pressure, Pa

$t$  : time, s

$T$  : temperature, K

$w$  : moisture content, kg/m<sup>3</sup>

$\delta_p$  : vapor permeability, kg/(msPa)

$\phi$  : relative humidity

#### 2.8.4 WUFI: Material input

To run a simulation using WUFI, material data for all construction layers must be defined.

There are built-in libraries to get the material data in WUFI, or it can be added manually.

The following property for each material is to be defined:

- Density [kg/m<sup>3</sup>]
- Specific heat capacity [J/kgK]
- Thermal conductivity [W/mK]
- Porosity [m<sup>3</sup>/m<sup>3</sup>]
- Water vapor diffusion resistance [-]

In this thesis, WUFI® Pro version 4.1 was used to simulate how the heat fluxes transport in a melting scenario with PV panels and a snow cover.

## 2.9 Simulation of the snowpack

Methods for numerical simulation of the snowpack have evolved and become more accurate in recent years. And there are now several simulation models developed and applied for forecasting snow-related influence on infrastructure.

Some of the simulation models available have different calculations for the mathematical model of the snowpack for various purposes. One model used in Norway, the seNorge model, is used to model spatial snow cover distributions on a daily basis (Saloranta, 2016).

SNOWPACK is a model developed by the Institute for Snow and Avalanche Research (SLF) in Switzerland and is used for forecasting the need for snow load removal from roofs in Japan (Barthelt & Lehning, 2002) (Hirashima, et al., 2020). The Energy Balance Snow Cover Integrated Model (ESCIMO) model represents a single-layer energy balance snow model that solves the snow surface's energy and mass balance equations by using physically based parameterizations of the relevant processes. The Energy Balance Snow Cover Integrated Model (ESCIMO) is applied in this thesis.

### 2.9.1 The Energy Balance Snow Cover Integrated Model (ESCIMO)

The model uses hourly temperature, precipitation, wind speed, relative humidity, global radiation, and incoming longwave radiation to simulate the hourly energy balance, the water equivalent, and melt rates of snow cover. ESCIMO includes a one-layer process model, 1-D, which assumes a homogeneous snowpack and uses simplified parameterizations to solve the energy and mass balance for the snow surface (Strasser & Marke, 2010).

The energy balance of the snow surface is calculated on an hourly time step considering the radiation balance ( $Q$ , balancing incoming and outgoing components of short- and longwave radiation), sensible ( $H$ ) and latent heat fluxes ( $E$ ), advective energy conducted by solid or liquid precipitation ( $A$ ), as well a soil heat flux ( $B$ ). The energy available for melt ( $M$ ) is calculated in the expression

$$Q + H + E + A + B = M \quad (17)$$

From formula 17,  $Q$  is divided in to four values, shortwave and longwave for both radiations down and up,  $Q_{l \text{ up}}$ ,  $Q_{l \text{ down}}$ ,  $Q_{s \text{ up}}$ , and  $Q_{s \text{ down}}$ . The shortwave and longwave radiation balance

is calculated by subtracting outgoing short- and longwave radiation from measured incoming shortwave and longwave radiation.

Longwave emission of the snow cover,  $Q_{l up}$ , is calculated from the snow emissivity  $\varepsilon$ , the Stefan-Boltzmann-constant  $\sigma$ , and the snow surface temperature  $T_s$

$$Q_{l up} = \sigma \cdot \varepsilon \cdot T_s^4 \quad (18)$$

Soil heat flux is set to  $2 \text{ W/m}^2$  as an assumption due to scarcely available measurements (Strasser & Marke, 2010).

Snow albedo ( $a$ ) is modelled with ageing curve approach

$$a = a_{min} + a_{add} \cdot e^{-k n} \quad (19)$$

Where  $a_{min}$  is the minimum albedo of the snow and  $a_{add}$  is an additive albedo (and adding these gives the maximum albedo),  $n$  is the number of days since last (considerable) snowfall and  $k$  is the recession factor (one for positive and one for negative temperatures, shown in table 8). The snow albedo is reset if a significant snowfall occurs.

Due to the lack of detailed measurements above the local scales, the model uses simple empirical descriptions of the turbulent fluxes, valid for medium roughness and a wide range of wind speeds. In areas where the contribution of the turbulent fluxes to the energy balance of the snowpack is small, the induced loss of accuracy is negligible. For neutral or stable conditions, the parameterizations applied here are valid.

The sensible heat flux  $H$  is expressed with wind speed  $W$  in m/s as

$$H = 18.85 \cdot (0.18 + 0.098 \cdot W) \cdot (T - T_s) \quad (20)$$

And the latent heat flux  $E$  is expressed through

$$E = 32.82 \cdot (0.18 + 0.098 \cdot W) \cdot (e_l - e_s) \quad (21)$$

where  $e_l$  is the water vapour partial pressure at measurement level and  $e_s$  the water vapour saturation pressure at the snow surface, with both calculated from

$$\delta e = \frac{E \cdot t}{l_s} \quad (22)$$

where the small mass changes  $\delta e$  in mm generated by sublimation or resublimation is simulated with  $t$  as the duration between two-time steps of 3600 s, and  $l_s$  is the sublimation/resublimation heat of snow.

Supplied by precipitation  $P$ , the advective energy  $A$  depends on its phase. An adjustable threshold temperature ( $T_w$ ) is assumed for the precipitation phase detection, if not measured. The energy advected by  $P$  in mm is calculated for rainfall on snow, without refreezing, as

$$A = P \cdot c_{sw} \cdot (T - 273.16) \quad (23)$$

where  $c_{sw}$  is the specific heat of water, shown in table 8.

For snowfall, the advective energy is calculated by

$$A = P \cdot c_{ss} \cdot (T - T_s) \quad (24)$$

where  $c_{ss}$  is the specific heat of snow.

For melting scenario where the air temperature is below 273.16 K, all fluxes are calculated with an assumed snow surface temperature of 273.16 K. Energy that remains is available for melt and is calculated by

$$melt = \frac{M \cdot t}{c_i} \quad (25)$$

where  $c_i$  is the melting heat of ice.

Parameter values and constants used in ESCIMO.spread are shown in table 8, reproduced from Strasser & Marke, 2010.

Table 8. Parameter values and constants used in ESCIMO.spread reproduced from (Strasser & Marke, 2010).

Parameter/constant	Symbol	Value	Unit
Soil heat flux	$B$	2.0	W/m <sup>2</sup>
Minimum albedo	$a_{min}$	0.45	
Maximum albedo	$(a_{min} + a_{add})$	0.90	
Recession factor ( $T \geq 273.16$ K)	$k$	0.12	
Recession factor ( $T < 273.16$ K)	$k$	0.05	
Hourly threshold snowfall for albedo reset		$0.5 \times 10^{-3}$	m
Threshold temperature for precipitation phase detection	$T_w$	275.16	K
Emissivity of snow	$\varepsilon$	0.99	
Specific heat of snow (at 0°C)	$c_{ss}$	$2.10 \times 10^3$	J/kg K
Specific heat of snow (at 5°C)	$c_{sw}$	$4.20 \times 10^3$	J/kg K
Melting heat of ice	$c_i$	$3.337 \times 10^5$	J/kg
Sublimation/resublimation heat of snow (at -5°C)	$l_s$	$2.8355 \times 10^6$	J/kg
Stefan-Boltzmann constant	$\sigma$	$5.67 \times 10^8$	W/m <sup>2</sup> K <sup>4</sup>

In contrast to ESCIMO.spread (v1), the model version ESCIMO.spread (v2) applied in this thesis, includes

- i) an improved detection of precipitation phase based on wet-bulb-temperature,
- ii) an approach for snow temperature estimation,
- iii) consideration of cold and liquid water content in the snowpack and last, not relevant in the context of this study,
- iv) a canopy sub-model to account for snow-vegetation interaction (Marke, et al., 2016).

## **3 Method**

The main method in this thesis is quantitative research using simulation models and analysis of the results. This chapter describes the implementation of the simulations, modelling and analysis performed in the thesis.

### **3.1 Validation of the simulation model**

This chapter explains the method of how the simulation of the snowpack was validated. To test if the simulation method is reliable, the registered snow load data from The Citycon “Down Town”, in Porsgrunn, Norway, is used to compare with a simulated situation with collected data.

#### **3.1.1 Approach of the validation**

The foundation for validation of the simulation method, was the event with heavy snowfall registered in Porsgrunn from 10<sup>th</sup> to 12<sup>th</sup> of March 2021. Simulating the same event with registered weather data in the snowpack model, simulating a snowpack, and then adding heat to compare with the registered snow loads from “Down Town”, from chapter 2.7. The validation process aimed to see if the simulation method fits with actual, registered snow load data.

The melting energy used at Down Town was 500 W per panel, with panel size of 1.65 m<sup>2</sup>, the power for every m<sup>2</sup> is approximately 303 W. Assuming that 1 kg/m<sup>2</sup> of new snow is equal to 1 cm/m<sup>2</sup> depth of snow. The SWE of the snowpack is assumed to be 1 mm per 1 cm new snow. If the registered snow load is 75 kg/m<sup>2</sup> at Down Town, it would correspond to a 75 mm SWE in the model when comparing snow load.

#### **3.1.2 Site characteristic and collection of weather data**

Porsgrunn is a city located on the south-east coast of Norway.

To simulate the snowpack, collection of the following weather parameters was needed: temperature, wind speed, relative humidity, precipitation and short- and longwave radiation. As there is no nearby weather station that supplies all needed parameters for this site in

Porsgrunn, it was necessary to investigate and combine several data sources. A total of four sets of different parameter source combinations. and local differences in climate were simulated.

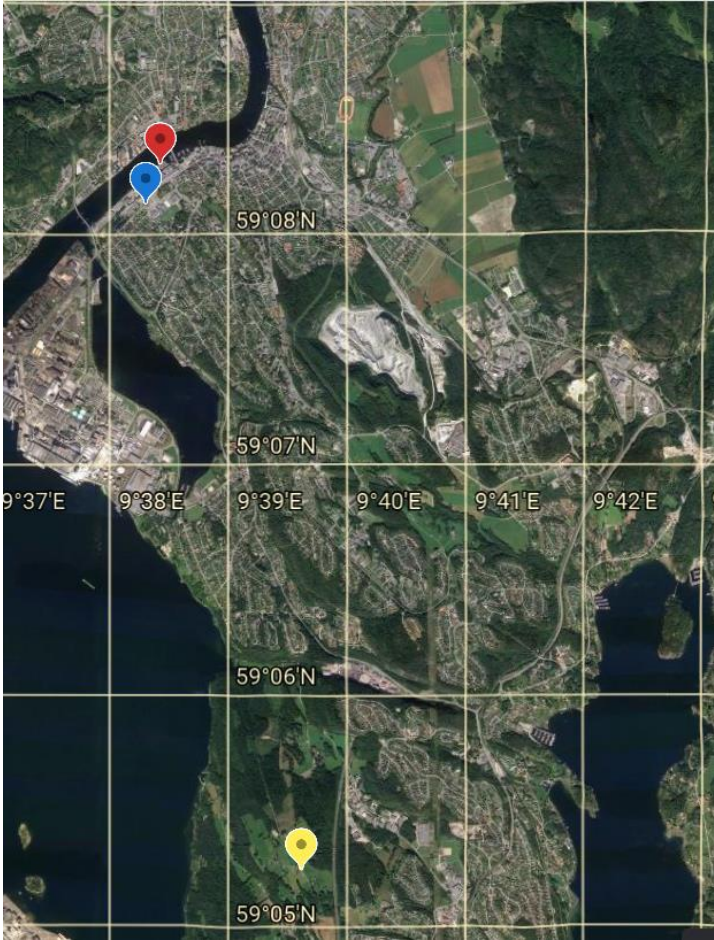


Figure 15. Locations of Down Town shopping center and the collected weather data source in Porsgrunn, Norway. Red: Down Town - Blue: SN30261 - Yellow: SN30255

Table 9. List lat/long and altitude of the collected weather data used in the simulation of the case at Down Town.

Source	Lat / Long	Height above sea level[m]
ERA5	59.25 / 9.75	216
SN30255	59.09 / 9.66	100
SN30261	59.14 / 9.64	10
Down Town	59.14 / 9.64	10

As there is not one source supplying all parameters for the simulation and validation process, it is necessary to exploit several data sources. All simulations have short- and longwave data from ERA5 due to the lack of collected data in this area.

Simulation number 1 has modelled weather data from ERA5 on all parameters.

The second simulation has parameters from the weather station, SN30255, which is located approximately 10 km in distance from Down Town.

Simulation number 3 have a combination of parameters from SN30255 and SN30261.

Weather station SN30261 is located approximately 500m distance from Down Town but collects only precipitation.

The fourth simulation have registered temperature from Down Town own panel's, relative humidity and wind speed from SN30255 and precipitation from SN3026. As the temperature registered at Down Town could be affected by the heat from when the PV panels are in heating mode, it was adjusted, explained in chapter 3.1.3.

*Table 10. Composition of the weather data sources used in the simulation of Down Town melting scenario.*

Combination of weather parameter sources in the simulations						
Simulation no.	Temperature	Relative Humidity	Wind Speed	Precipitation	Global radiation	Incoming longwave radiation
1	ERA5	ERA5	ERA5	ERA5	ERA5	ERA5
2	SN30255	SN30255	SN30255	SN30255	ERA5	ERA5
3	SN30255	SN30255	SN30255	SN30261	ERA5	ERA5
4	Down Town	SN30255	SN30255	SN30261	ERA5	ERA5

### 3.1.3 Adjusted temperature data

When melting was engaged at Down Town, the recorded temperatures from the panels were affected by the heat. Therefore, the values recorded with heating were adjusted as input data in ESCIMO. Comparing temperature data from the previous hours for both Down Town panel and the closest weather station SN30255 before melting started, indicates a temperature difference. Temperatures registered at Down Town panel showed a temperature of 1 K lower than SN30255, when comparing 39 hours of data before melting started. To correct the



temperature from the panel, after hour 9 at 11<sup>th</sup> march, SN30255 temperature is used with an adjustment of minus 1 K for each hour.

Figure 16 show that at some hours the Down Town panel have higher temperatures, but the trend is the temperatures are lower. It was assumed in beforehand that the data validation would show some differences, but all data from the 39 hours were included when calculating the mean delta.

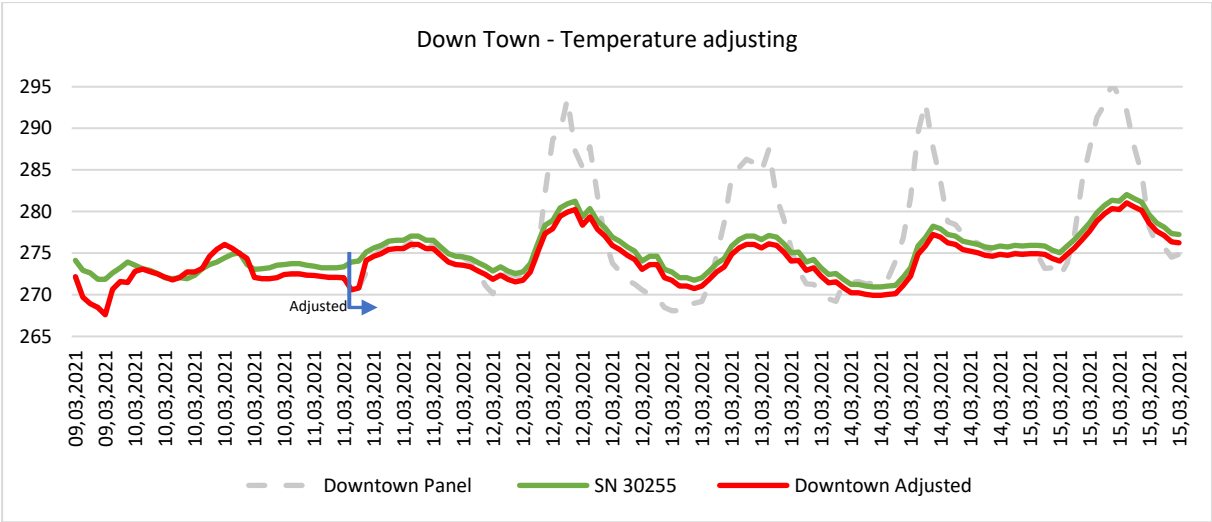


Figure 16. Temperature registered at Down Town PV panel adjusted with the mean difference value of the closest location of a weather station.

### 3.2 Simulation of the energy efficiency

The PV panels in reverse mode produce heat to melt the snow, but there is little to no documentation of the PV panel's efficiency in the melting scenarios. As described in the theory chapter 2, snow insulates and might affect the heat flux in the melting scenarios. In this study, the simulations have both excellent, equal to 1, and reduced, below 1, energy efficiency from the PV panels to compare the differences in energy demand of the melting strategies. The simulations conducted in WUFI are a simplified and theoretical interpretation of a melting situation with PV heating systems.

#### 3.2.1 Simulation of heat transfer

The main idea behind simulating how the heat transportation distributes from the PV panels in a simplified melting scenario, is to find a general expectation of the effect and efficiency. The results can then be used to calculate the energy demand in more extensive areas than the studied area, e.g., by having case studies where the effect and efficiency only apply for the specific local conditions in that case. Using a simulation program that simulates the percentage of heat flux that transports up in the snowpack in a melting scenario over a set time, will indicate efficiency of the PV panels. The efficiency will probably vary according to the snowpack conditions such as thickness, density, etc., materials used in the panels, and quality of the panels.

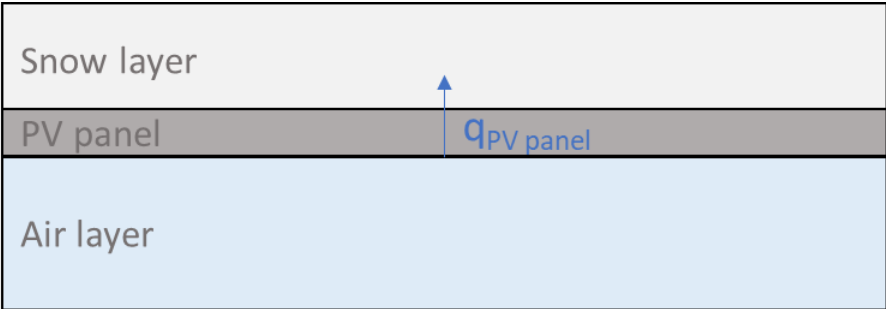


Figure 17. Model of the air layer under the PV panel and snowpack above. Where  $q_{PV\ panel}$  is the heat from the PV panel.

The illustration in figure 17 is a model of a horizontal PV panel with an air layer below and a snow layer above.  $q_{PV\ Panel}$  is the heat from the PV panels. For simplification, the PV panels are horizontal and not with an angle.

Heating or ventilation sources can be added to the layers from the model using WUFI. Adding a heat source that hourly emits a specific amount of heat over the simulated period in the PV panel layer will show how the heat transports throughout the layers. Adding an air change over time in the air layer might affect heat transport. The layers and settings in WUFI are constant and the potential melting of the snowpack due to the added heat source is not considered in the simulation. Therefore, the constants of the snowpack aim to fit the snow properties that match a snowpack's right before it starts to melt. WUFI provides monitoring of heat transport in all layers.

### **3.2.2 Structure and procedure**

The procedure in WUFI is first to create a project that allows making different varieties of simulation. For each variant, there are three main groups of settings and conditions. The first group is the “construction,” which has four sub-categories, determined by the user to fit the desired construction for simulation. The first sub-group is the layers and monitoring positions. Where each layer in the construction from left (outside) to right (indoor). Material definitions, thickness, and sources of heat and/or moist are defined in each layer. The monitoring positions for later analysis is selected.

The next sub-group is the determination of the orientation, slope and height of the construction. Adding the orientation of the construction in cardinal directions (north, east, south and west). Slope or angle, and categorizing of the height (below 10m, more than 20m, etc.) of the construction is also selected.

The next step is the surface transition coefficient. Where the outer surface settings, or boundaries, are determined with values on heat resistance, SD-value, short-and long wave radiation emissivity, explicit radiation balance, and rainwater absorption. Also, the inner surface is defined by heat resistance and SD-value.

The last sub-group is the determination of initial conditions which is defined by setting values for humidity and temperature at the simulation start.

The next group is “settings”, with two sub-categories for the user to set simulation profile and specify the calculation type. Deciding the simulation time, from start-date to end-date, and defining the time interval in the simulation. Defining the calculation type if it is heat- and/or

moist-transport. Hygrothermal advanced settings, increased accuracy, and convergence improvement can also be selected.

The last main group is the determination of climate on the two sides of the construction, outside and indoor. Both sides of the construction have a climate and it is possible to add climate file, using standards, or manually choose the relevant category and type in temperature and relative humidity with amplitudes or have the values constant.

### **3.2.3 Input materials and settings**

Four sets will be simulated in WUFI. The layers simulated vary in each set, table 11 shows an overview of which layers that are included in which set. The PV panel is divided into two layers, a glass layer on top and a metal layer on the bottom. Set 1, is a simplified construction consisting of a snow layer and PV panel with outdoor climate on both sides. Set 2 simulates with the snow layer, PV panel and an air layer with outdoor climate on each side. Set 3 and 4 have the same construction with the snow layer, PV panel, air layer and a flat roof construction with an indoor climate below the roof and an outdoor climate above the snow layer. Set 3 have half the thickness in the air layer than set 4.

The thickness of the snow and air layer varies throughout the sets. All sets have simulations with 10, 50 and 100mm of snow thickness. The air layer is 5mm in set 3 and 10mm in set 2 and 4. Table 11 lists the construction layers for all sets.

Table 11. Overview of the sets run in WUFI with the construction composition of layers and thickness.

Simulation Set no.	Layer	Thickness [mm]
1	Snow	10/50/100
	Glass	1
	Aluminium	1
	Air	10
2	Snow	10/50/100
	Glass	1
	Aluminium	1
	Air	10
3	Snow	10/50/100
	Glass	1
	Aluminium	1
	Air	5
	Compact roof	502
4	Snow	10/50/100
	PV system	1
	Air	10
	Compact roof	502

Table 12. Roof construction used in set 3 and 4. The construction with the material properties and thicknesses collected from built-in library in WUFI.

Compact roof	
Layer	Thickness [mm]
PVC coating	1
Mineral wool	300
PE-foil	1
Concrete B45	200

An illustration of all the simulated sets is shown in figure 18.

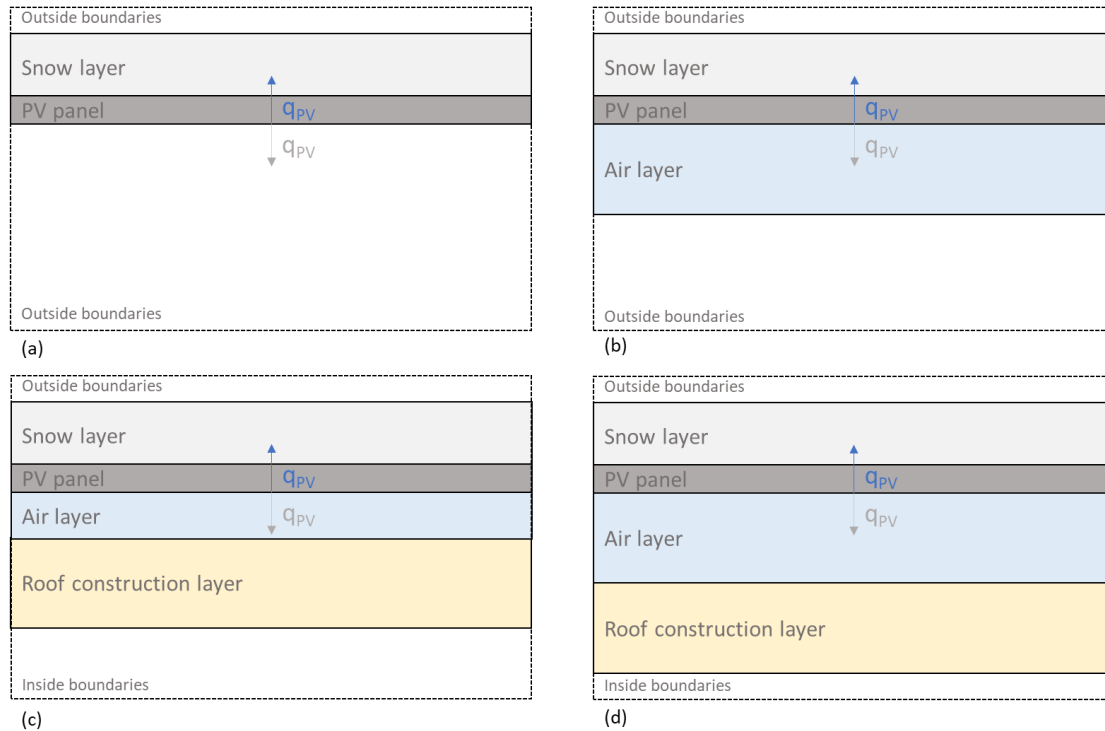


Figure 18. Illustration of the sets run in WUFI: (a) set 1, (b) set 2, (c) set 3, (d) set 4. Differences in thickness of the snow layer are not illustrated. Where  $q_{PV}$  is heat transportation up in the snow layer and  $q_{PV}$  is heat transportation down in air layer.

The simulation emphasizes heat transportation/heat flux and will not simulate moist transportation. The time profile for all sets was 24 hours with a heat source of 300 W per hour in the glass layer. The construction orientation is to the south with a construction angle of  $0^{\circ}$ C, simulating a flat roof. The outdoor climate is constant, with  $0^{\circ}$ C and 80 % relative humidity (RH), with the start conditions in the middle of the structure as the same. The climate inside is constant for sets 3 and 4, with  $22^{\circ}$ C and 40 % RH. The start conditions as mean values with  $10^{\circ}$ C and 60 % RH in the middle of the construction. Set 1 only consists of three layers; the metal layer is the inner surface with an R-value of 0.11.

The inner surface of set 2 is the air layer, and has one reflecting, the roof, and one non-reflecting surface, the back of the PV panel, and the R-value is 0.33. For set 3 and 4, the inner surface is inside the roof construction and have a standard R-value of 0.04 (SINTEF Byggforsk, 2014).

The R-value is a measure of resistance to heat flow through a given thickness of material. For the outer surface, snow layer was calculated from the thermal conductivity of snow and the results is shown in table 13.

*Table 13. R-value of the outer surface, snow layer*

R-value of the outer surface – snow layer		
Thickness [mm]	Equation: thickness/thermal conductivity	R
10	0.01/0.2	0.05
50	0.05/0.2	0.25
100	0.10/0.2	0.50

### 3.2.4 Material definitions

For each material, in addition to thickness, five material properties were entered. These are density, porosity, specific heat capacity, thermal conductivity, and vapor diffusion. The materials are snow, glass, metal/aluminium, air, and the roof components, shown in table 14.

*Table 14. Material data input used for the construction layers simulating the snowpack, PV panel and air layer with WUFI.*

Material data	Snow	Glass	Aluminium	Air	Unit
Density	300	2400	2700	1.3	kg/m <sup>3</sup>
Porosity	0.5	0	0	0.999	m <sup>3</sup> /m <sup>3</sup>
Specific heat capacity	2.05	900	900	1000	J/kgK
Thermal Conductivity	0.2	1	150	0.071	W/mK
Vapor diffusion	1	100000	100000	0.73	-

The snow layer is considered a homogeneous material with no changing throughout the simulation, as this simulation focuses on the heat flux and not snow melting. For the simulation to be as close to a real melting scenario as possible, the determination of the material properties of the snow layer represents a snowpack's properties right before it melts. The air layer was chosen from a built-in library, “General material”, in WUFI.

The glass layer has the material properties of a soda-lime glass and the aluminium layer have anodized aluminium alloy. The construction of the compact roof was found in the NTNU construction library in WUFI for a “compact flat roof”. Table 14 shows the values on each layer in the compact roof.

*Table 15. Material data input for the roof construction layers for simulations in WUFI. The construction is extracted from a built-in library, “NTNU”, in WUFI.*

Material data	PVC	Mineral wool	PE-folie	Concrete	Unit
Density	1000	60	130	2220	kg/m <sup>3</sup>
Porosity	0.0002	0.95	0.001	0.18	m <sup>3</sup> /m <sup>3</sup>
Specific heat capacity	1500	850	2200	850	J/kgK
Thermal Conductivity	0.16	0.04	1.65	1.6	W/mK
Vapor diffusion	15000	1.3	87000	248	-

After simulating all the sets, the next step was to observe how air changes affect the heat flux. In set 2, with a 10mm snow layer, an air change was added to the air layer with a 10, a 100 and a 1000 air changes per hour for 24 hours was simulated.



### 3.3 Simulation of the energy demand

The simulations in ESCIMO are used for several purposes, finding the maximum yearly snow load, energy demand with an added heating source, and years with overload, all run with different strategies and conditions. Before simulations with melting and strategies were implemented, the design limit and subsequent melting limit were found simulating the "base" snowpack. The aim of using ESCIMO to simulate the "base" snowpack from weather data is to collect it and extract yearly maximum snow load for as many years with weather data available. The data could then be used to find the snow load's return period and decide the melting limit.

#### 3.3.1 Site characteristics

A total of six sites in Europe were selected for the simulations: Tromsø, Oslo, and Bergen in Norway, Copenhagen in Denmark, Cortina d'Ampezzo in Italy, and Grenoble in France. The choice of locations was based on several reasons:

- Sites in various parts of Europe
- Variation in climate classification
- Differences in the average amount of snow and characteristic snow load from the snow load standard
- Various altitudes

Table 16 contains reproduced values of the characteristic snow load on the ground,  $S_{k,0}$ , from the EN 1991-1-3:2003 The Snow Load standard. Altitude is the height above sea level for the site in question.

Table 16. Characteristic snow load on the ground and climate region from the Snow Load Standard and National annex.

Site	Altitude [m]	$S_{k,0}$ [kN/m <sup>2</sup> ]	Climate region
Tromsø	0-150	3,5	Norway
Oslo	0-150	3,5	Norway
	151-250	4,5	
	251-350	5,5	
	>350	6,5	
Bergen	0-150	2,0	Norway
Copenhagen	0-100	1,0	Central mid-west
Cortina d'Ampezzo	200-1500	5.31	Alpine
Grenoble	200-500	0.67	Central west

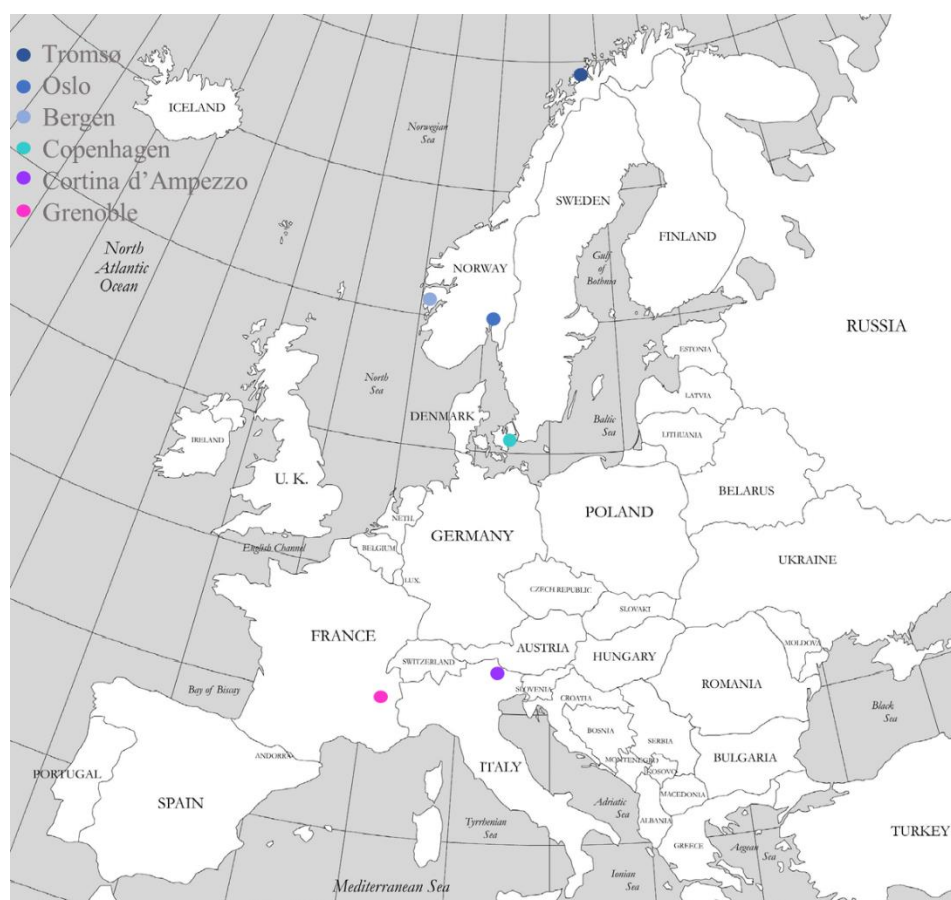


Figure 19. Map of the sites used for simulations in ESCIMO.

The ERA5 files was retrieved on the selected locations. Because the ERA5 map covers a great area of a latitude/longitude grid of 0.25 x 0.25 degrees, it is not given that the modelled weather data have the same latitude/longitude and altitude as the selected locations originally have.

All locations have differences in altitude compared to the ERA5 data. The values of the height above sea level were found using an easily accessible and public online map service (Google maps), which also correspond with the site's characteristic snow load data listed in table 15. Copenhagen is the only site which has an insignificant altitude difference, while the other sites spread from having 100 m and up to 750 m in difference. Table 17 show the original lat/long and altitude to the retrieved ERA5 data, it also shows the climate classification on each site.

Three sites have the same classification category from Köppen-Geiger classification system. Bergen, Copenhagen, and Grenoble are categorized are “Cfb”, which is temperate, no dry season and warm summers. Tromsø, Oslo and Cortina d’Ampezzo have Df, continental with no dry season, with the last group different, with respectively c (cold summer), a (hot summer) and b (warm summer).

*Table 17. Site characteristics: latitude and longitude, altitude, and the climate category from the Köppen-Geiger climate classification system.*

Site	Lat/Long	Altitude [m]	Lat/Long ERA5	Altitude [m] ERA5	Köppen- Geiger
Tromsø	69.67 / 18.96	13	69.75 / 19	211	Dfc
Oslo	59.92 / 10.75	5	60 / 10.75	247	Dfa
Bergen	60.22 / 5.2	5	60.5 / 5.25	117	Cfb
Copenhagen	55.68 / 12.57	6	55.75 / 12.5	12	Cfb
Cortina d’Ampezzo	46.54 / 12.14	1223	46.5 / 12.25	1652	Dfb
Grenoble	45.19 / 5.73	218	45.25 / 5.75	985	Cfb

### **3.3.2 Procedure using the snow cover integrated model**

In chapter 2.4.6, the recommended procedure for determining the snow load on the ground is by using a distribution of a minimum of 20 years. For Tromsø, Oslo, and Bergen, weather data of 39 years, from 1981-2019, were collected. For Copenhagen, Cortina d'Ampezzo, and Grenoble, weather data of 40 years, from 1981-2020, was collected.

Using the extracted weather data. The model application is an excel-spreadsheet where the input data is added on the *Meteorological input*-sheet, and the results are shown in the Model calculation sheet. The model calculation sheet contains rows for a set of hourly time steps, usually a year, and columns with the calculations at each time step. The results are collected directly on the sheet of the model calculation sheet, the model parameters are defined, which makes it easy for the user to change. To simulate the heat from the PV panel, a row for PV heat flux was added in the spreadsheet and the calculation of the energy.

### **3.3.3 Extreme values**

The snow load on the ground is dependent on several meteorological parameters such as temperature, precipitation, radiation, wind speed, and humidity. The snow load on roofs is usually related to the snow load on the ground.

The common method for calculating the return period of the snow is to use the extreme values from the analysis of snow load measurements over a specific period.

From chapter 2.4.6, the proposal from the European standard, prEN 1991-1-3, on determining the snow load and annual maximum snow load is by using a log-normal distribution of fitted measured data. This thesis uses the proposed method to find 5- and 50-year return periods (YRP) with modelled weather data. Because the data used is not from actual weather stations with accurate measures, it may differ from the return period in the current snow load standard and national annex for the areas included in this study. The characteristic snow load was extracted from the log-normal distribution where 20 % is the 5 YRP, and 2 % is the 50 YRP.

### **3.3.4 Melting strategies**

From chapter 2.1.4, previous research concludes that meltwater from the PV panels may refreeze if the air temperature is equal to or below 0°C. In that case, the snow load is not

reduced, just displaced, or moved from one place to another. If a building structure depends on the PV panels to reduce the snow load due to reliability and structural matters, melting the snow load from the PV panel will be unnecessary if the meltwater refreezes directly at the roof or gutters. The structure will even have a lower capacity for snow loads due to extra weight from the PV panels, and additional alternatives for snow load control are required.

This thesis has four strategies for modelling the melting of the snowpack, shown in table 18. Strategy A and B have two sub-strategies with melting energy of 100 W/m<sup>2</sup> and 300 W/m<sup>2</sup>. Whereas strategies C and D, only melting energy of 300 W/m<sup>2</sup> are simulated. In total, six melting results plus the base case of the “base” snowpack with no added energy.

All strategies initiated or terminated melting energy at a specific melting limit. The melting limit was determined based on which strategy of use and on each site's base case of snow load. The melting limit for strategies A, B, and D was determined when the snow load and the weight of the PV panel were equal to or higher than the 5 YRP characteristic snow load for each site.

For strategy A, melting energy is initiated with no consideration to the air temperature.

The rest of the strategies, B, C, and D only initiated melting energy if the temperature was equal to or above 0°C.

Strategy A have the melting limit when the snow load and the weight of the PV panel equal or higher than the 5 YRP characteristic snow load. Melting power of both 100 W/m<sup>2</sup> and 300 W/m<sup>2</sup> and with no consideration to the air temperature, melting was initiated even though the temperature is lower than 0°C.

Strategy B have the same melting limit and melting power as strategy A, but with temperature restrictions. Melting will only be initiated if the temperature is equal or more than 0°C.

From strategy B, the melting limit for strategy C was found. Using the maximum overload from strategy B and reducing the melting limit with the overload percentage to the 5 YRP characteristic snow load. Strategy C have temperature restrictions only melting equal to or above 0°C and with 300 W/m<sup>2</sup> melting power. There is a potential risk that the snow accumulates faster than melting can mitigate with temperature restrictions. Lowering the melting limit with the most significant continuous snowfall creates a snow load buffer.

Strategy D have the same melting limit and temperature restrictions as strategy B. The melting power in strategy D have reduced the efficiency of the power with the result from the simulations in WUFI, 85 %. For Norway, only 300 W/m<sup>2</sup> of melting power were simulated.

*Table 18. Melting strategies for simulations in ESCIMO.*

Strategy	Snow load	Temperature	Melting power
A	$S_{pv} + S \geq S_5$	N/A	100 W/m <sup>2</sup> , 300 W/m <sup>2</sup>
B	$S_{pv} + S \geq S_5$	$T \geq 0$ [C°]	100 W/m <sup>2</sup> , 300 W/m <sup>2</sup>
C	$S_{pv} + S \geq S_{\max\text{StrategyB}}$	$T \geq 0$ [C°]	300 W/m <sup>2</sup>
D	$S_{pv} + S \geq S_5$	$T \geq 0$ [C°]	300*0.85 W/m <sup>2</sup>

# 4 Results

This chapter presents the results and analysis using the methods described in chapter 3.

## 4.1 Validation

There were run four simulations in ESCIMO with various sources on the weather parameters. All results basis on that 1 kg/m2 is equal to 1 mm SWE and is used as the comparing unit. Figure 20 show the results from long-term simulation from January until the end of March 2021 if simulation number 1 to 3.

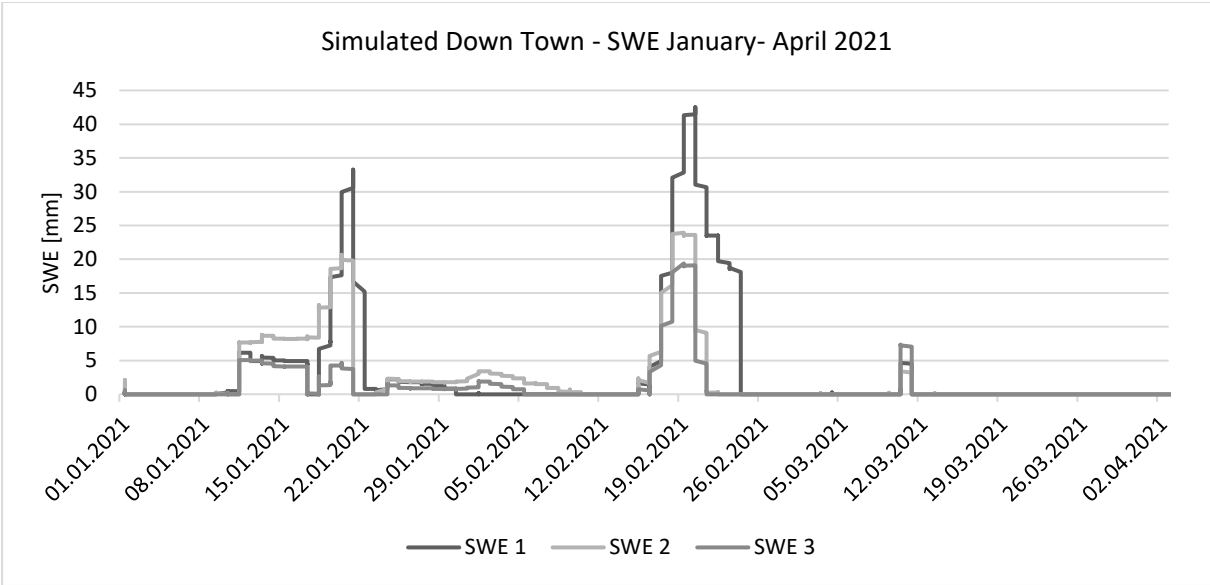


Figure 20. Base SWE for simulation number 1-3 in January-March.

The snow load result from simulation number 1 to 3 has a significantly lower value than the registered snow load at Down Town. It shows a slight increase in the snow in the period 10-12<sup>th</sup> of March, but far from the same amount. On another note, the different simulation has the same trends for snow accumulation but with different amounts.

As the figure 21 show, with the base SWE results from simulation 1-3, the simulation shows a significantly lower value of SWE on 10<sup>th</sup> to 12<sup>th</sup> of March than the registered SWE at Down Town. Simulation 1 to 3 are all under 7 mm SWE, while Down Town registered SWE from the range of 50 mm to 80 mm.

For simulation 4, only 9<sup>th</sup> to 15<sup>th</sup> of March was simulated. As the load peaks right above 50 SWE, two of the registered snow loads at Down Town with a similar maximum snow load was inserted in this chart for comparison. The base SWE is the simulated snow load without any added heat to the energy balance. It stabilizes and holds steady after a small decrease after the peak. The purple and blue dotted lines are the two registered snow loads. The simulation with added heat has a similar shape with only minor differences. The simulation with the reduced efficiency on the panels to 85 % and temperature condition, has a similar shape at the end before the SWE goes to zero after melting. Snow load 4 Down Town has an increase late at 12<sup>th</sup> of March, which none of the simulated or the Snow load 2 Down Town does.

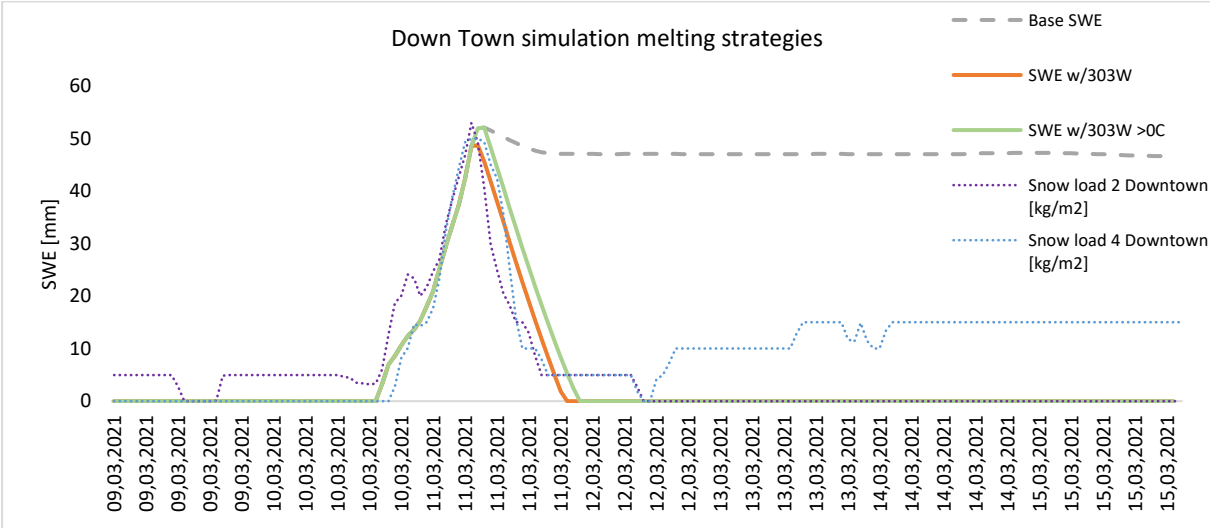


Figure 21. Simulation 4 - Compared to the registered snow load at Down Town. Base SWE, strategy A SWE and strategy B SWE.

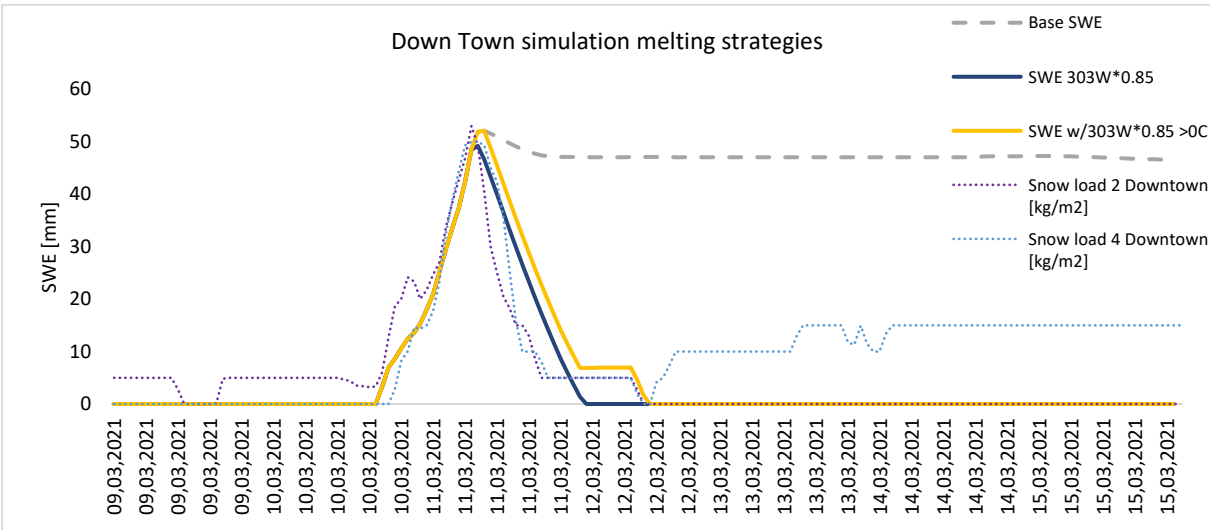


Figure 22. Simulation 4 - Compared to the registered snow load at Down Town. Base SWE, strategy D SWE.



## 4.2 Efficiency

The output in WUFI was hourly data of the heat flux distribution in the construction. In table 19, the percentage of heat flux that transported up in the snow layer is listed. Calculation of the efficiency was found by dividing the fraction of heat flux that moves up in the snowpack by the total amount of heat.

*Table 19. Percentage of the heat flux transportation from the PV panel and up in the snow layer.*

Efficiency of the heat flux from the PV panels in heating mode				
Snow depth	Set 1	Set 2	Set 3	Set 4
10 mm	52%	85%	99%	98%
50 mm	18%	49%	90%	89%
100 mm	10%	32%	80%	79%

This simulation aimed to find a general efficiency that could be applied to estimate the energy demand in melting scenarios. The increase in thickness of the snow layer decreases the percentage of heat flux moving upwards. Set 3 and 4 have excellent efficiency with the minimum snow depth. This indicates that if there is a warm indoor climate on the inside of the roof, the heat flux from the roof will increase the efficiency of the PV system. Set 3 and 4 will not be used further in this thesis as there are no assumptions of other heat sources than from the PV heating system.

None of the simulation sets above include the possible effect of air changes in the air layer. Set 2 was simulated with 10, 100 and 1000 air changes per hour. The efficiency of the PV panel decreases with the increase of air changes.

*Table 20. Efficiency of the heat flux from PV panels with air change in the air layer. Percentage of the heat flux moving up into the snow layer.*

Efficiency with air exchange			
Air change	10 /h	100 /h	1000 /h
Set 2 - 10mm	82 %	81 %	69 %

In a scenario with a 10 m long “tunnel” of PV panel, with a wind of 1 m/s wind. The air under the tunnel will have completely changed in 10 seconds. And by an hour there will be 360 air changes per hour.

As this is a general simulation and for no specific scenario, the result of 85 % efficiency will be used further for simulation of the snowpack in strategy D.

All sites have different limits of snow load for when melting is initiated in the simulations in ESCIMO. Therefore, the result with the least snow depth of 10mm for set 2, will be used further in the following snowpack simulation.

### 4.3 Extreme value analysis of snow load

By extracting the yearly maximum value of SWE on the base case for all years simulated, the 5- and 50- YRP was found, using lognormal distribution. This distribution was used on all sites. Figure 23 show the 5 YRP (20% of the lognormal) for Tromsø, charts for all sites and each strategy are in the appendix part A2.

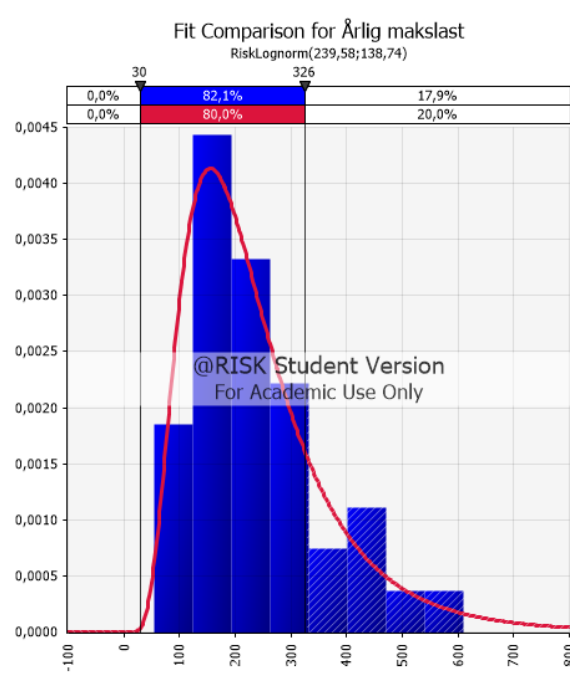


Figure 23. Log-normal distribution of the 5-year return period in Tromsø.

From the 5 YRP, or the characteristic five-year snow load, the PV share of load capacity was calculated. The weight of a PV panel is determined to be 20 kg/m<sup>2</sup> in this thesis and the percentage of PV load on the S5 was calculated. Selection of the melting limits for the respectively location is determined from the characteristic five-year snow load, S5, and subtracting the PV load. This was used on all strategies, except strategy C which were determined based on the results in strategy B. Table 21 shows the characteristic 5-YRP of snow load, the PV share of load capacity, the characteristic 50- YRP snow load and average temperatures in January and the Winter season (from December until March). The mean

average temperatures were calculated from the weather parameters from ERA5 on all years simulated.

*Table 21. Results from simulation of 5- and 50 YRP characteristic snow load, share load capacity and average temperature for winter season and January.*

Site	S <sub>5</sub> [kN/m <sup>2</sup> ]	PV share of load capacity [%]	S <sub>50</sub> [kN/m <sup>2</sup> ]	T <sub>JanuaryAverage</sub> [C°]	T <sub>WinterAverage</sub> [C°]
Tromsø	3.26	6	6.25	-7.8	-6.4
Oslo	1.35	15	3.91	-4.7	-3.0
Bergen	0.32	63	0.73	1.7	2.2
Copenhagen	0.15	135	0.51	0.9	1.8
Cortina d'Ampezzo	4.44	5	8.39	-7.1	-5.0
Grenoble	2.07	10	5.26	-1.1	0.7

## 4.4 Snow load simulation – long term

This chapter covers yearly maximum snow load, expressed as SWE, annual energy demand, and the percentage of annual overload on the selected sites. The results from the strategies are presented graphicly for each location. Presentation of the yearly maximum snow load with all strategies is shown in charts, where the "base" SWE and the specific melting limit is marked with dotted lines. The energy used in melting and the calculation of overload, defined as roof load exceeding 5 YRP where the roof load is the snow load plus the load of the PV panel, is presented in the same charts. For the energy demand and overload results, only the years where melting occurs are shown. Energy demand and overload results on strategies A and B are shown on the same chart for easy comparison. Strategy D has the same conditions as strategy B, 300 W/m<sup>2</sup> and air temperature above 0°C to melt, but with an added efficiency of 85 % on the panels' power, due to heat flux and loss of energy.

### 4.4.1 Results

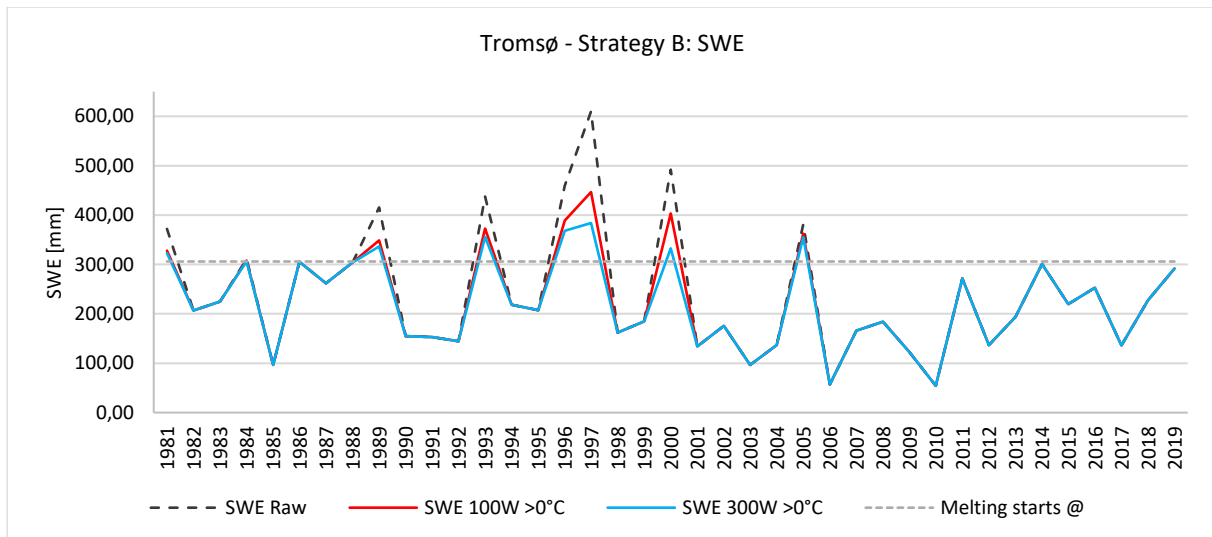
For strategy A, B and D, the melting limit is calculated from table 22 with the subtraction of the PV system load. The melting limit for strategy C are based on the year with the highest percentage overload from strategy B with melting energy 300 W/m<sup>2</sup>.

Table 22. SWE limits for when melting, heat, was initiated in the snowpack model

Site	Melting limits	
	SWE Strategy A, B, D [mm]	SWE Strategy C [mm]
Tromsø	306	233
Oslo	115	70
Bergen	012	3
Copenhagen	0.1	-
Cortina d'Ampezzo	424	377
Grenoble	187	99

## Tromsø

The most northern located site is Tromsø. The share load capacity used for the PV panels is 6 %.

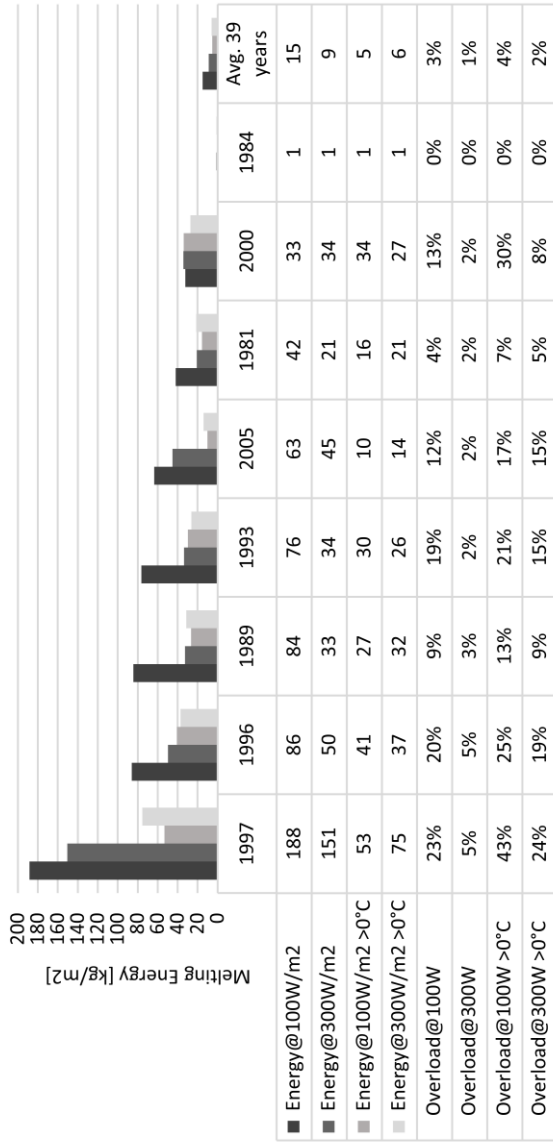


Melting occurred in 8 of 39 years. The energy demand and overload for strategy A, where there are no temperature criteria for melting, show that melting with  $100 \text{ W/m}^2$  requires more energy than melting with  $300 \text{ W/m}^2$ . Melting with  $300 \text{ W/m}^2$  (strategy A) gives the lowest degree of overload in all years but requires a fair amount of energy compared to strategy B. The lowest energy demand and overload combined is strategy B with  $300 \text{ W/m}^2$ .

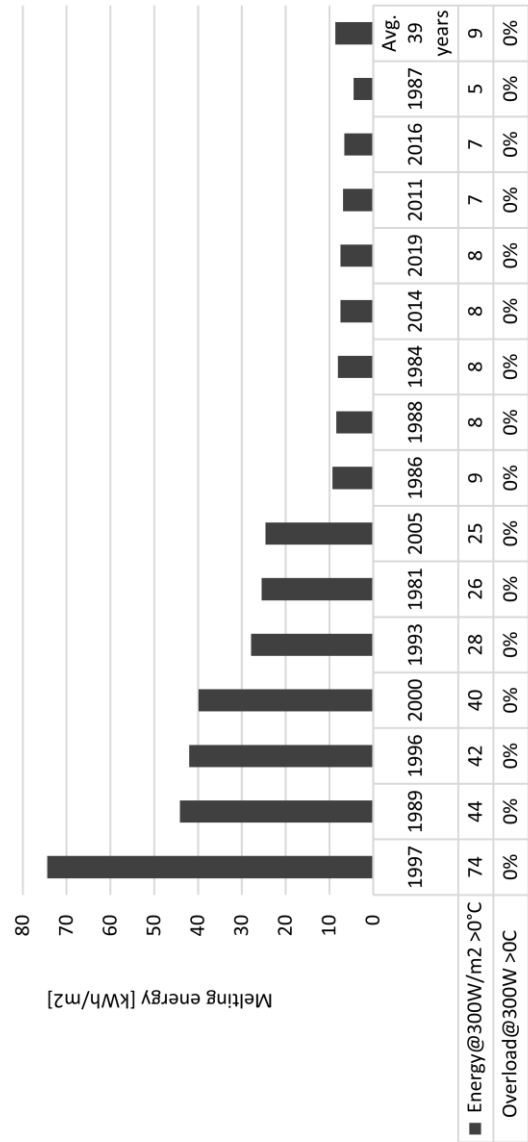
The melting limit for strategy C was determined using the maximum overload from strategy B, 24 %. The results show that strategy C gives 15 years with melting and zero years with overload. In 1997, the energy demand was  $74 \text{ W/m}^2$  and zero overload, whereas strategy B had  $75 \text{ kW/m}^2$  and 24% overload. However, the average energy demand of 39 years is higher. The average energy demand for strategy C was  $9 \text{ kWh/m}^2$  and  $6 \text{ kWh/m}^2$  for strategy B, with temperature restrictions in both strategies.

Both the energy demand and overload were higher in strategy D, than in strategy B. In 1997, the energy demand with strategy B was  $75 \text{ kWh/m}^2$ , whereas strategy D has  $90 \text{ kWh/m}^2$ . The overload in the same year is 24 % in strategy B and 27% in strategy D. They have the same number of years with melting.

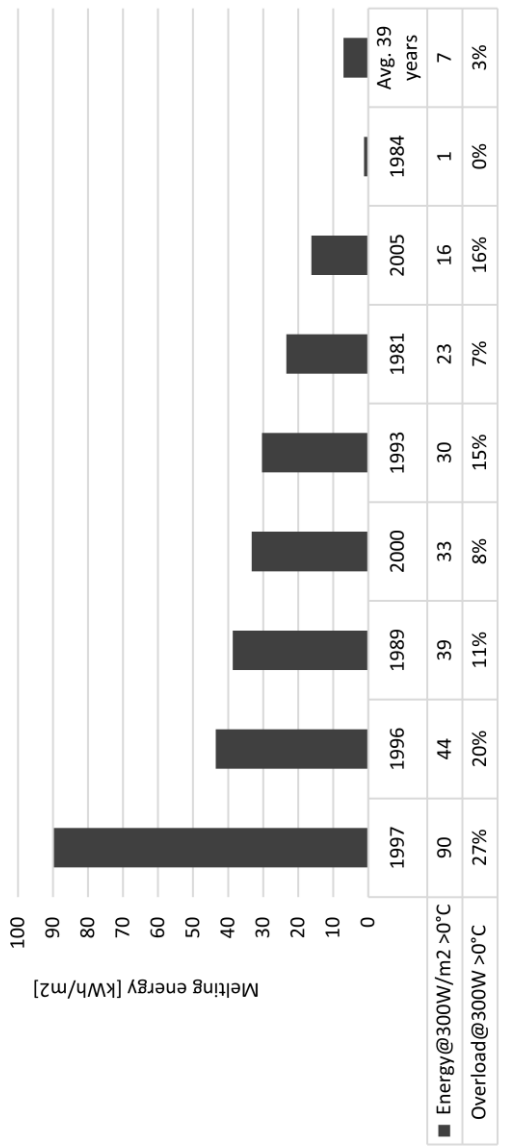
Tromsø - Strategy A + B: Energy demand and overload



Tromsø - Strategy C: Energy demand and overload



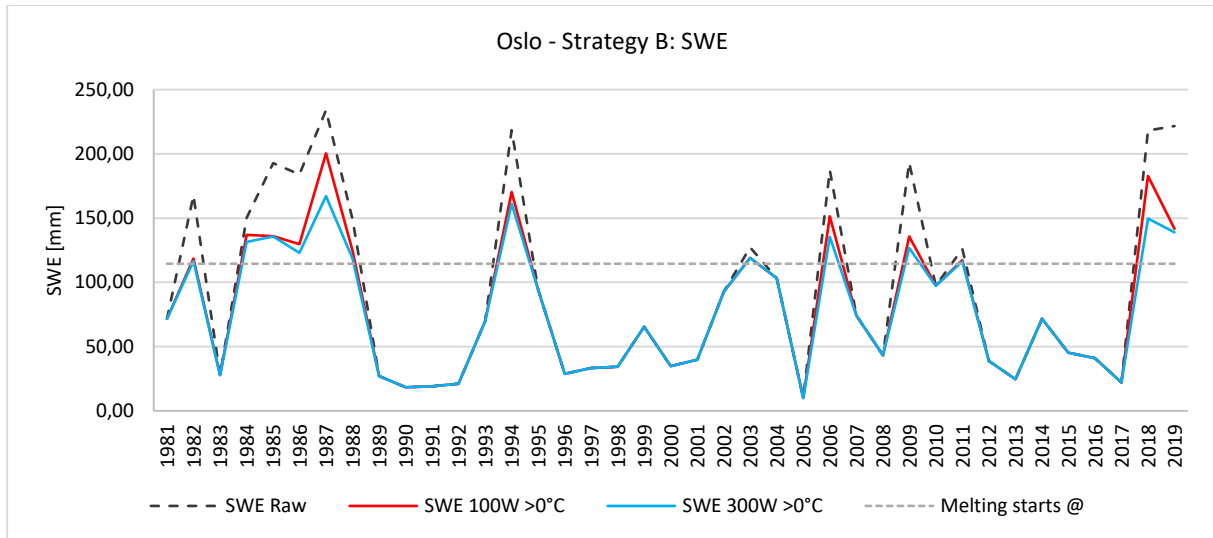
Tromsø - Strategy D: Energy demand and overload





## Oslo

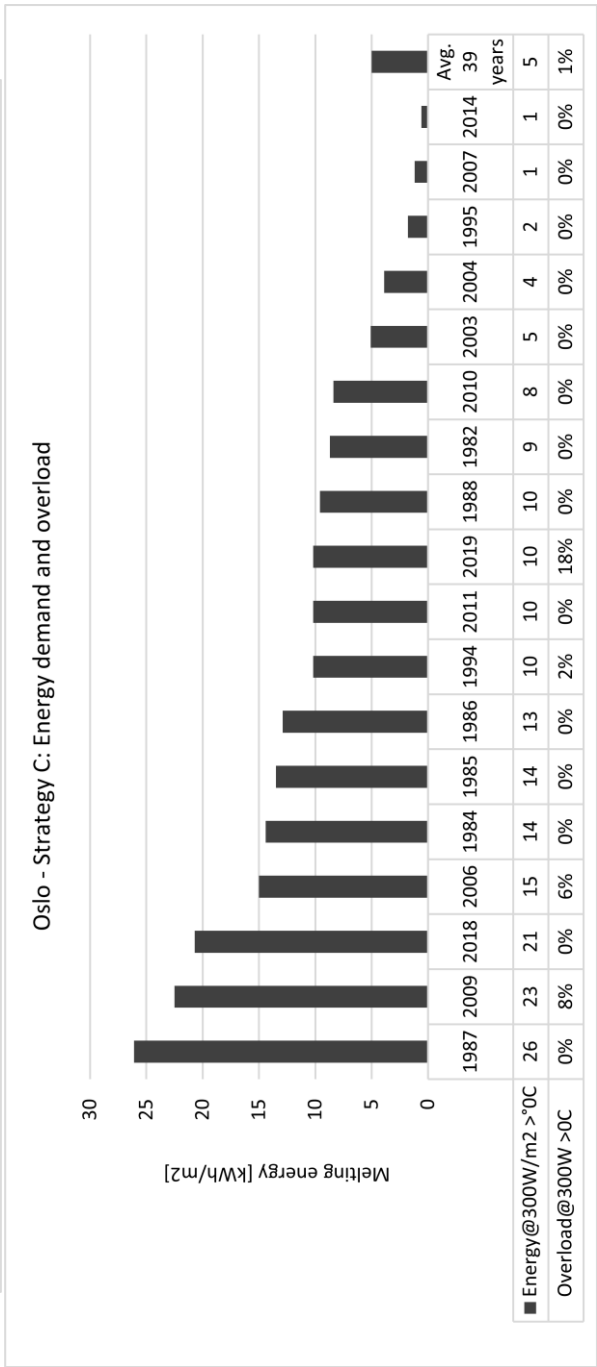
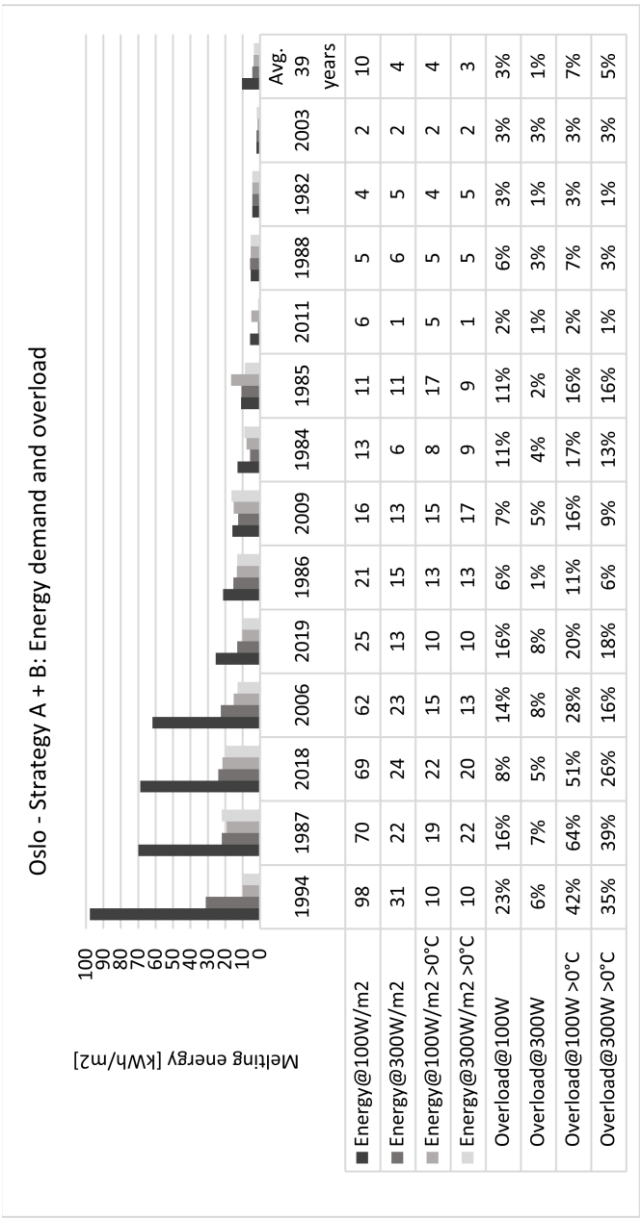
With a continental climate, Oslo has relatively cold winters. The share load capacity for the PV panels is 15 %.



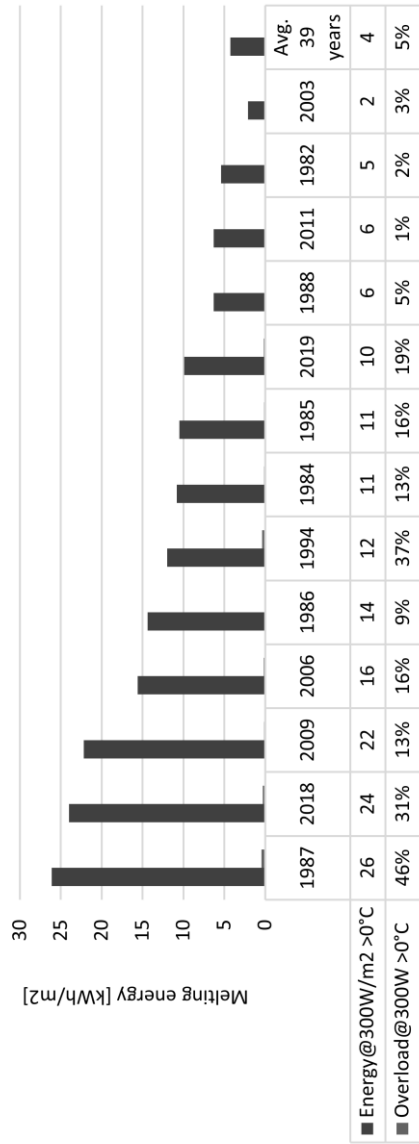
The results show 13 of 39 years with overload. Melting with  $100 \text{ W/m}^2$  in strategy A required more than doubled energy than the other strategies. The strategy with the least overload is strategy A with  $300 \text{ W/m}^2$ . In strategy B, melting with  $300 \text{ W/m}^2$  has the lowest energy demand and overload. In 1987, strategies A and B with  $300 \text{ W/m}^2$  used  $22 \text{ kWh/m}^2$ , but strategy A had 7 % overload, whereas strategy B had 39 % overload.

The melting limit for strategy C was found from the maximum overload of 39 % from strategy B. Resulting in 18 years with melting and 4 years with overload. The energy demand is higher with strategy B, but the overload was lower. In 1987, strategy B had  $22 \text{ kWh/m}^2$  and an overload of 39%, but strategy C had  $26 \text{ kWh/m}^2$  and 0% overload. The average overload on 39 years is 1%.

With a reduced efficiency of 85 %, strategy D shows an average overload of 5%, same as strategy B. The average energy is  $4 \text{ kWh/m}^2$ , where strategy B has  $3 \text{ kWh/m}^2$ .

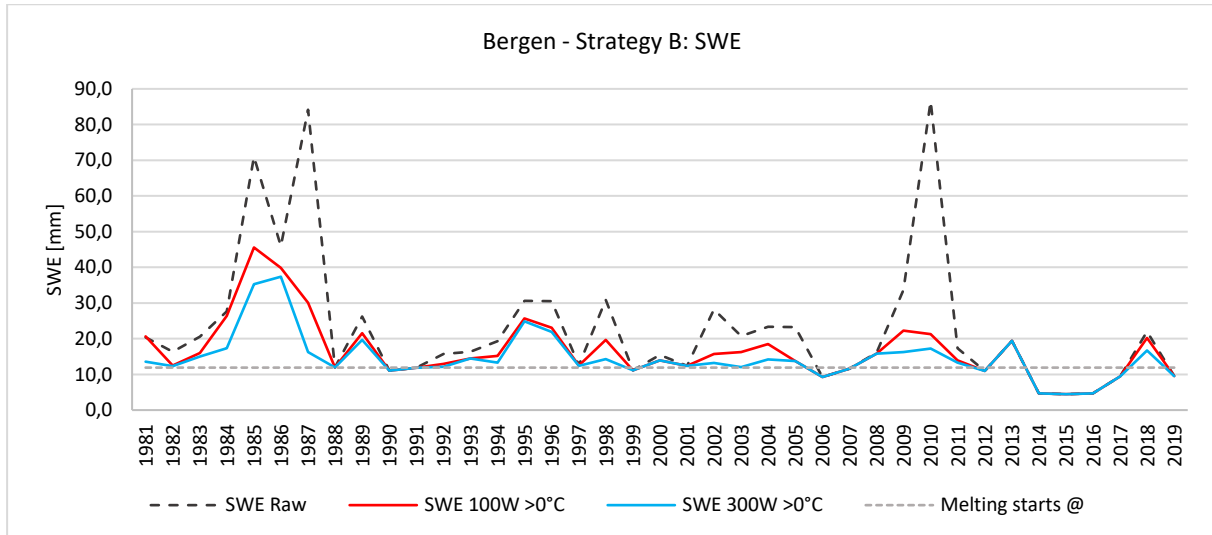


Oslo - Strategy D: Energy demand and overload



## Bergen

The climate in Bergen is defined as temperate with no dry season and warm summers and has considerably higher average temperatures in the winter season. The share load capacity for the PV panels is 63%.



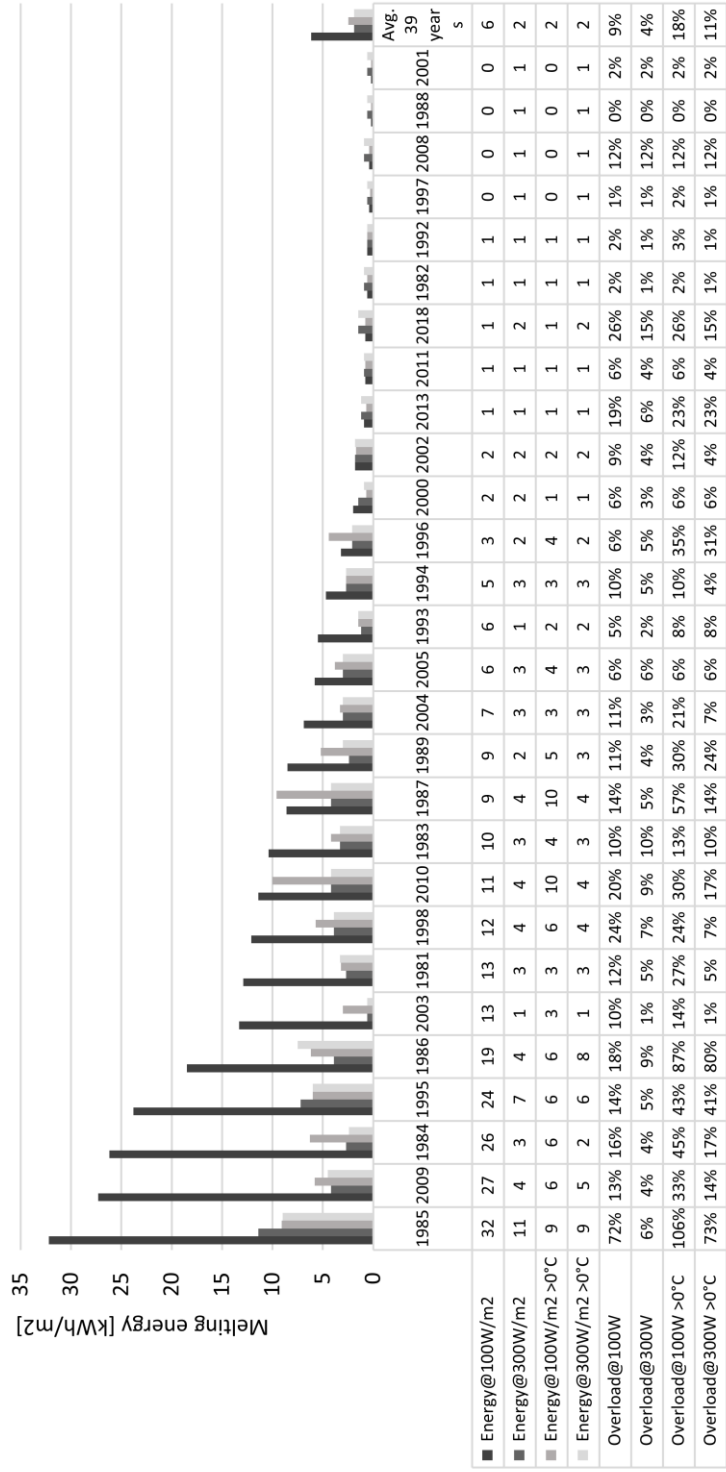
The simulations show that melting is needed in 28 of 39 years. A fair number of years needs a low amount of energy but has a high overload percentage. The melting limit is considerably lower than other sites, resulting in the snow load quickly reaching the maximum capacity limit. Melting energy were below 5 kWh/m<sup>2</sup> for 13 years.

The average energy demand is the same in strategy B for both cases, but the overload is higher for 100 W/m<sup>2</sup> with an average of 18% compared to 11% using 300 W/m<sup>2</sup>.

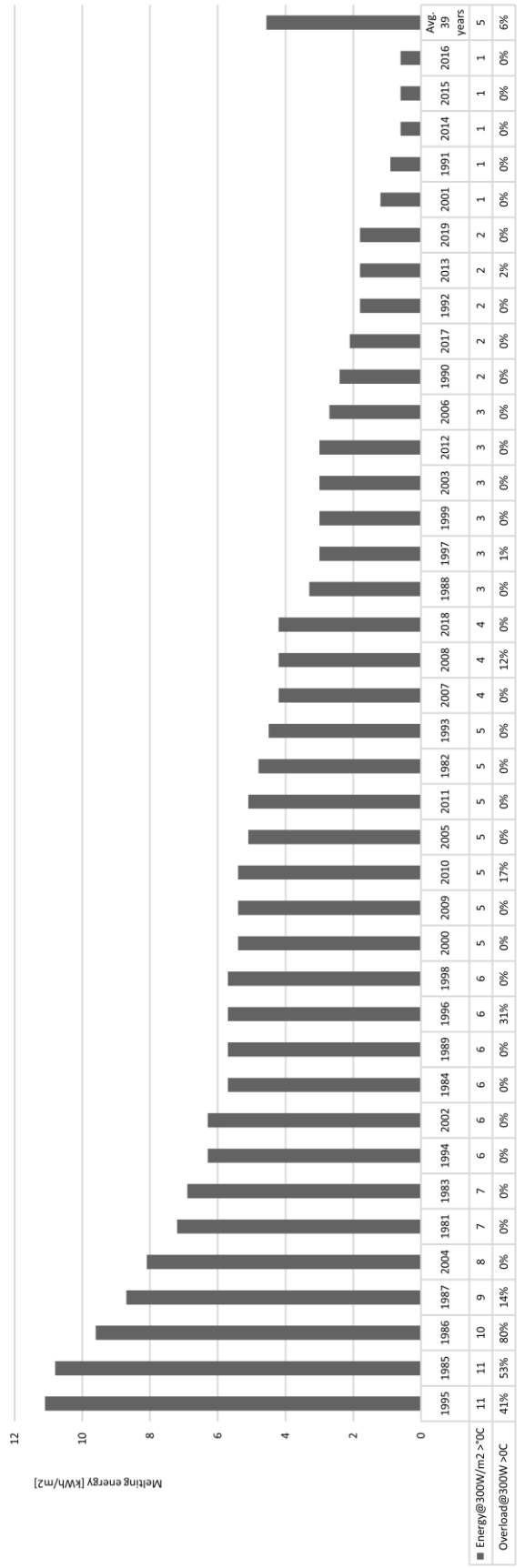
For strategy C, with a new melting limit considering 73% overload from strategy B, the overload is almost halved, and energy demand doubled compared to strategy B. A total of 39 years needs melting with this melting limit.

Results from strategy D with 85% efficiency from the PV panels show that melting was needed in 28 of 39 years. The average overload was 12% and the average energy demand was 2 kWh/m<sup>2</sup>. This is approximately equal to strategy B, with an average energy demand of 2 kWh/m<sup>2</sup> and an overload of 11%.

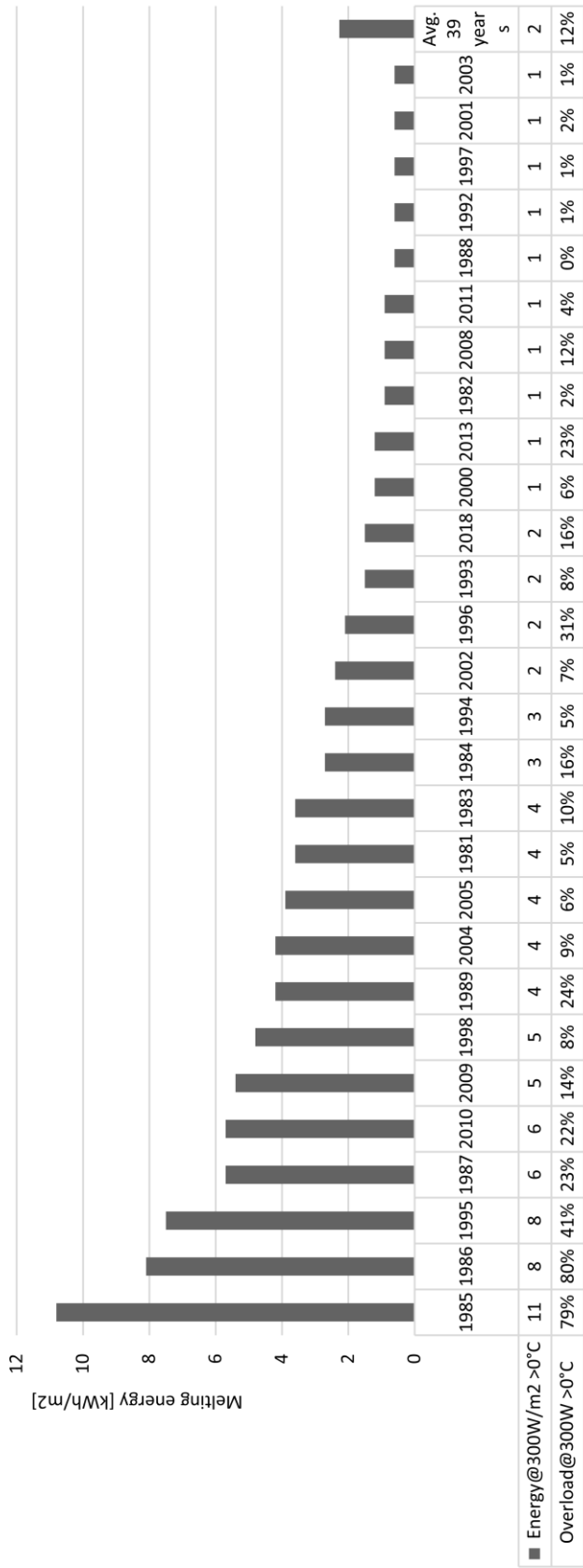
Bergen - Strategy A + B: Energy demand and overload



Bergen - Strategy C: Energy demand and overload

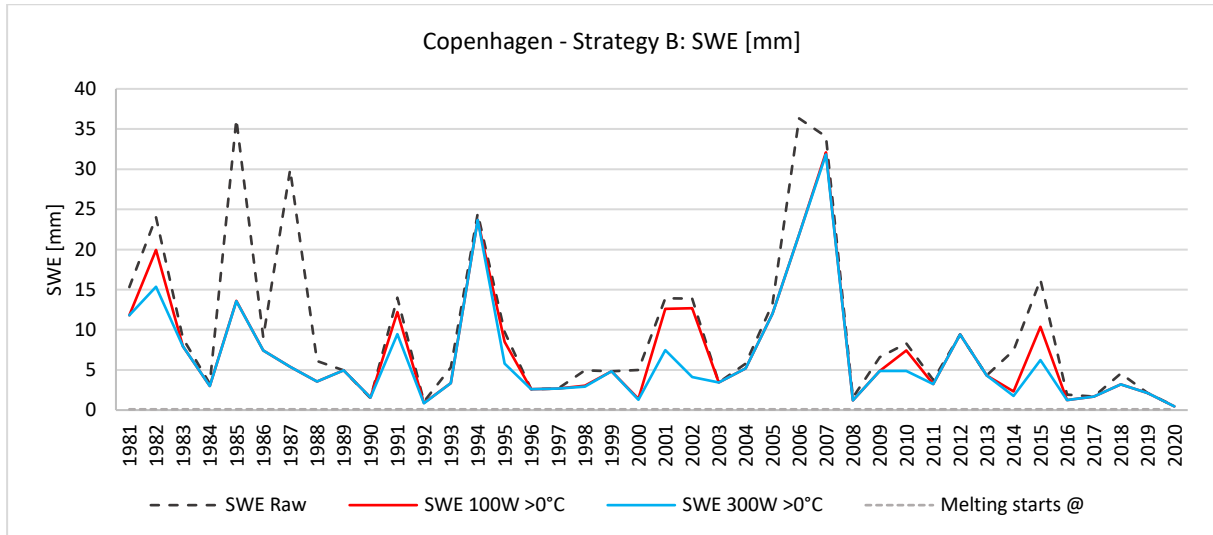


Bergen - Strategy D: Energy demand and overload



## Copenhagen

The climate in Copenhagen is similar to Bergen, located further south. The share load capacity for the PV panels is 135%, the highest percentage of all locations. Due to the low melting limit, strategy C is not relevant for this site.

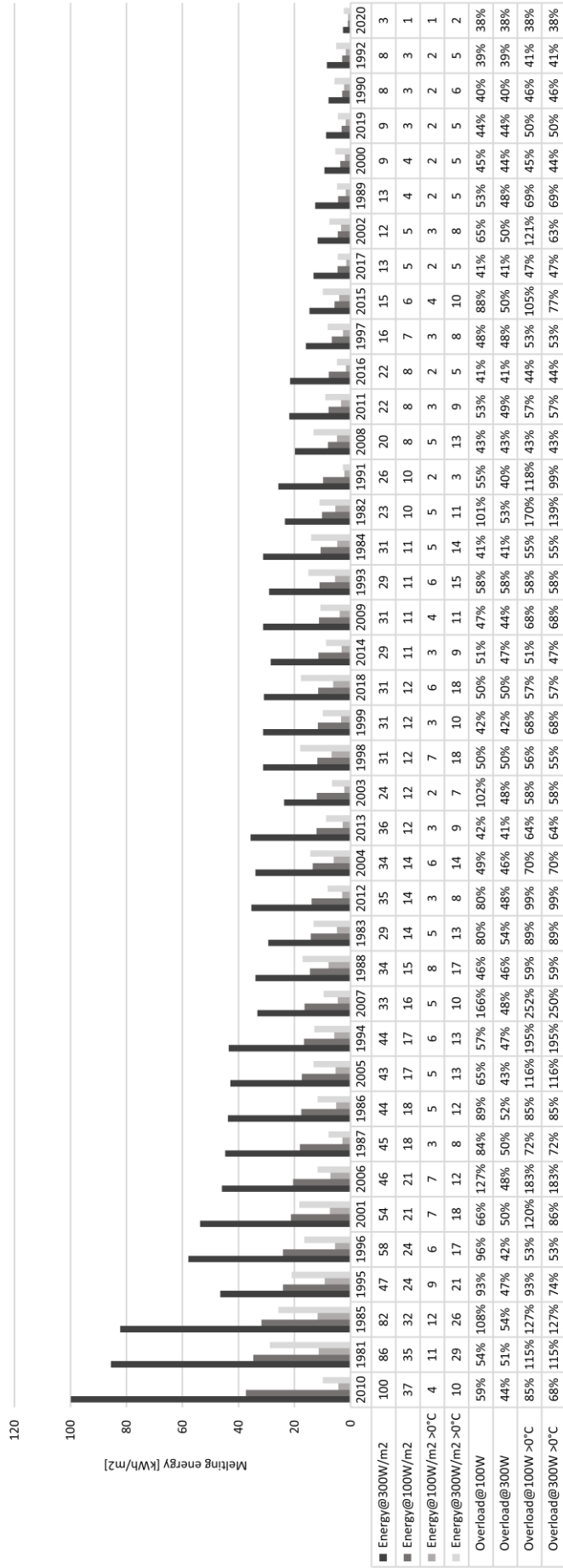


The results show melting in 39 of 39 years with melting limit at 0.1 mm SWE. Melting with 100 W/m<sup>2</sup> in Strategy A gave the highest energy demand with more than doubled melting energy compared to the other. This site reaches the melting limit instantaneous with snowfall, and all years have an overload.

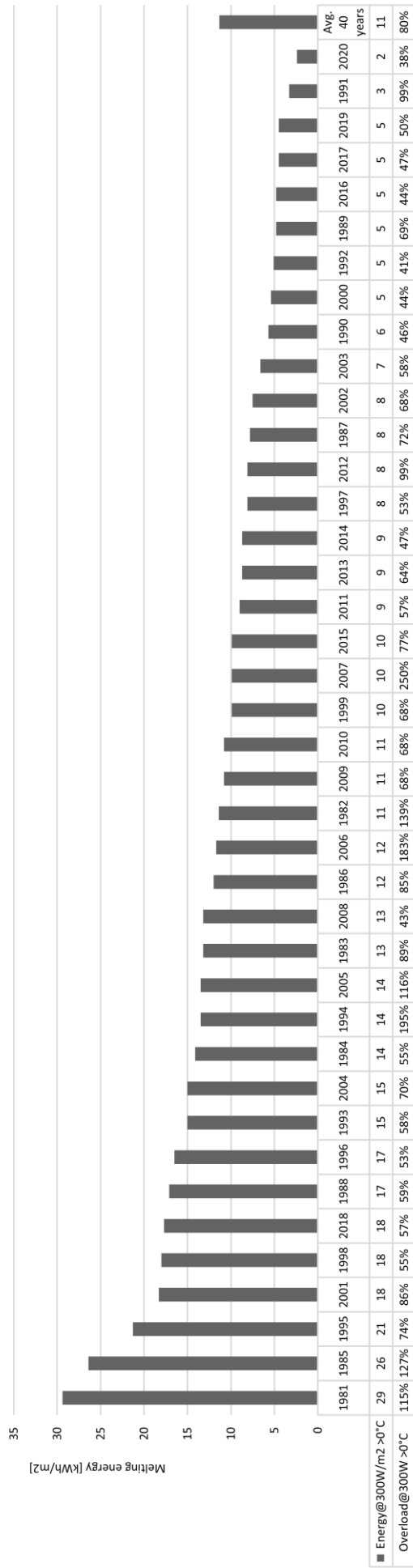
Strategy D has an average energy demand of 11 kWh/m<sup>2</sup> and an average overload of 80 %.



Copenhagen - Strategy A + B: Energy demand and overload

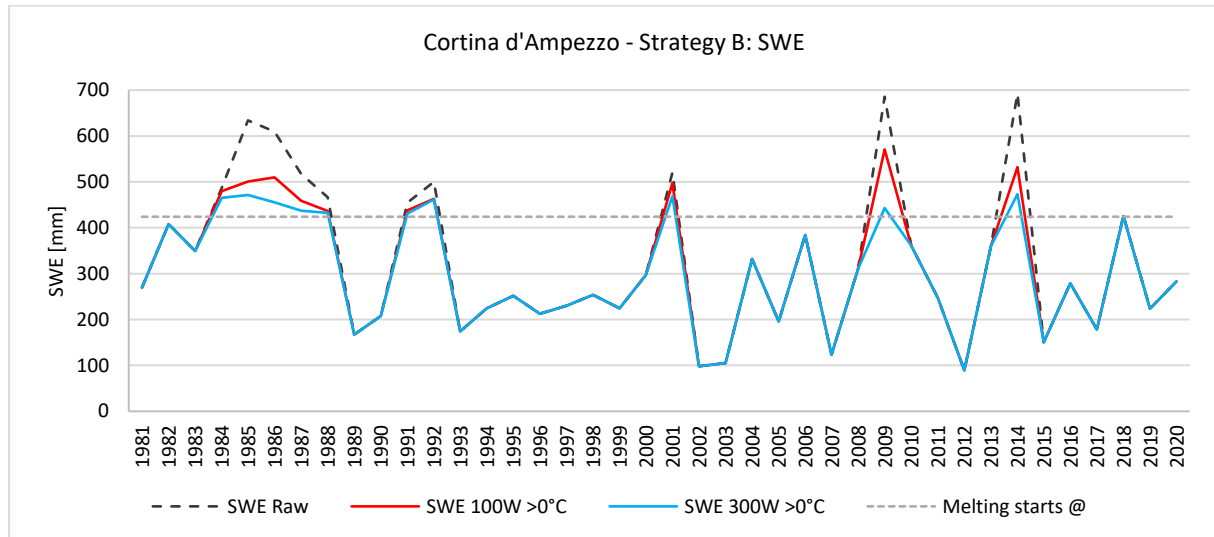


Strategy D: Energy demand and overload



## Cortina d'Ampezzo

With a location height data at 1 652 m, the site with the highest altitude is Cortina d'Ampezzo. Located more than 20 degrees further south, Cortina has similar values of average winter temperatures to Tromsø. The share load capacity for the PV panels is 5 %, the lowest share load of the sites.

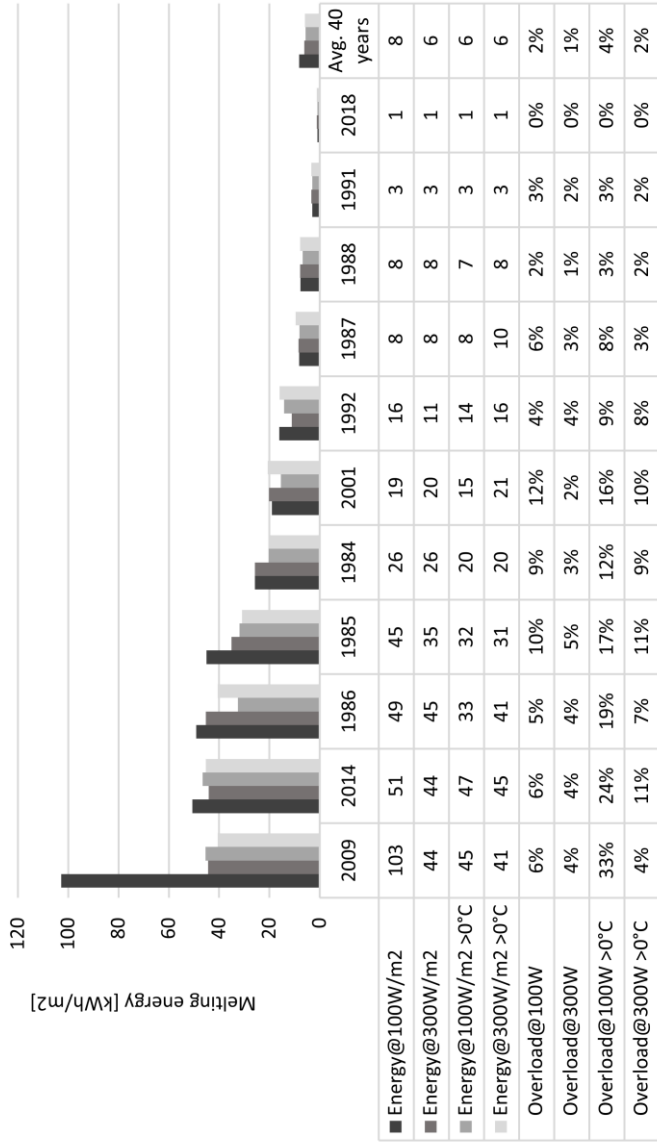


There were 11 years of melting using strategies A and B. The highest energy demand was with strategy A, using melting energy of  $100 \text{ W/m}^2$ . Except for strategy B, with  $100 \text{ W/m}^2$ , the overload with these strategies is generally low. The lowest overload is strategy A, with  $300 \text{ W/m}^2$ , resulting in an average overload of 1%. Both strategies A and B, using  $300 \text{ W/m}^2$ , have the lowest overload and energy demand on average combined. The difference is relatively low, having an air temperature above  $0^\circ\text{C}$  or not on this site.

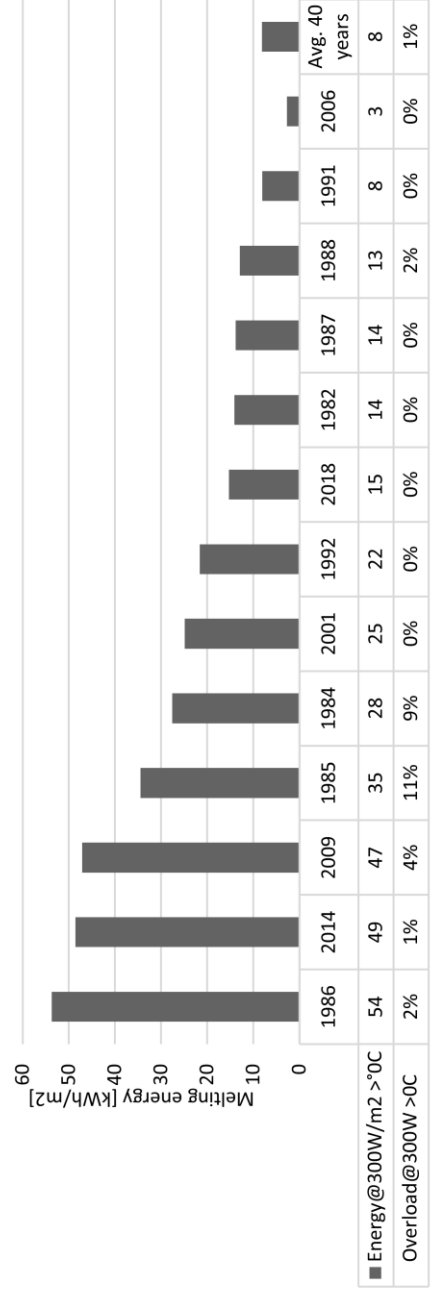
Using the maximum overload of 11% from strategy B, the new melting limit shows melting in 13 of 39 years. The average energy demand is slightly higher with  $8 \text{ kWh/m}^2$  compared to strategy B with  $6 \text{ kWh/m}^2$ . The overload is zero in 7 of the years with melting.

The results from strategy D show that 11 years need melting when changing the efficiency of the PV panels to 85%. The highest overload in 2014 was 14%, wherein strategy B was 11%. With reduced efficiency, strategy D has higher energy demand than B, with a difference of  $1 \text{ kWh/m}^2$ .

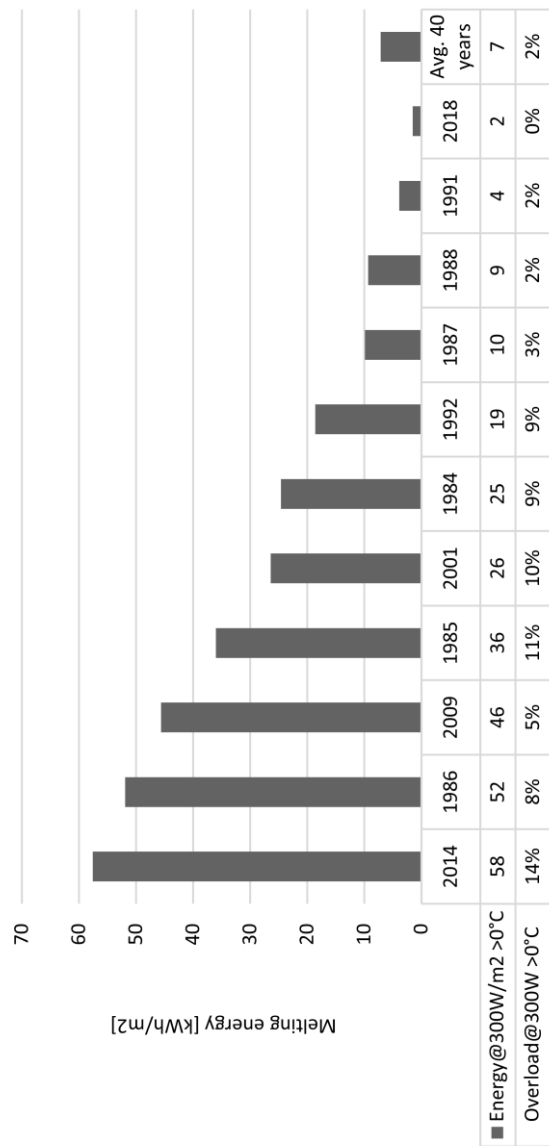
Cortina d'Ampezzo - Strategy A + B: Energy demand and overload



Cortina d'Ampezzo - Strategy C: Energy demand and overload

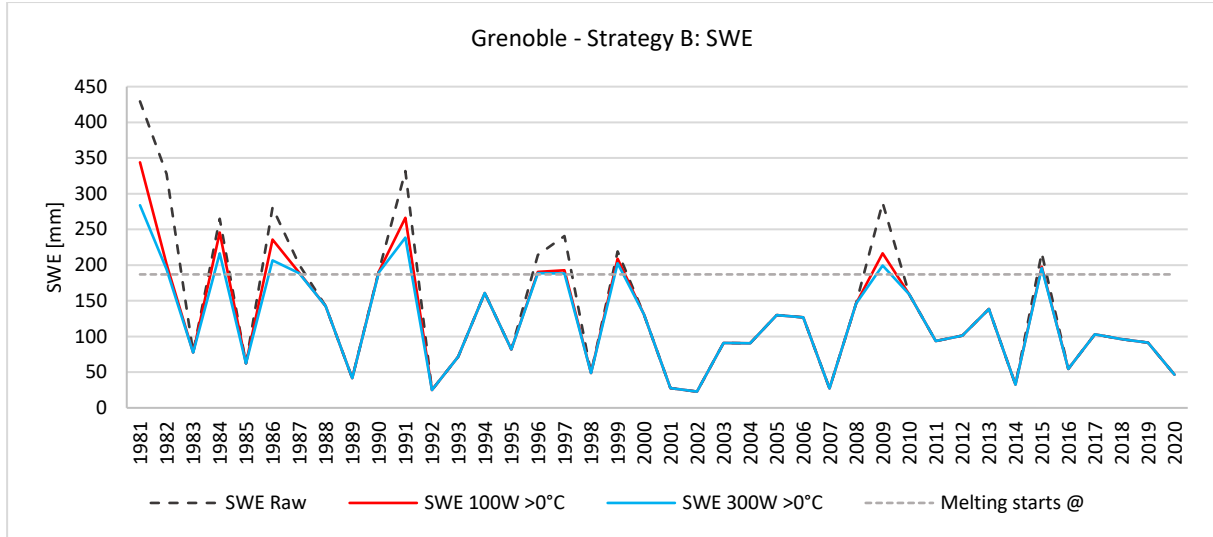


Cortina d'Ampezzo - Strategy D: Energy demand and overload



## Grenoble

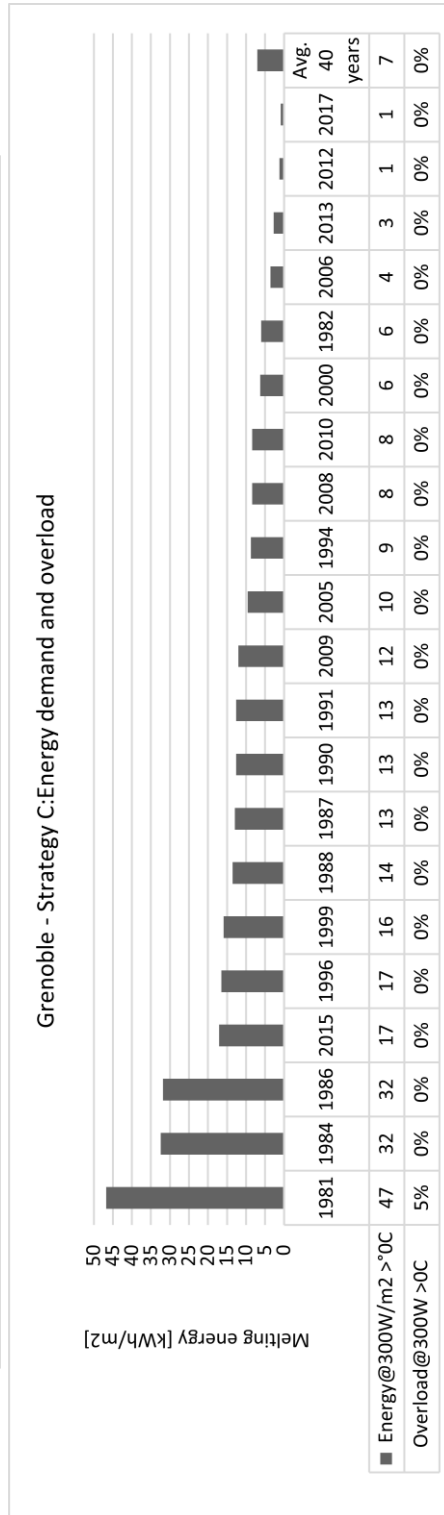
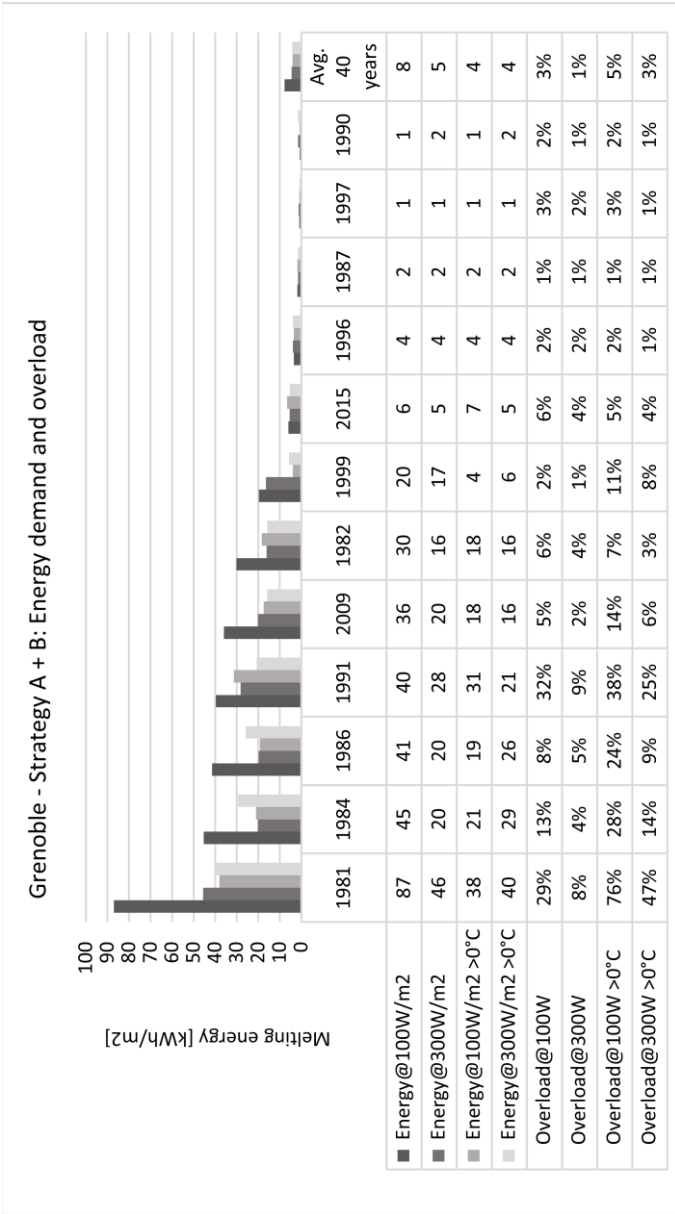
Grenoble is located at 985 m above sea level, and the average winter temperature is close to 0°C. The share load capacity of the PV panels is 10 %.

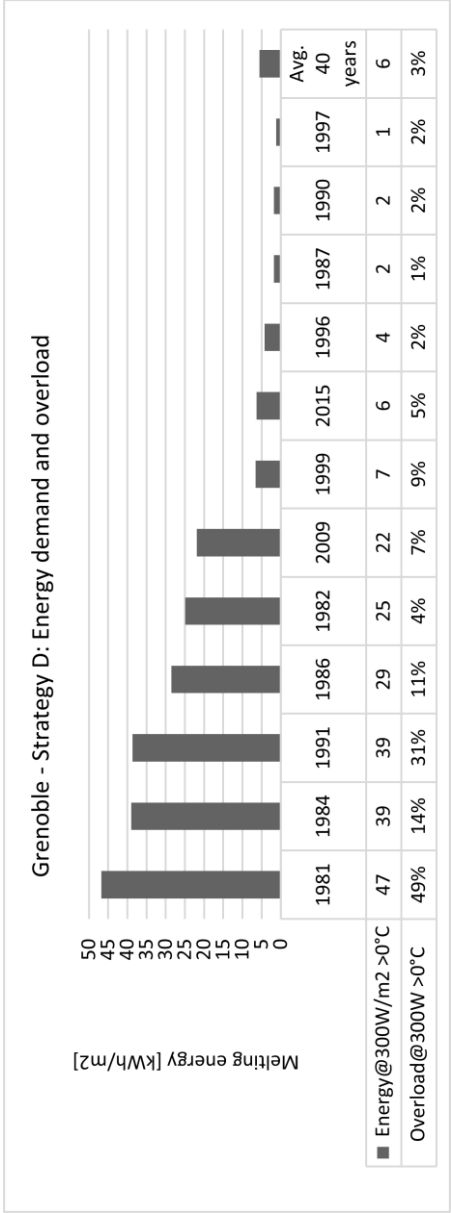


Melting occurred in 12 of 39 years. Strategy A, with 100 W/m<sup>2</sup>, is the most energy-demanding strategy on average. In 1981, strategy B, with 100 W/m<sup>2</sup>, the overload is 76% and is the highest in all years simulated. The lowest overload percentage is using strategy A, with 300 W/m<sup>2</sup>, where the maximum is 8%, and the average is 1%.

When changing the melting limit according to the maximum overload from strategy B, 25%, the results show 21 years of melting. The energy demand in 1981 was 47 kWh/m<sup>2</sup>, while strategy B had 40 kWh/m<sup>2</sup>. On 40 years average, the energy demand was kWh/m<sup>2</sup> with C, while B has 4 kWh/m<sup>2</sup>. In 1981, the maximum overload was 5%, the rest of the years with melting have zero overloads.

The results with strategy D show 12 years of melting with an efficiency of 85 % on the PV panel. The average energy demand was 6 kWh/m<sup>2</sup> and the overload was 3% for strategy D, whereas strategy B had 4 kWh/m<sup>2</sup> of average energy demand and 3% overload.







#### 4.4.2 Summary of average values

The average values on energy demand and percentage overload, depicted on the tables in chapter 4.4.1, are listed in the tables below.

*Table 23. Average energy demand and overload in Tromsø.*

Tromsø – Average Energy and Overload			
Strategy	Energy [kW/m <sup>2</sup> ]		Overload [%]
A - 100W	15		3
A - 300W	9		1
B - 100W >0°C	5		4
B - 300W >0°C	6		3
C - 300W >0°C	9		0
D - 300W >0°C	7		3

*Table 24. Average energy demand and overload in Oslo.*

Oslo – Average energy and overload			
Strategy	Energy [kW/m <sup>2</sup> ]		Overload [%]
A - 100W	10		3
A - 300W	4		1
B - 100W >0°C	4		7
B - 300W >0°C	3		5
C - 300W >0°C	5		1
D - 300W >0°C	4		5

*Table 25. Average energy demand and overload in Bergen.*

Bergen – Average energy and overload			
Strategy	Energy [kW/m <sup>2</sup> ]		Overload [%]
A - 100W	6		9
A - 300W	2		4
B - 100W >0°C	2		18
B - 300W >0°C	2		11
C - 300W >0°C	5		6
D - 300W >0°C	2		12

Table 26. Average energy demand and overload in Copenhagen.

Copenhagen – Average energy and overload		
Strategy	Energy [kW/m <sup>2</sup> ]	Overload [%]
A - 100W	33	66
A - 300W	13	47
B - 100W >0°C	5	86
B - 300W >0°C	11	80
D - 300W >0°C	11	80

Table 27. Average energy demand and overload in Cortina d'Ampezzo.

Cortina d'Ampezzo – Average energy and overload		
Strategy	Energy [kW/m <sup>2</sup> ]	Overload [%]
A - 100W	8	2
A - 300W	6	1
B - 100W >0°C	6	4
B - 300W >0°C	6	2
C - 300W >0°C	8	1
D - 300W >0°C	7	2

Table 28. Average energy demand and overload in Grenoble.

Grenoble – Average energy and overload		
Strategy	Energy [kW/m <sup>2</sup> ]	Overload [%]
A - 100W	8	3
A - 300W	5	1
B - 100W >0°C	4	5
B - 300W >0°C	4	3
C - 300W >0°C	7	0
D - 300W >0°C	6	3

### 4.4.3 Extreme values analysis of the snow load

All yearly maximum snow loads coming out of the different strategies on each site, were fitted to a lognormal distribution to compare with the base case results.

The results from the extreme value analysis of the Tromsø simulations are listed in table 29. Strategy C has the highest percentage of reduction on the characteristic snow loads, while strategy B with 300 W/m<sup>2</sup> has the lowest. Strategy B and D, both with 300 W/m<sup>2</sup>, have the same reduction percentage.

*Table 29. Results from extreme value analysis of Tromsø. Lognormal distribution with 5 YRP and 50 YRP based on yearly maximum snow load.*

Tromsø - Extreme value analysis		
Strategy	S <sub>5</sub> [kN/m <sup>2</sup> ]	S <sub>50</sub> [kN/m <sup>2</sup> ]
Base	3,26	6,26
A - 100W	2,97 (- 9 %)	5,29 (- 15 %)
A - 300W	2,85 (- 13 %)	4,95 (- 21 %)
B - 100W >0C	3,05 (- 6 %)	5,54 (- 12 %)
B - 300W >0C	2,96 (- 9 %)	5,27 (- 15 %)
C - 300W >0C	2,66 (- 18 %)	4,41 (- 30 %)
D - 300W >0C	2,97 (- 9 %)	5,30 (- 15 %)

Table 30 lists the results from the extreme value analysis of the Oslo strategies. Strategy C represents the highest percentage of reduction on the characteristic snow loads, while strategy B with 300 W/m<sup>2</sup> has the lowest reduction. Strategy B and D, with 300 W/m<sup>2</sup>, have the same percentage of reduction for S<sub>5</sub> and a difference of 2 % for S<sub>50</sub>.

*Table 30. Results from extreme value analysis of Oslo. Lognormal distribution with 5 YRP and 50 YRP based on yearly maximum snow load.*

Oslo - Extreme value analysis		
Strategy	S <sub>5</sub> [kN/m <sup>2</sup> ]	S <sub>50</sub> [kN/m <sup>2</sup> ]
Base	1,35	3,91
A - 100W	1,10 (- 19 %)	2,65 (- 32 %)
A - 300W	1,06 (- 21 %)	2,49 (- 36 %)
B - 100W >0°C	1,18 (- 13 %)	2,99 (- 24 %)
B - 300W >0°C	1,13 (- 16 %)	2,78 (- 29 %)
C - 300W >0°C	0,97 (- 28 %)	2,16 (- 45 %)
D - 300W >0°C	1,14 (- 16 %)	2,84 (- 27 %)

Table 31 lists the results from the extreme value analysis of the Bergen simulations. Here, the highest percentage of reduction on the characteristic snow loads comes from strategy A for S<sub>50</sub> and strategy C for S<sub>5</sub>. Strategy B and D, with 300 W/m<sup>2</sup>, have the same percentage of reduction for S<sub>5</sub> and a difference of 1 % for S<sub>50</sub>.

*Table 31. Results from extreme value analysis of Bergen. Lognormal distribution with 5 YRP and 50 YRP based on yearly maximum snow load.*

Bergen - Extreme value analysis		
Strategy	S <sub>5</sub> [kN/m <sup>2</sup> ]	S <sub>50</sub> [kN/m <sup>2</sup> ]
Base	0,32	0,73
A - 100W	0,18 (- 44 %)	0,29 (- 60 %)
A - 300W	0,15 (- 53 %)	0,22 (- 70 %)
B - 100W >0°C	0,23 (- 28 %)	0,41 (- 44%)
B - 300W >0°C	0,19 (- 41 %)	0,32 (- 56 %)
C - 300W >0°C	0,14 (- 56 %)	0,27 (- 63 %)
D - 300W >0C	0,19 (- 41 %)	0,33 (- 55 %)

The results from the extreme value analysis of the Copenhagen simulations are listed in table 32. The highest percentage of reduction on the characteristic snow loads is strategy A, with 300 W/m<sup>2</sup>. Strategy B and D, with 300 W/m<sup>2</sup>, have the same reduction percentage.

*Table 32. Results from extreme value analysis of Copenhagen. Lognormal distribution with 5 YRP and 50 YRP based on yearly maximum snow load.*

Copenhagen - Extreme value analysis		
Strategy	S <sub>5</sub> [kN/m <sup>2</sup> ]	S <sub>50</sub> [kN/m <sup>2</sup> ]
Base	0,15	0,51
A - 100W	0,06 (- 60 %)	0,20 (- 61 %)
A - 300W	0,02 (- 87 %)	0,04 (- 92 %)
B - 100W >0°C	0,11 (- 27 %)	0,35 (- 31 %)
B - 300W >0°C	0,09 (- 40 %)	0,29 (- 43 %)
D - 300W >0°C	0,09 (- 40 %)	0,29 (- 43 %)

Table 33 shows the extreme value analysis results of Cortina d'Ampezzo. The highest percentage of reduction on the characteristic snow loads is strategy C, while strategy B with 100 W/m<sup>2</sup> has the lowest reduction. Strategy B and D, with 300 W/m<sup>2</sup>, have the same percentage of reduction.

*Table 33. Results from extreme value analysis of Cortina d'Ampezzo. Lognormal distribution with 5 YRP and 50 YRP based on yearly maximum snow load.*

Cortina d'Ampezzo - Extreme value analysis		
Strategy	S <sub>5</sub> [kN/m <sup>2</sup> ]	S <sub>50</sub> [kN/m <sup>2</sup> ]
Base	4,44	8,39
A - 100W	4,00 (- 10 %)	7,00 (- 17 %)
A - 300W	3,94 (- 11 %)	6,82 (- 19 %)
B - 100W >0°C	4,16 (- 6 %)	7,48 (- 11 %)
B - 300W >0°C	4,01 (- 10 %)	7,03 (- 16 %)
C - 300W >0°C	3,90 (- 12 %)	6,70 (- 20 %)
D - 300W >0°C	4,02 (- 10 %)	7,05 (- 16 %)

Table 34 lists the results on the extreme value analysis from Grenoble. Strategy C gives the highest percentage of reduction on the characteristic snow loads, while strategy B with 100 W/m<sup>2</sup> has the lowest reduction. Strategy B and D, with 300 W/m<sup>2</sup>, have the same percentage of reduction for S<sub>5</sub> and a difference of 1 % for S<sub>50</sub>.

*Table 34. Results from extreme value analysis of Grenoble. Lognormal distribution with 5 YRP and 50 YRP based on yearly maximum snow load.*

Grenoble - Extreme value analysis		
Strategy	S <sub>5</sub> [kN/m <sup>2</sup> ]	S <sub>50</sub> [kN/m <sup>2</sup> ]
Base	2,07	5,26
A - 100W	1,79 (- 14 %)	4,10 (- 22%)
A - 300W	1,73 (- 16 %)	3,89 (- 27 %)
B - 100W >0°C	1,87 (- 10 %)	4,42 (- 16 %)
B - 300W >0°C	1,80 (- 13 %)	4,13 (- 22 %)
C - 300W >0°C	1,31 (- 37 %)	2,51 (- 52 %)
D - 300W >0°C	1,81 (- 13 %)	4,18 (- 21 %)

## 4.5 Snow load simulation - yearly

This chapter show the hourly results for the snow water equivalent (SWE) and melt rates from a one-year simulation on all sites. The selected year was the year with the highest percentage overload from strategy B, with  $300 \text{ W/m}^2$ .

### Tromsø 1996-1997

In both strategy A and B, melting with  $100 \text{ W/m}^2$  does not contribute as good as  $300 \text{ W/m}^2$  to the reduction of the SWE. The melting limit is reached much earlier by melting with  $300 \text{ W/m}^2$ . Comparing strategy D, with strategy B, with  $300 \text{ W/m}^2$ , shows only a small difference, where strategy D has slightly higher SWE values.

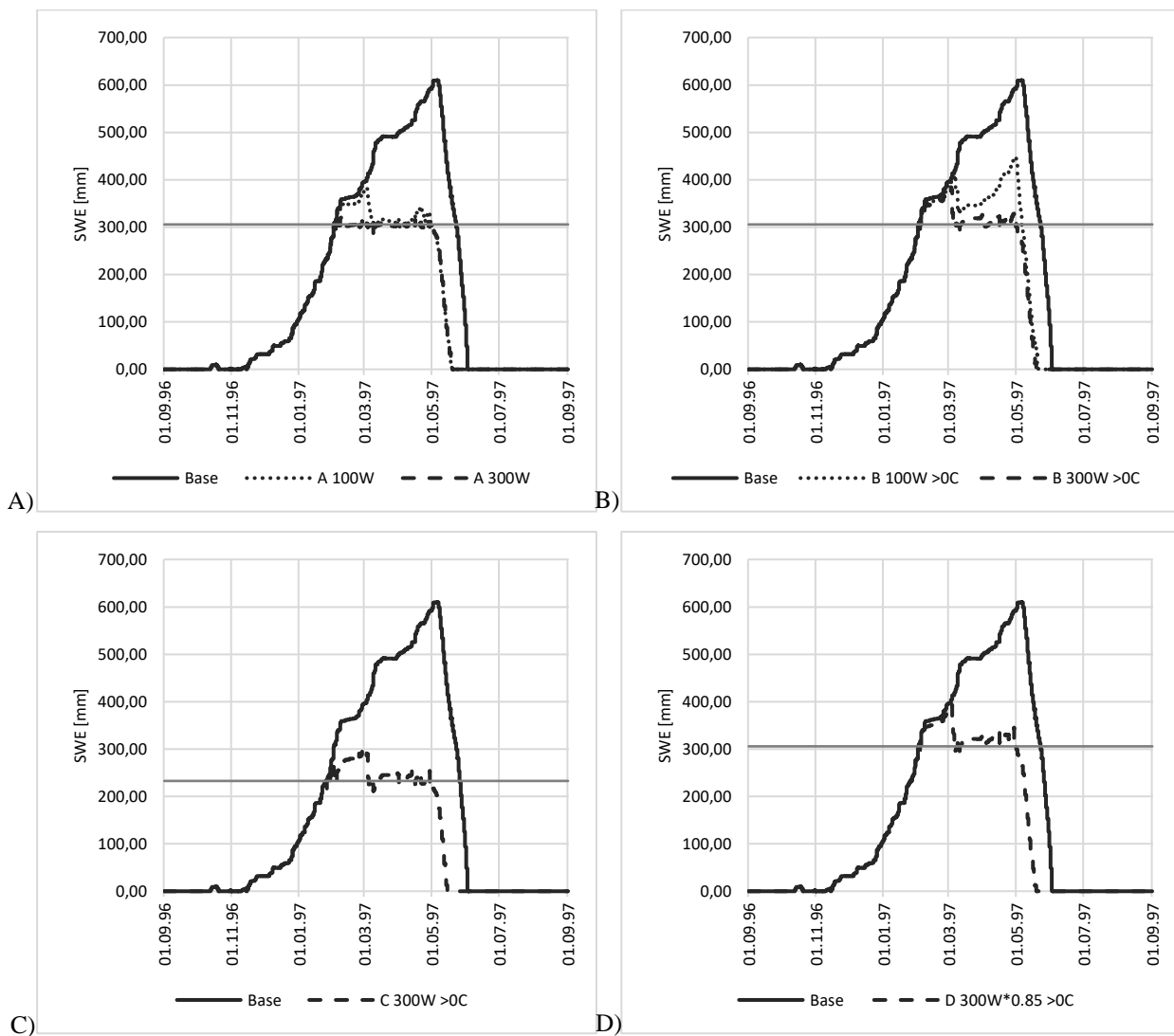
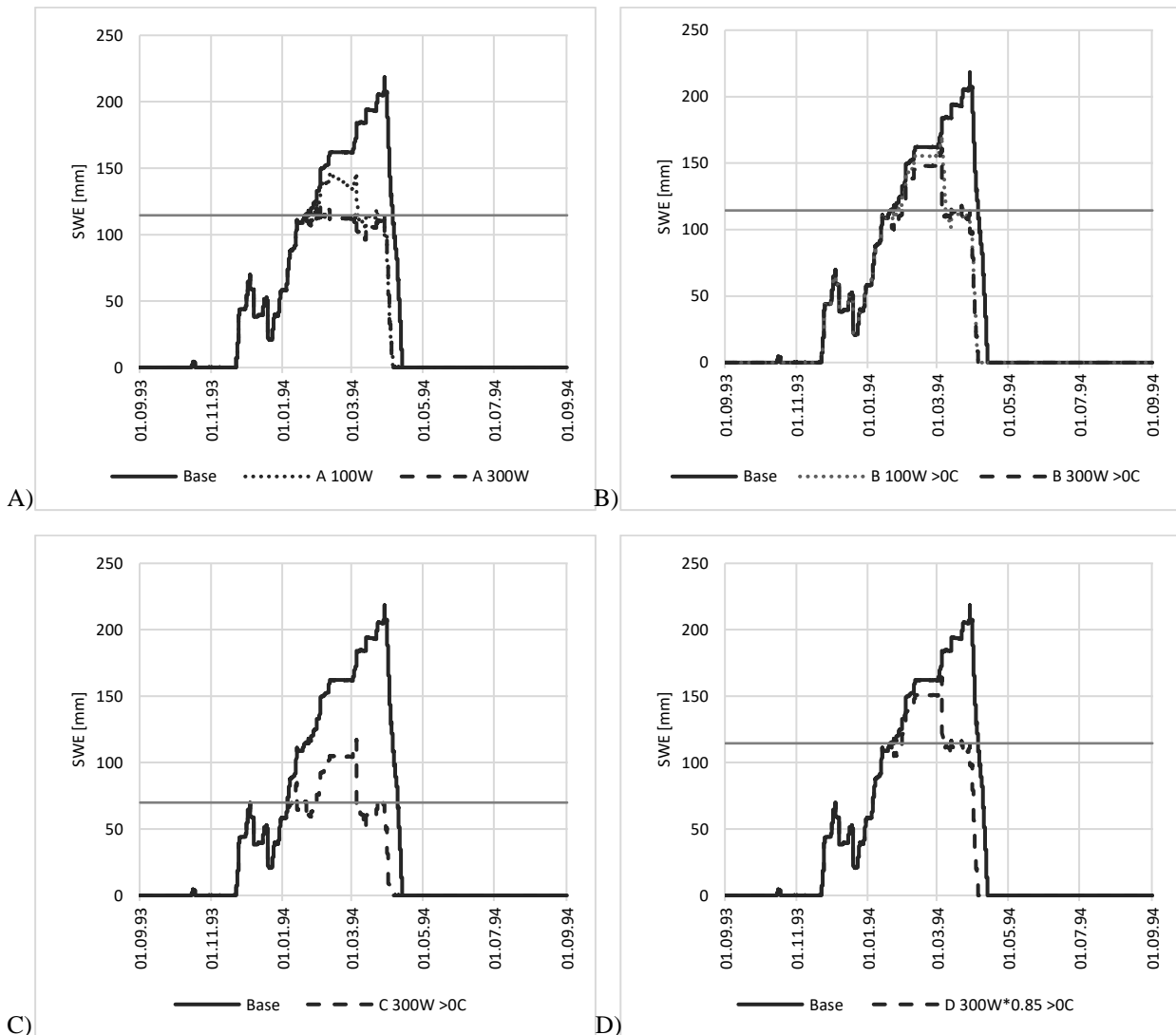


Figure 24. Yearly simulation of the snow water equivalent and melt rates for Tromsø 1996-1997.

*Oslo 1993-1994*

In strategy A, melting with  $100 \text{ W/m}^2$  does not contribute as good to the melt rate as with  $300 \text{ W/m}^2$ . The melting limit is reached earlier by melting with  $300 \text{ W/m}^2$ . In comparison, implementation of Strategy B gives melt rates remarkably similar at both  $100 \text{ W/m}^2$  and  $300 \text{ W/m}^2$ . Due to the lower melting limit, strategy C has the lowest SWE values and stays below the melting limit on all the other strategies. Strategy D gave a similar SWE to strategy B with  $300 \text{ W/m}^2$ .



*Figure 25. Yearly simulation of the snow water equivalent and melt rates for Oslo 1993-1994.*



*Bergen 2009-2010*

All strategies show a significant reduction of the SWE compared to the base case. Melting with 300 W/m<sup>2</sup> has a slightly higher melt rate than using 100 W/m<sup>2</sup> on strategies A and B. Strategy C has the lowest SWE values due to the low melting limit.

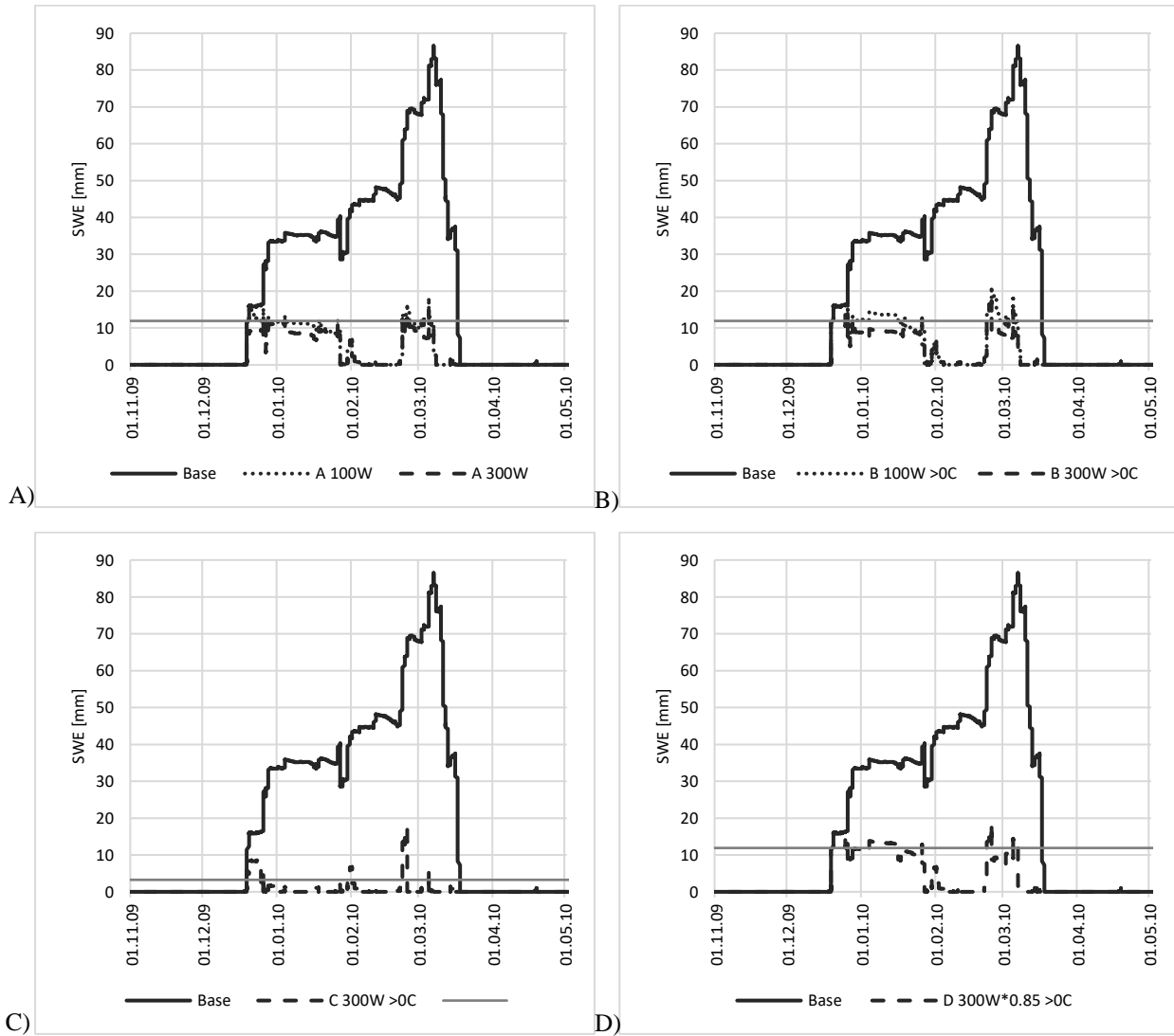


*Figure 26. Yearly simulation of the snow water equivalent and melt rates for Tromsø 1996-1997.*

Copenhagen 2009-2010

Strategy A has a significantly higher melt rate than strategy B, where melting with 300 W/m<sup>2</sup> has the most successful rate. Strategy B and D gave similar values of the SWE and did not melt at a sufficient rate.

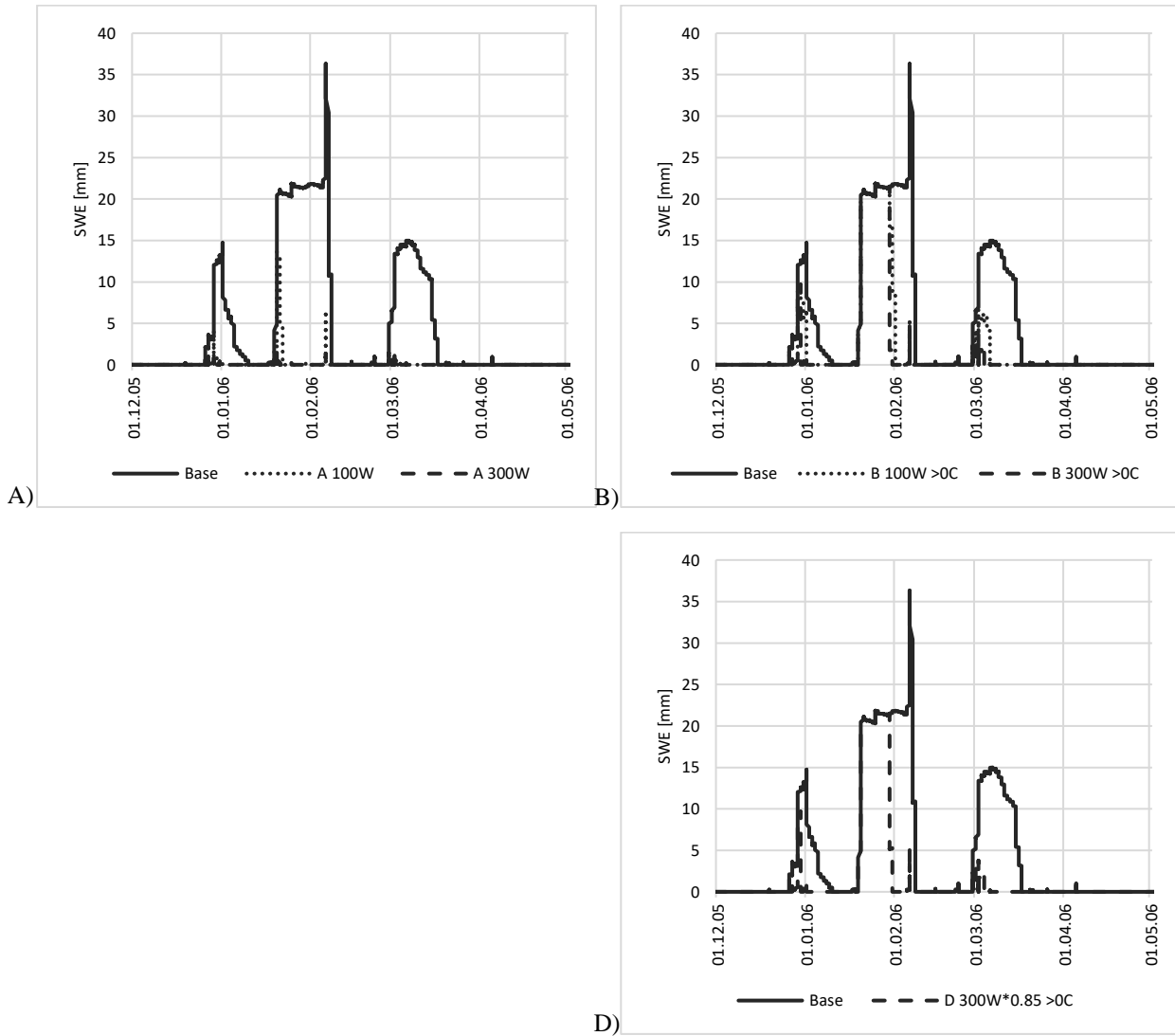
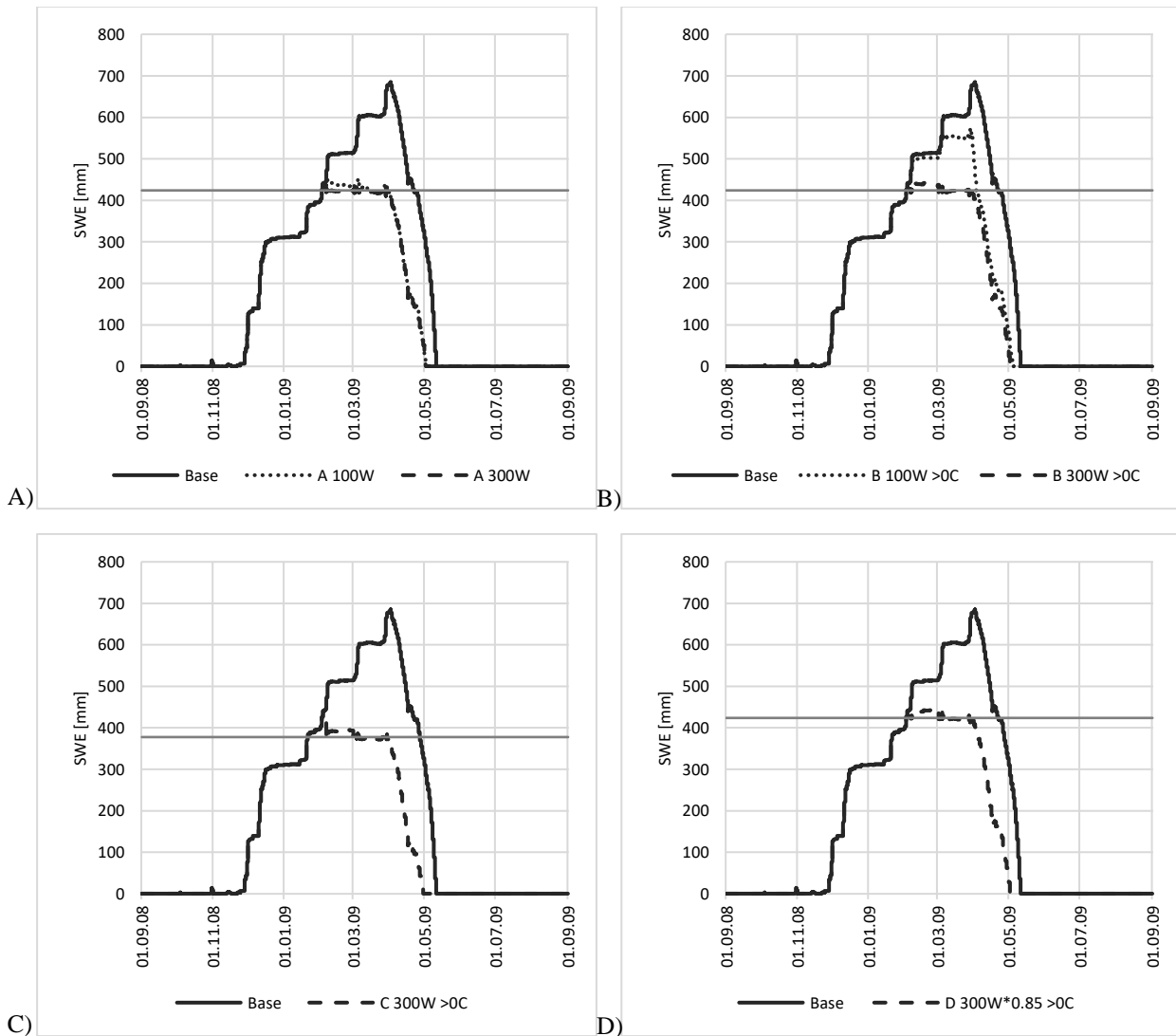


Figure 27. Yearly simulation of the snow water equivalent and melt rates for Tromsø 1996-1997.

*Cortina d'Ampezzo 2008-2009*

In strategy A, melting with  $100 \text{ W/m}^2$  shows a slightly higher value of the SWE than melting with  $300 \text{ W/m}^2$ . Melting with  $100 \text{ W/m}^2$  in strategy B shows a significantly lower melt rate than  $300 \text{ W/m}^2$ . Strategy D has only minor differences compared to strategy B with  $300 \text{ W/m}^2$ .



*Figure 28. Yearly simulation of the snow water equivalent and melt rates for Tromsø 1996-1997.*

*Grenoble 1981-1982*

In strategy A, melting with  $100 \text{ W/m}^2$  has a slightly lower the melt rate compared to  $300 \text{ W/m}^2$ . Strategy B, have a great difference when melting with  $100 \text{ W/m}^2$  and  $300 \text{ W/m}^2$ . Melting with  $100 \text{ W/m}^2$  show a lower melt rate and the difference between  $100 \text{ W/m}^2$  and  $300 \text{ W/m}^2$  exceeds  $100 \text{ mm SWE}$ . Due to the lower melting limit, strategy C has the lowest SWE values and stays below the melting limit on the other strategies. Strategy D gave a similar SWE to strategy B with  $300 \text{ W/m}^2$ .

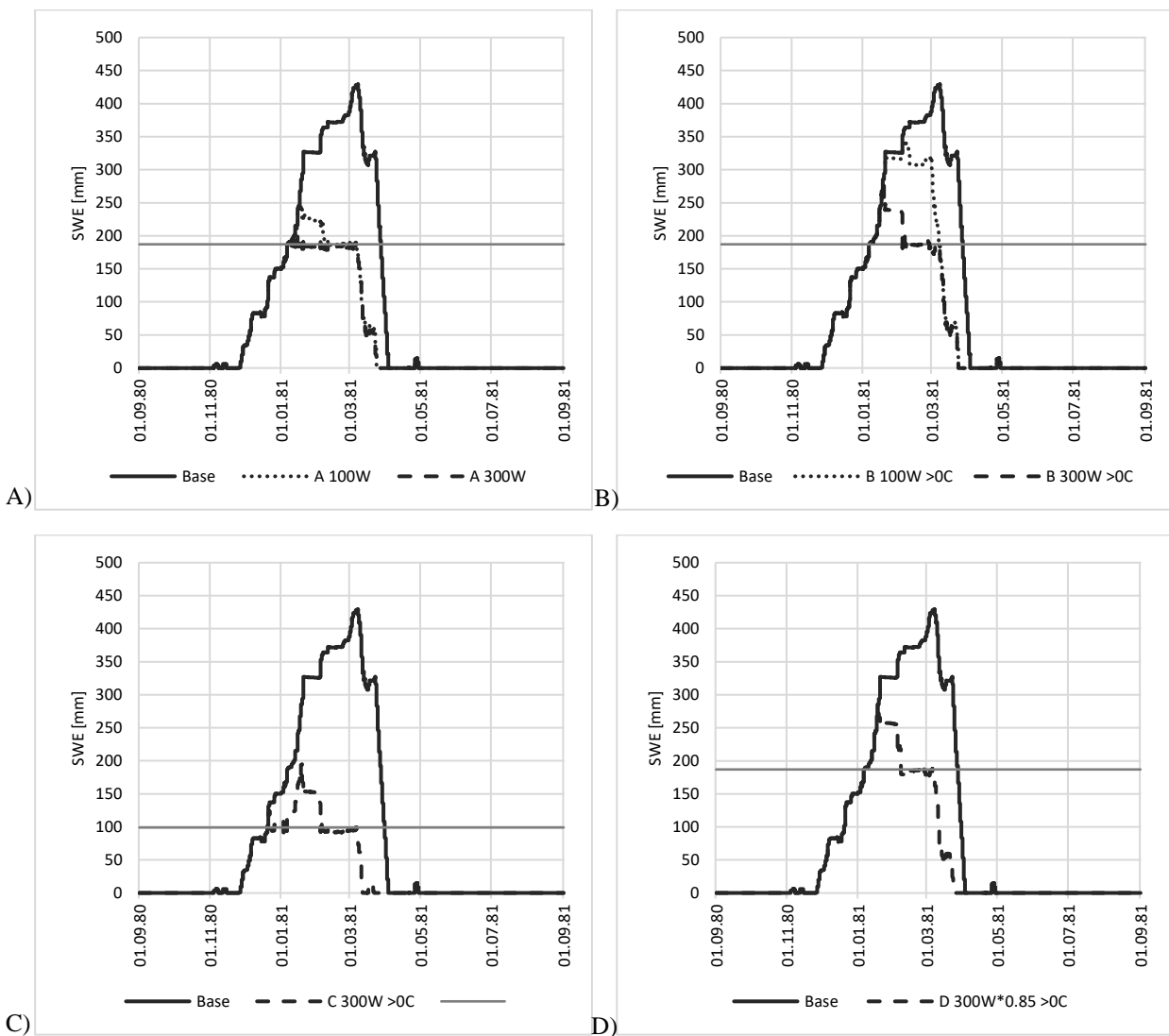


Figure 29. Yearly simulation of the snow water equivalent and melt rates for Tromsø 1996-1997.

## 5 Discussion

This chapter aims to answer the research questions stated at the beginning of this thesis. Also the limitations of the research approach and recommended further studies in this field will be discussed. The main problem was stated as follows in the beginning of this thesis:

*Energy demand for photovoltaic snow mitigation systems to reduce roof snow load on building structures*

with the support of three research questions. The next subchapters address and discuss the research sub-questions based on relevant theory and the results from the simulations and analysis.

### 5.1 Validation

The first sub-problem stated in the first chapter of the thesis:

*Validation of simulation method using measured data from an observed melting scenario using photovoltaic heating systems.*

The model (ESCIMO) provided results comparable with registered snow load reduction at Down Town, which is used as validation data for the research in this thesis. A validation was required to substantiate the research approach and the results. The research approach can briefly be described as snowpack simulation with an inserted heat source to reduce the snow load. Data collection from an actual event with PV systems in heating mode could indicate whether this model is valid compared to a similar simulated scenario with registered weather parameters.

The collection of registered weather parameters was slightly challenging as no source near Down Town could supply all the required parameters for the simulation. As the results on base SWE from simulations number 1-3 were considerably lower than the registered snow load at Down Town, only the results from simulation number 4 were simulated with melting. The snow load on the Down Town panels was registered at 12 individual weight sensors, and

there were differences in the maximum snow load before melting was initiated. There was no information provided that could determine the correct snow load for comparing the result from the simulation. The simulated snow load was compared to the registered snow load that had approximately the same amount of maximum snow load before melting was initiated. Consequently, this might embellish the results and research method.

There are several events that could be the reason why the registered snow load had individual differences. For example, this could be caused by wind drafts or orientation to the wind, inaccuracies or fault of weight sensor, or areas on the roof that could be affected by heat flux from the roof if it is poorly insulated. As the Down Town's roof has an area of 10 000 m<sup>2</sup> with PV heating systems installed on 6000 m<sup>2</sup> of it, uneven distribution of the snow load does not seem unlikely. This thesis does not go further into this, but the problem should be further addressed in field tests to identify sources of error.

To prevent the added heat from the PV panels at Down Town affecting the registered temperature above the panels, the temperature was adjusted. Weather station SN30255 was the closest weather station providing hourly air temperature. In figure 16 in chapter 3.1, the temperatures are shown, and it is apparent that the temperatures fluctuate, as well as crossing each other several times in the hours that make the base for adjusting. By calculating the mean difference from the first 24 hours, which indicated that Down Town was -1°C lower on average than SN30255, the temperature from the following days was adjusted accordingly. Adjusting the input data is not optimal as it does not necessarily represent as accurate as observed local weather data.

The result shows that the model (ESCIMO) is sensitive considering input temperature and snow accumulation. Temperature is the only difference in the input data in simulations 3 and 4, but the results were very different. The results showed a maximum SWE of 7 mm in simulation 3 and 50 mm in simulation 4. From the 11th of March, the only difference in temperature in the two simulations is minus one degree for all hours.

With the maximum snow load at 50 SWE in the base case in simulation number 4, two registered snow loads at Down Town with a similar maximum value was used for comparison. The base case has no added heat to the energy balance, and after reaching the

maximum, the snow load stabilizes and stays steady for the next days. Strategies A-D with the added heat source with the same energy, 303W per m<sup>2</sup>, were then initiated at Down Town. All strategies provided the same melt rate in the chart, with minor differences. The strategies with temperature restriction have a small displacement at the apex where the melting started. Reduced efficiency shows that the melt rate stops and evens out before it reaches zero.

Efficiency from the PV heating system at Down Town is not considered. If the roof at Down Town is poorly insulated, it might show better results than what the melting from PV systems provides. If it is assumed that the local weather at Down Town during the melting had zero wind it is probable that the roof provided heat flux transportation increasing the melting efficiency. The simulation does not consider a reduction of the efficiency, which might be an offset if this is the case.

### **Limitations**

The registered snow load data and amount of melting energy used from Down Town is the source of information in the validation case and only reflect one short melting scenario with a photovoltaic snow mitigation system. A larger dataset with more information on the local climate conditions could possibly provide results that show the advantages and disadvantages of this method and sources of errors in the model.

The weather parameters used in the simulation are a combination of several sources. A complete dataset of weather parameters from the site would provide more precise and reliable results.

## 5.2 Energy efficiency

The second sub-problem stated in the thesis:

*Estimation of the energy efficiency of photovoltaic heating systems by simulation.*

This analysis compared how snow depth and snow properties affected heat flux transportation. The simulations were run with 10-, 50- and 100-mm thickness of the respective snow layer. Boundaries of outside climate were defined with a constant temperature of 0°C and 80 % relative humidity, but these parameters change naturally in real life. The indoor climate was determined with a steady temperature at 22°C and a 40 % relative humidity for sets 3 and 4.

The simulations with the best results and the highest efficiency are set 3 and 4. The heat from the indoor climate was transported through the roof construction and into the air layer.

Not surprisingly, the efficiency of the PV panel decreased as the snow depth increased in all sets of simulations. The insulation increased as the snow depth got deeper, and the heat flux transportation changed accordingly. Snow is a complex material and there are many stages in the melting process. The insulating effect of snow might increase the temperature on the PV panel surface and may also provide shelter from the wind in a real scenario. A melting process in wintry conditions is likely to be more easily performed for thick rather than thin snowpacks.

WUFI does not provide all materials and components in its built-in library needed for this simulation, and some layers were added manually. The snow layer is constant with the same properties in 24 hours as no function changes layers throughout the simulation in WUFI. The snow layer was determined to be wet, as it could simulate the snowpack right before it melts. For simplification, the PV panel was represented by two thin layers of glass and metal with an added heat source in the glass layer. The air layer was found in the library. In simulations 3 and 4, with a compact roof and indoor climate on one side, a built-in construction from the WUFI library was used.

There was no moist transportation in the calculation. As moist transportation is a natural part of an outside climate this could be a source of error in the melting scenario.



PV systems are often installed with an air layer or a gap between the roof and the module. A poorly insulated roof that used to have the snow load distributed directly on the roof, may experience an increased snow load after installing PV systems. When an air change occurs in the air gap, the heat flux transported through the roof will likely dissipate. Before installing modules, the snow is in direct contact with the roof, and the heat flux from a poorly insulated roof will melt the snow load directly.

Another indication from the simulation is that the wind affects the efficiency. If there is a strong wind, it requires more energy to melt the snow than when there is no wind. Wind can also cause the snow load to redistribute on the roof and create concentrated and heavier loads on some parts of the roof, which should be avoided if the roof is under-designed.

The results from set 2 with snow depth 10 mm were determined to be of further use in the research. This is an optimistic value as the results show that the efficiency varies depending on snow depth and air change. Due to the amount of data simulated with the snow cover model (ESCIMO) of 39 years, the efficiency needed to be a generic value. All the simulated sites had different melting limits because the amount of SWE changes through the melting scenario. Therefore, it was necessary to simplify the efficiency calculations. Any influence from air change was also not considered, however the results showed that air change influenced the efficiency.

A snowpack has layers with different material properties, and the simplification of the snowpack in this simulation might also have affected the results. For example, if the top layer in the snowpack is iced or the bottom layer consists entirely of slush, the ice on top will affect how the heat distributes in the snowpack.

Due to all the influencing factors listed above, the calculation in this thesis of the efficiency using PV heating systems is a rough estimate and might be somewhat optimistic. A more advanced simulation model could simulate the efficiency more precisely.

A case study might be the most accurate if different constructions with varied heat flux transportation, local climate changes such as temperature, wind, and relative humidity are included.

## **Limitations**

The efficiency simulation is simplified and do not include moist transportation or that the snow consistency changes over time due to the added heat. There is no consideration in the analyses of the possible variations of the local weather, except for the simulation with a temperature boundary.

Transportation direction of heat flux in the simulation model is limited from one side of the construction to the other, passing through the layers.

### 5.3 Melting strategies and energy demands

The third sub-problem stated in the thesis:

*Simulation of the energy demands of photovoltaic snow mitigation systems in varying climatic conditions, and the optimal melting strategy to minimize energy loss.*

#### *Strategy A*

With  $100 \text{ W/m}^2$  of melting energy, Strategy A has the highest energy demand on all sites. And have a higher percentage of overload than  $300 \text{ W/m}^2$  of melting energy. The results show that melting at  $100 \text{ W/m}^2$  is insufficient with a significantly slower melt rate. The sites' long-term average energy demand and overload show satisfactory results in melting with  $300 \text{ W/m}^2$  for load reduction. In the extreme value analysis, chapter 4.4.3, the sites have a higher reduction on the 5- and 50-YRP characteristic snow load using  $300 \text{ W/m}^2$  rather than  $100 \text{ W/m}^2$ .

The simulations model does not consider how the meltwater drains off. There is a high probability of refreezing the meltwater using this strategy. This is the only strategy that does not have a temperature boundary at  $0^\circ\text{C}$  for melting, and even with a drainage system, the stakes for refreezing are high. If the air temperature is below the freezing point, the refreezing may occur near the drainage or gutters, displacing the snow load and making it difficult to remove.

#### *Strategy B*

As discussed in strategy A, melting with  $100 \text{ W/m}^2$  does mitigate the snow load at the same rate as using  $300 \text{ W/m}^2$ . The results show that all the sites have a higher reduction of the 5- and 50-YRP characteristic snow load using  $300 \text{ W/m}^2$  rather than  $100 \text{ W/m}^2$ .

This strategy has a temperature boundary where it can only melt if the temperature is equal to or above  $0^\circ\text{C}$ , a measure to minimize the risk of meltwater refreezing on the roof.

#### *Strategy C*

Strategy C has the best results regarding overload on all the sites, excluding Copenhagen, which was not simulated with this strategy due to the already low melting limit. This strategy

also considers the risk of the meltwater to refreeze, and only initiated heat when at 0°C or above. The overload with this strategy is generally lower, but the number of years with melting is higher and therefore has a higher energy demand. If it is desired not to exceed the original melting limit, melting with strategy C is optimal.

#### *Strategy D*

Strategy D has the same conditions as strategy B, with 300 W/m<sup>2</sup>, except for the efficiency reduction. This is the only strategy with a reduced efficiency from the panels. The results indicate that strategy D reduces the same snow load, but the energy demand is naturally slightly higher.

Assuming that 100 %, as used in the other strategies, or 85 % of the heat from the melting system is transferred to the snowpack would be optimistic. Four of the sites have a melting limit above 100 mm SWE, which is estimated to be 100 cm of fresh snow. The insulating effect of a thick layer decreases the efficiency.

The average 39-year energy demand seems less significant than a single year with melting. Depending on the site's climate characteristic, target level, and the number of years that required melting, the energy demands was between 3-11 kWh/m<sup>2</sup> using strategy B, C, or D.

The energy required to keep an under-designed roof safe depends on the energy demand and the number of intervals on single load reduction. There are various magnitudes of under-design in building structures that determines the frequency of load reduction. Also, the snow load varies each year, means it would be unnecessary to melt every year. With regards to the safety of the structure, this is one reason the snow is not reduced from the start of the accumulation. Thus, the removal of the snow allows energy production from the panels. Whether it is cost efficient to remove the full snow cover in favour of energy production should be examined taking into account the location of the building and the amount of solar radiation in the wintry season. For example, Tromsø, located 69 degrees north, has polar nights for a large part of the wintry season, and snow removal for energy production might not be cost efficient in these months.

Installing a PV heating system might affect the snow accumulation on a flat roof, as discussed in chapter 5.2, but the systems also change the roof's surface, and this might affect other

factors—as the roof shape changes, especially if it is installed with an air gap and with an angle tilt. In chapter 2.3.1, it was considered how the load is arranged by the shape coefficient that adjusts the shape, angles, and pitches of the roof on the determination of the snow load. Depending on the arrangement and design on the PV system, there is a risk of an uneven snow load distribution due to drifting. A tilt on the modules or a gap between modules risks being filled up with a bulk of snow load from the wind drifting the snow. If there are only a few modules with an installed snow weight sensor, they will not necessarily register the heavy load.

Adding a PV heating system on a roof raises questions regarding the added dead load. If extra dead load is applied to an already under-designed building structure, it becomes even more dependent on the snow load control to function. The reaction time will probably, before reduction of the snow load is necessary, be shortened. Risk factors such as climatic conditions or technical difficulties/failures could possibly interfere with the PV system's efficiency. This could influence the reliability of the roof. Predefined reliability levels in the design standard must be satisfied by the building to avoid structural failure. The PV system has a certain probability of delivering sufficient load reduction in a heavy snow load scenario, which should be added to the reliability calculation of the roof. Documentation guaranteeing load reduction must be provided for the design snow load to be reduced. This is highly dependent on the climate where the load reduction is performed.

From the ISO 4355 standard, Annex F, which concerns snow load control described in chapter 2.6, it is stated that the determination of snow load on roofs can be reduced if a sufficient and reliable device controls the snow load. The snow load control needs field research and testing to guarantee snow load reduction before calculation. It is also necessary to find the annual maximum value of snow accumulation in the return period of years based on observed meteorological data. PV heating systems qualify as sufficient and reliable control devices, but they require documentation with observed meteorological data and field tests that guarantee the differential snow load reduction to reduce the snow load on a roof.

Three sites that are categorized as *Cfb* are Bergen, Copenhagen, and Grenoble. Bergen and Copenhagen are the sites with the lowest characteristic snow load, which results in low melting limits for both places. Melting occurred in 39 of 39 years for Copenhagen and 28 of

39 years for Bergen. Copenhagen, with only 0.1 mm for melting limit, has overloaded all the years in the simulations and all the strategies. Copenhagen's average energy demand and overload for strategies B and D are 11 kW/m<sup>2</sup> and 80 % overload. Therefore, there is no difference in the average of 40 years with 100 % or 85 % efficiency from the PV panel. A low melting limit and 5-YRP give many years of melting and high energy demand. The results on the distributed fitting of the 5-YRP of Bergen and Copenhagen might not be reflecting the accurate local climate and could explain these results.

Grenoble, has a significant difference regarding the altitudes from ERA5 and Grenoble city. With more than 700 m in altitude difference, the weather data probably deviates from the accurate local climate in Grenoble.

Tromsø and Cortina d'Ampezzo are located 2500 km apart, and they are the two sites with the highest characteristic snow loads, and both sites have long-lasting snow covers in the winter season. Both sites have average temperatures below 0°C for January and the winter season. In areas with stable cold winters, snow will build up continuously until spring, and usually, a period of rapid melting was found. The snow load is more intermittent in climates where the winter temperature varies around the freezing point. The winter might consist of several independent snow episodes separated by snow melting.

For the melting that restricts melting below freezing degrees, the snow can accumulate faster than the melting system is able to melt. A solution is to reduce the melting limit, creating a snow load buffer. The results from strategy C showed an overall greater reduction of the snow load on both the yearly and the extreme values.

## **Limitations**

Snow as a complex natural system was simplified as a homogenous material simulating the snowpack. It does not consider how internal layers in a snowpack may change over time, especially with an added heat source.

The focus of this thesis was snow loads not exceeding target levels and the structural resistance and capacity of a specific roof has not been considered.

The climatic data used as model input increase uncertainty in the results compared to actual, observed climatic data.

## **5.4 Further studies**

The research performed in this thesis is limited, and the field demands more investigation to determine if photovoltaic systems are sufficient for snow load reduction in varying climatic conditions.

It is necessary to conduct further studies of load reduction under varying climatic conditions. Simulation with a collection of registered weather data may give more accurate results. Case studies of PV heating systems should be performed under various climatic conditions with different snow depths to measure energy efficiency.

Applying heat for snow mitigation with PV modules should be investigated for a long-term effect and provide documentation for the system's load reduction capabilities in structural design standards.

## 6 Conclusion

Simulation and analysis of the energy demand for roof mounted photovoltaic snow mitigation systems to reduce snow load on the structural building have been explored and researched. This thesis conducted simulations with observed weather data for validation and modelled weather data to simulate energy demand on various sites over 39 years. The energy efficiency of a photovoltaic panel was simulated in a program that calculates heat transportation through building components. Six locations in Norway and Europe, with various climate conditions, were chosen to be simulated over 39 years of snow load with several melting strategies, exploring the potential energy demand and the optimal strategy for various locations using PV snow mitigation systems. All melting scenarios were based on target levels calculated from the return period of the snow loads using a fitted distribution on the yearly maximum snow load for simulated years.

Moreover, the simulation model provided results comparable with registered snow load reduction from an actual melting case which is used as validation data for the research in this thesis. Due to some heat flux from the PV panel transporting in the opposite direction of the snow cover in the simulation, the PV panel's energy efficiency was reduced to 85 % in one of the melting strategies.

Furthermore, the optimal melting strategy was using  $300 \text{ W/m}^2$  of melting power and a temperature restriction equal to or above  $0^\circ\text{C}$  for initiated melting power—reducing potential meltwater refreezing and re-distributing the snow load on the roof. For areas with a low melting target, the results showed many years of melting and overload compared to the areas experiencing snow cover during winter. As snow could accumulate faster than the heating system could melt with temperature restriction in some cases, a snow load buffer based on the target level and amount of overload showed the most reduction. The average energy demand over 39- years was less significant, depending on the site's climate characteristic, target level and the number of years with required, yearly average of melting was between 3-11 kWh/m<sup>2</sup>. In conclusion, the photovoltaic snow mitigation system shows results of reduction of the snow load for seasonal use and in the long term. For future development and research, the input data in the model should be based on historically registered weather data for more accurate results on determining the melting targets and optimal strategies for local climate conditions. The energy efficiency and optimal melting strategy are yet to be documented in field tests with various climate conditions.



## References

- Barthelt, P. & Lehning, M., 2002. A physical SNOWPACK model for the Swiss avalanche warning: Part I: numerical model. *Cold Regions Science and Technology*, pp. 123-145.
- CEN/TC 250, 2020. *prEN-1991-1-3*. s.l.:European Committee for Standardization .
- Coléou, C. & Lesaffre, B., 1998. Irreducible water saturation in snow: Experimental results in a cold laboratory. *Annals of Glaciology* 26, pp. 64-68.
- Croce, P. et al., 2018. The snow load in Europe and the climate change. *Climate Risk Management* 20, pp. 138-154.
- ECMWF, 2021. [Online]  
Available at: <https://www.ecmwf.int/en/forecasts/dataset/ecmwf-reanalysis-v5>  
[Accessed 2021].
- Frimannslund, I., 2017. *Measurements and analysis of snow load reduction on flat roof using photovoltaic system in heating mode*, Norwegian University of Life Sciences: Department of Mathematical Sciences and Technology.
- Frimannslund, I. & Thiis, T. K., 2019. A feasibility study of photovoltaic snow mitigation systems for flat roofs. *Technical Transactions*, Vol. 7 2019, pp. 81-96.
- FUSen, 2021. *Solenergibloggen*. [Online]  
Available at: <https://blogg.fusen.no/snosmelting-med-solceller>.  
[Accessed 20 03 2021].
- Hirashima, H., Kawashima, K. & Sano, H., 2020. Development of a Snow Load Alert System "YukioroSignal" for Aiding Roof Snow Removal Decisions in Snowy Areas in Japan. *J. Dis. Res.*
- Innos, 2021. *Innos*. [Online]  
Available at: <https://www.innos.no/>  
[Accessed 2021].
- Karagiozis, A., Künzle, H. & Holm, A., 2001. WUFI-ORNL/IBP—A North American Hygrothermal model. *Buildings VIII Proceedings*.
- Kvande, T., Tajet, H. T. T. & Hygen, H. O., 2013. *Klima- og sårbarhetsanalyse for bygninger i Norge*, Trondheim: SINTEF Byggforsk.
- Köntges, S. A. T. H. U. J. K. B., 2018. Mean Degradation Rates in PV Systems for Various Kinds of PV Module Failures. *32nd European Photovoltaic Solar Energy Conference and Exhibition*, pp. 1435-1443.

- Marke, T. et al., 2016. *ESCIMO.spread (v2): parameterization of a spreadsheet-based energy balance snow model for inside-canopy conditions*, *Geosci. Model Dev.*, 9. [Online]  
Available at: <https://doi.org/10.5194/gmd-9-633-2016>  
[Accessed 2021].
- MathWorks, 2021. *MathWorks*. [Online]  
Available at: <https://www.mathworks.com/help/stats/lognormal-distribution.html>  
[Accessed 2021].
- Meløysund, V., 2010. *Prediction of local snow loads on roofs*, Trondheim: Norges Teknisk og Naturvitenskaplige Universitet, Fakultet for ingeniørvitenskap og teknologi, Institutt for konstruksjonsteknikk.
- Nuijiten, A. D. & Høyland, K. V., 2016. Comparison of melting processes of dry uncompressed and compressed snow on heated pavements. *Cold Regions Science and Technology*, pp. 69-76.
- Nuijten, A. & Høyland, K. V., 2017. Modelling the thermal conductivity of a melting snow layer on a heated pavement. *Cold Regions Science and Technology 140*, pp. 20-29.
- NVE, T. N. W. R. a. E. D., *Homepage NVE*. [Online]  
Available at: <https://www.nve.no/hydrologi/sno/?ref=mainmenu>  
[Accessed 22 February 2021].
- Oke, T. R., 1987. *Boundary layer climates*. Second edition ed. London: Routledge .
- Saloranta, T. M., 2016. Operational snow mapping with simplified data assimilation using the seNorge snow model. *J. Hydr*, 538, pp. 314-325.
- Schill, C., Brachmann, S. & Koehl, M., 2015. Impact of soiling on IV-curves and efficiency of PV-modules. *Solar Energy 112*, pp. 259-262.
- seKlima, 2021. *seKlima*. [Online]  
Available at: <https://seklima.met.no/observations/>  
[Accessed 2021].
- SINTEF Byggforsk, 2014. *Trehus*. 5 ed. Oslo: SINTEF akademiske forlag .
- SLF, 2021. *WSL Institute for Snow and Avalanche Research SLF*. [Online]  
Available at: <https://www.slf.ch/en/snow/snow-as-a-material.html>
- Smets , A. et al., 2016. *Solar Energy*. Cambridge: UIT Cambridge Ltd.
- Standard Norge, 2003. *NS-EN 1991-1-3:2003+NA:2008*. s.l.:Eurocode 1: Actions on structures - Part 1-3: General actions - Snow loads: Standard Norge.

Standard Norge, 2008. Nasjonalt tillegg NA. In: s.l.:N.A.4.1 Karakteristiske verdier. Norway.

Store Norske Leksikon, 2019. *Snl*. [Online]

Available at: <https://snl.no/entalpi>

[Accessed 15 10 2021].

Store Norske Leksikon, 2019. *Snl*. [Online]

Available at: <https://snl.no/varmekapasitet>

[Accessed 15 10 2021].

Strasser, U. & Marke, T., 2010. ESCIMO.spred - a spreadsheet-based point snow surface energy balance model to calculate hourly snow water equivalent and melt rates for historical and changing climate conditions. *Geosci. Model Dev.*, pp. 643-652.

Tipler, P. A. & Mosca, G., 2008. *Physics for Scientists and Engineers*. Sixth Edition ed. s.l.:W. H. Freeman and Company .

Tsanakas, J., Ha, L. & Buerhop, C., 2016. Faults and infrared thermographic diagnosis in operating c-Si photovoltaic modules: A review of research and future challenges.. *Renewable and Sustainable Energy Rev.* 62, pp. 695-709.

Wikipedia, 2021. *Koppen climate classification*. [Online]

Available at: [https://en.wikipedia.org/wiki/K%C3%B6ppen\\_climate\\_classification](https://en.wikipedia.org/wiki/K%C3%B6ppen_climate_classification)

[Accessed 2021].

Wikipedia, 2021. *Wikipedia Climate classification*. [Online]

Available at: [https://en.wikipedia.org/wiki/Climate\\_classification](https://en.wikipedia.org/wiki/Climate_classification)

[Accessed 2021].

WUFI, 2021. *WUFI*. [Online]

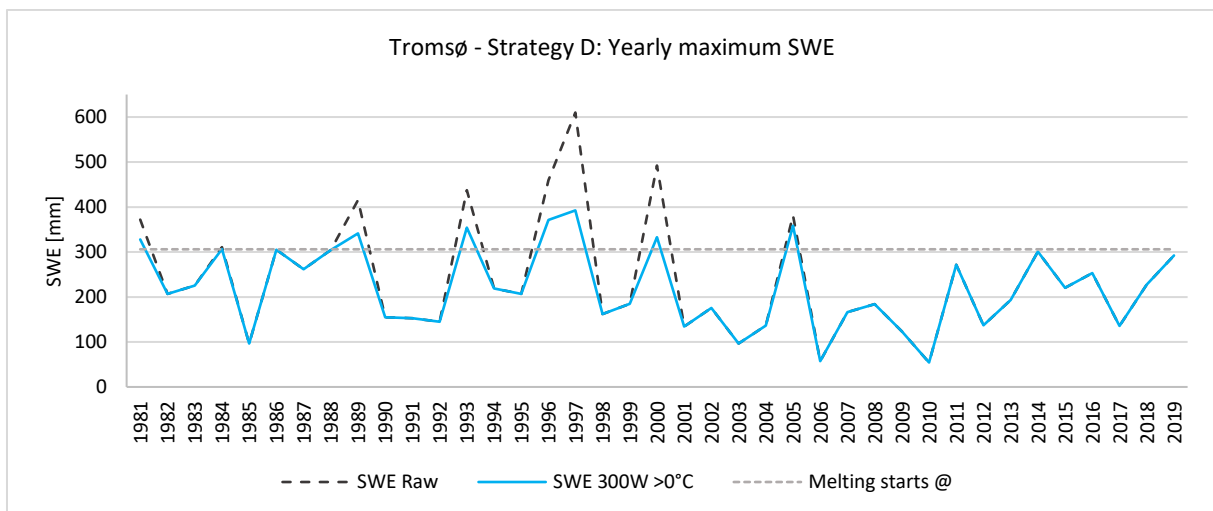
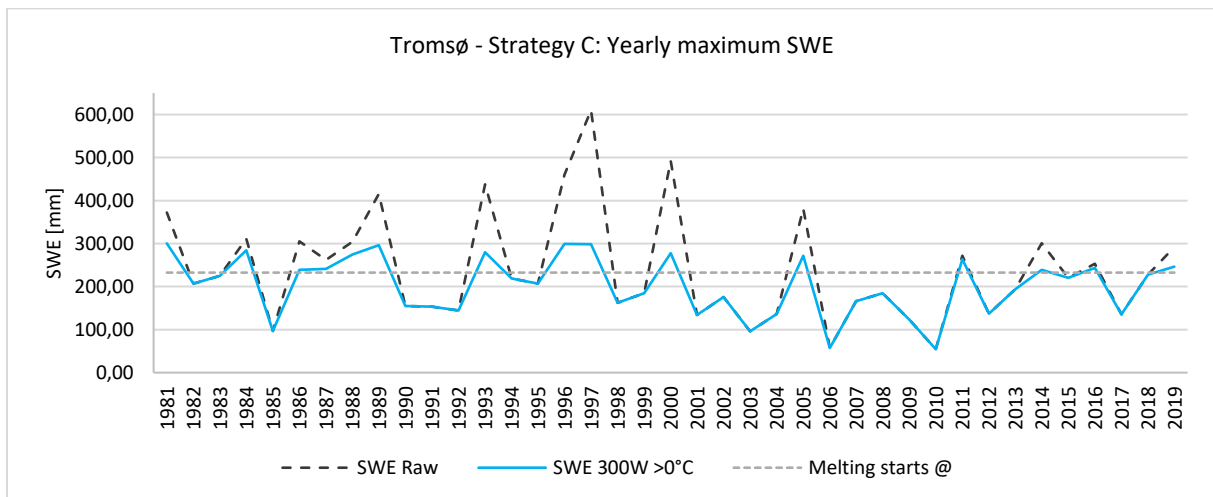
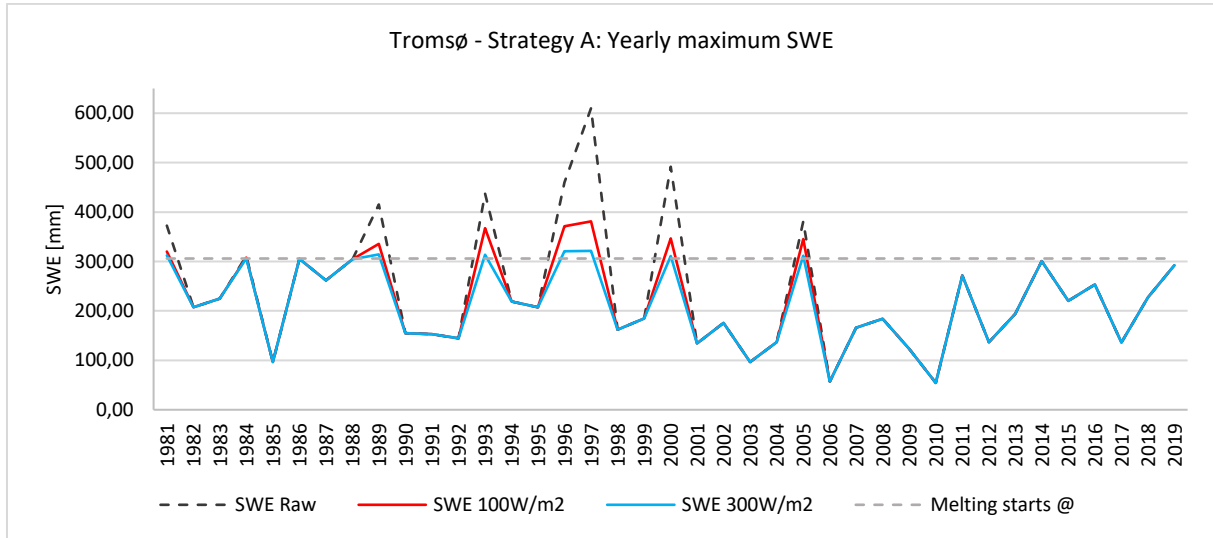
Available at: <https://wufi.de/en/software/what-is-wufi/>

[Accessed 21 09 2021].

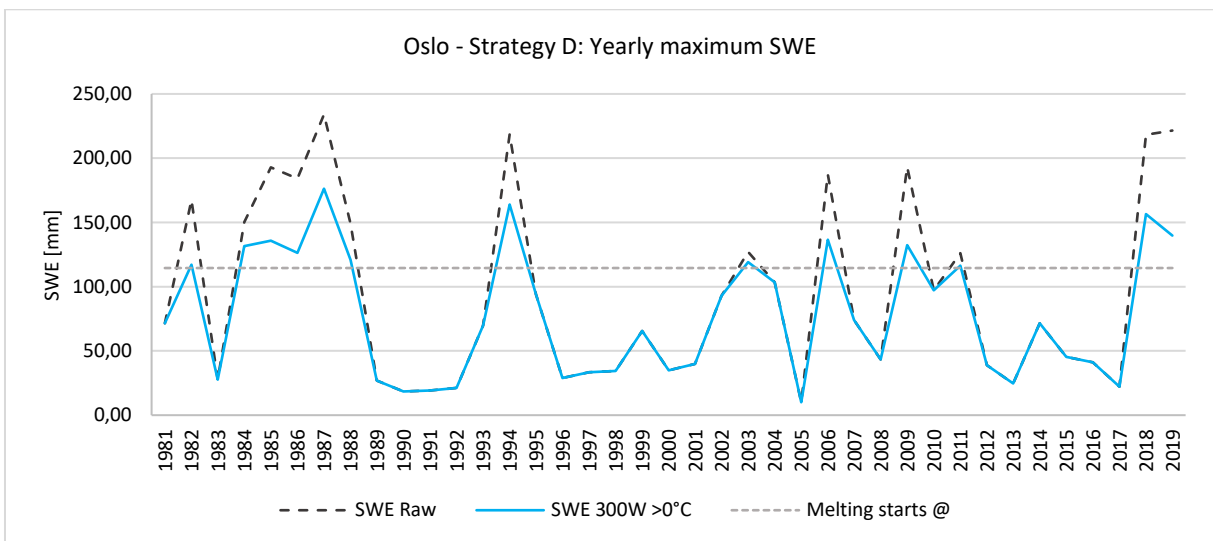
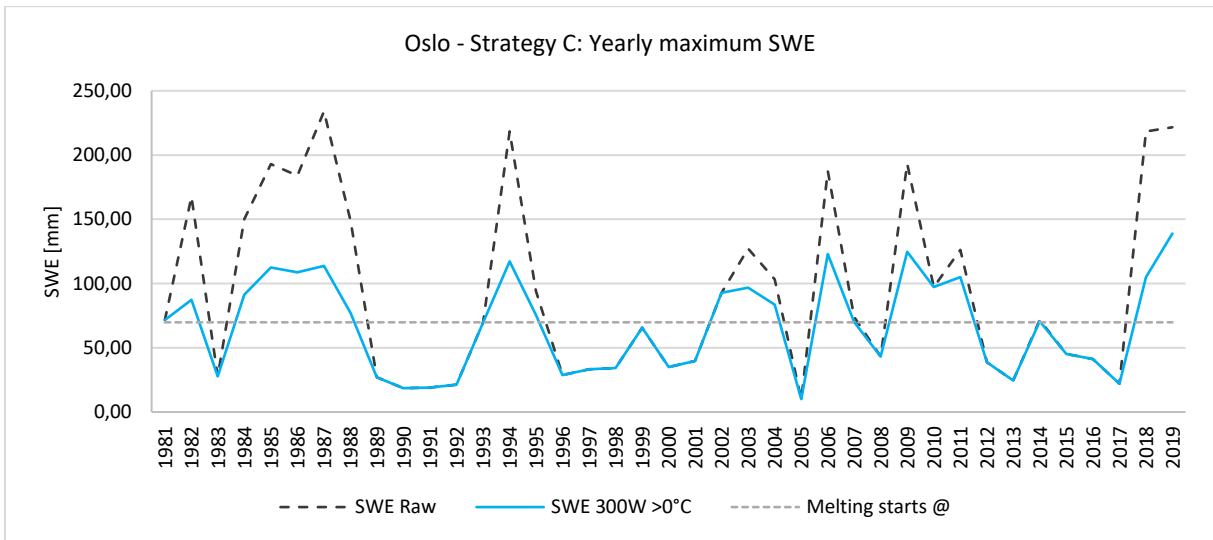
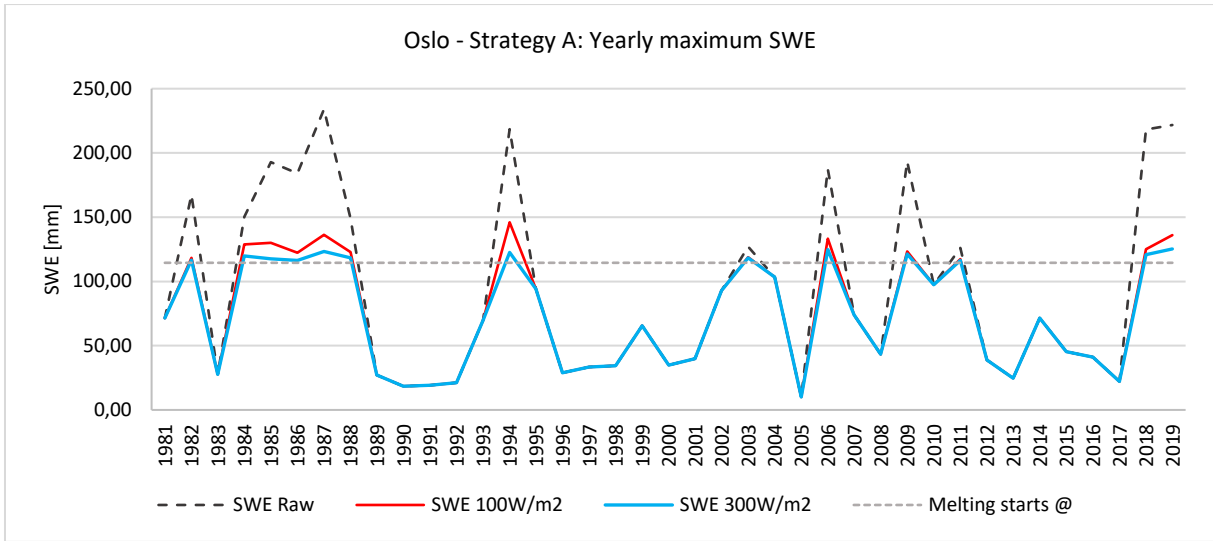
# Appendix

## A.1 Yearly maximum SWE

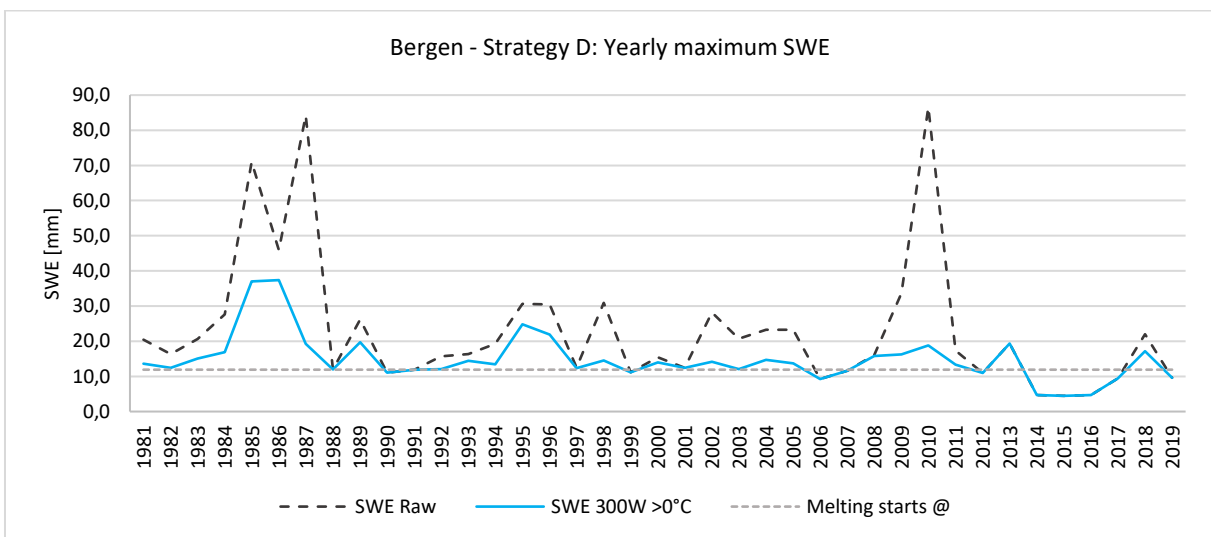
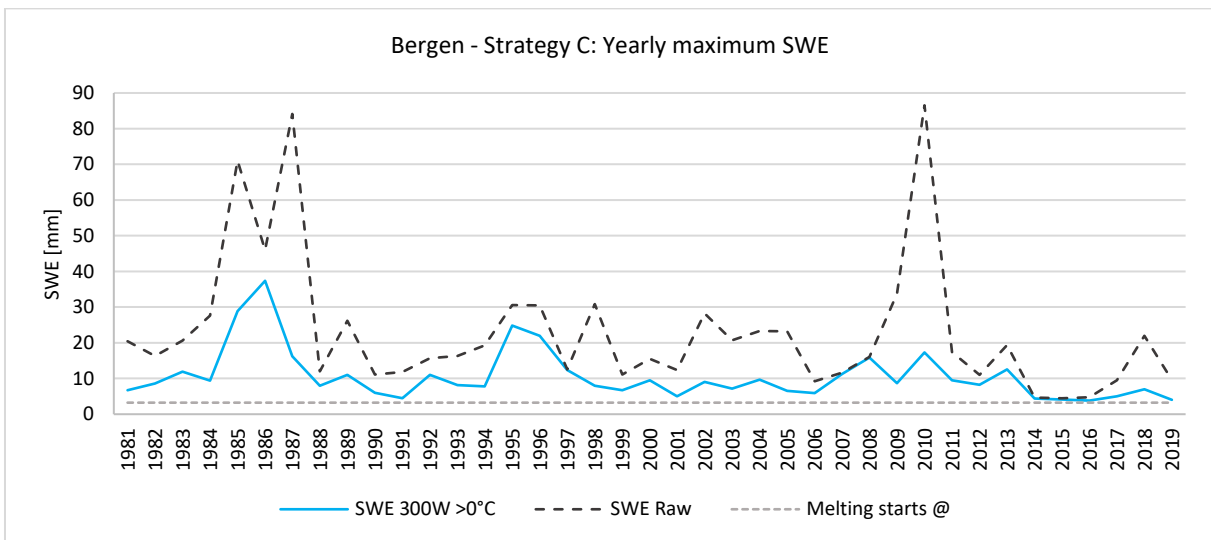
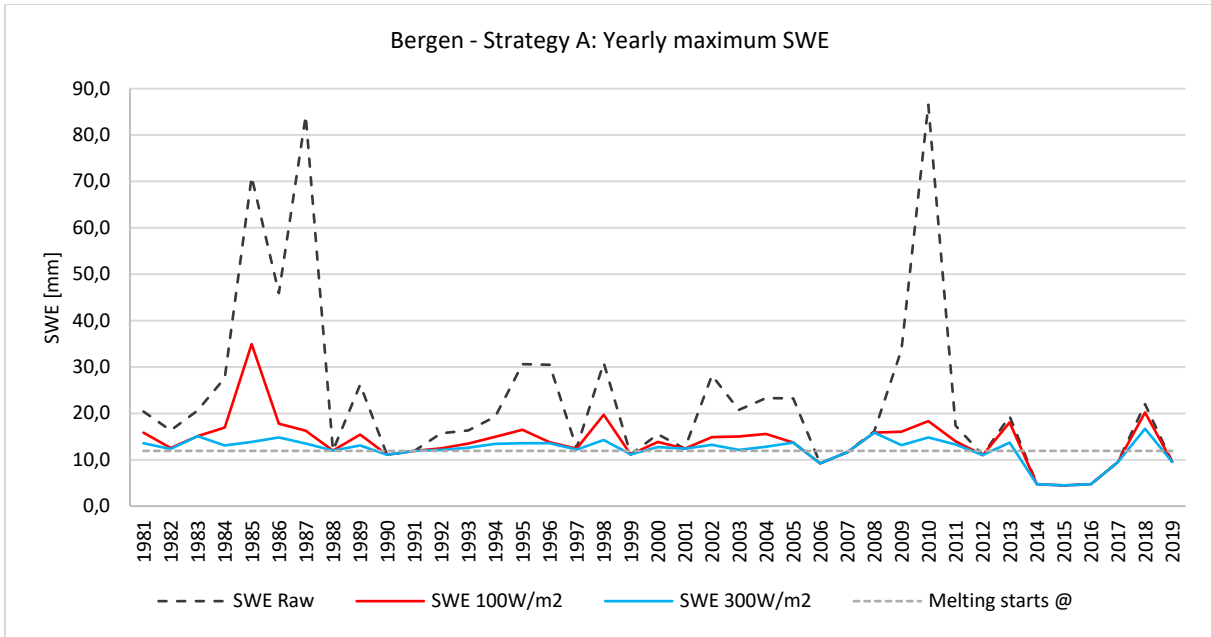
Tromsø



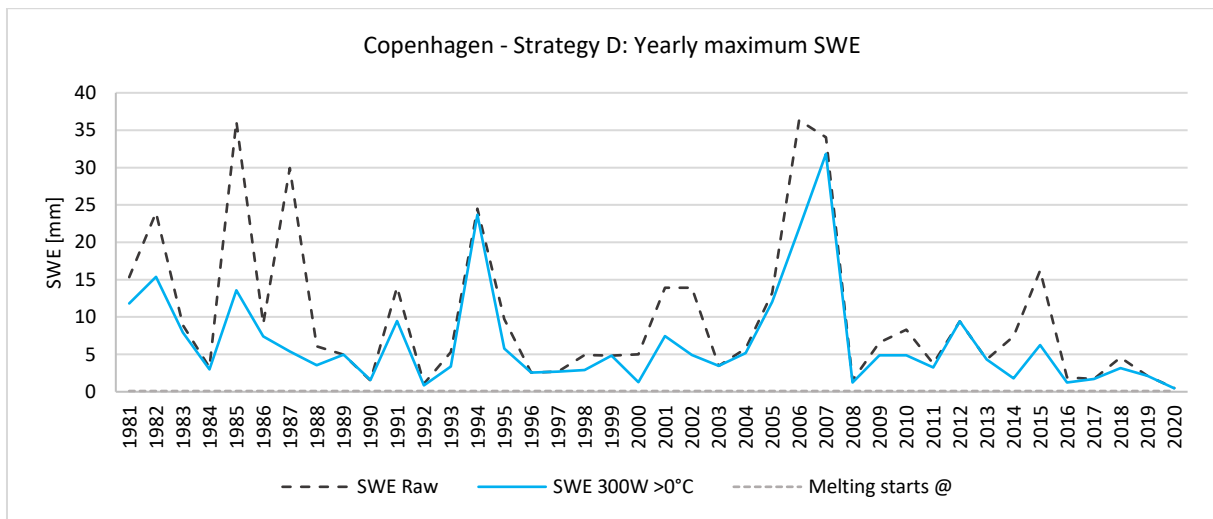
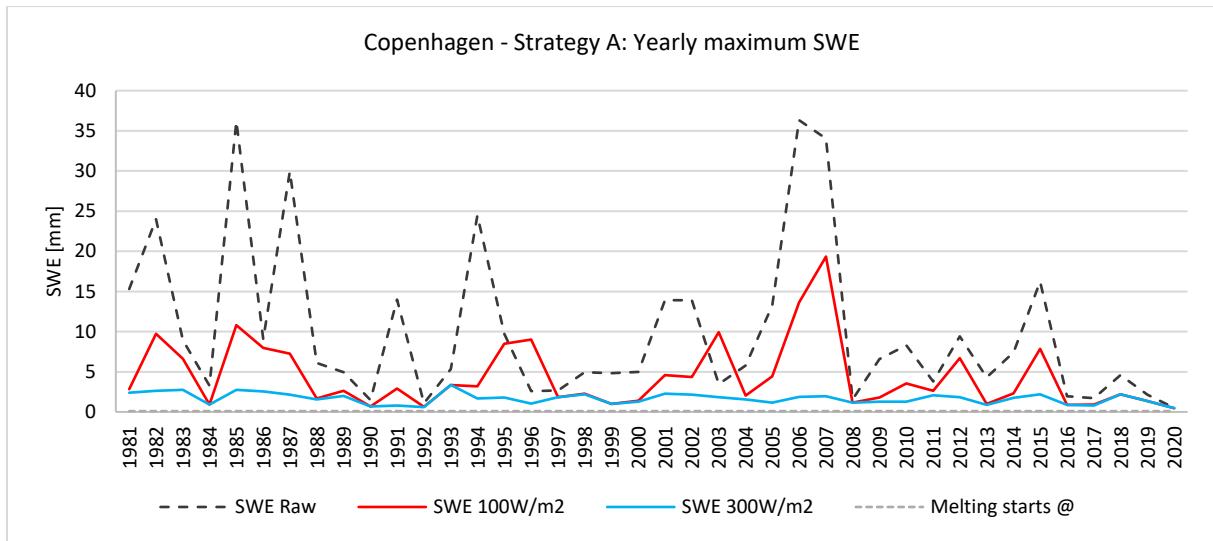
Oslo



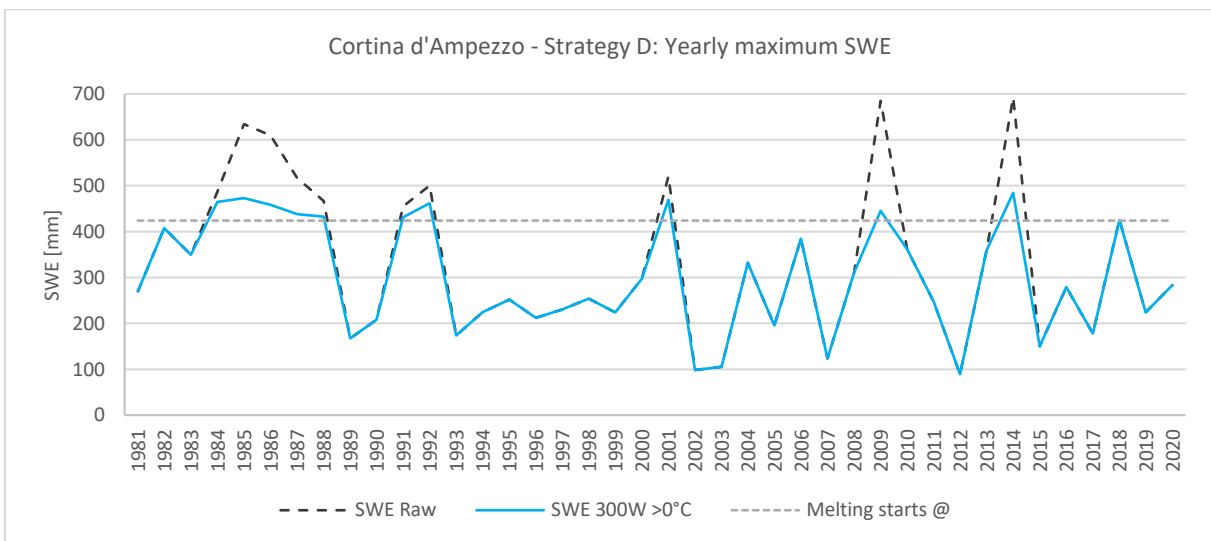
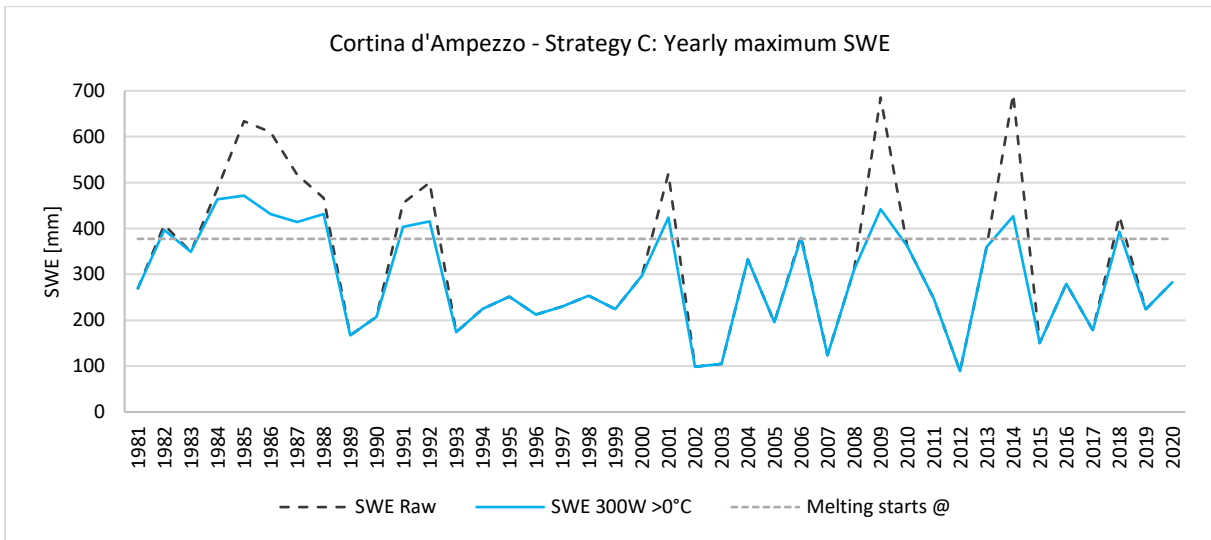
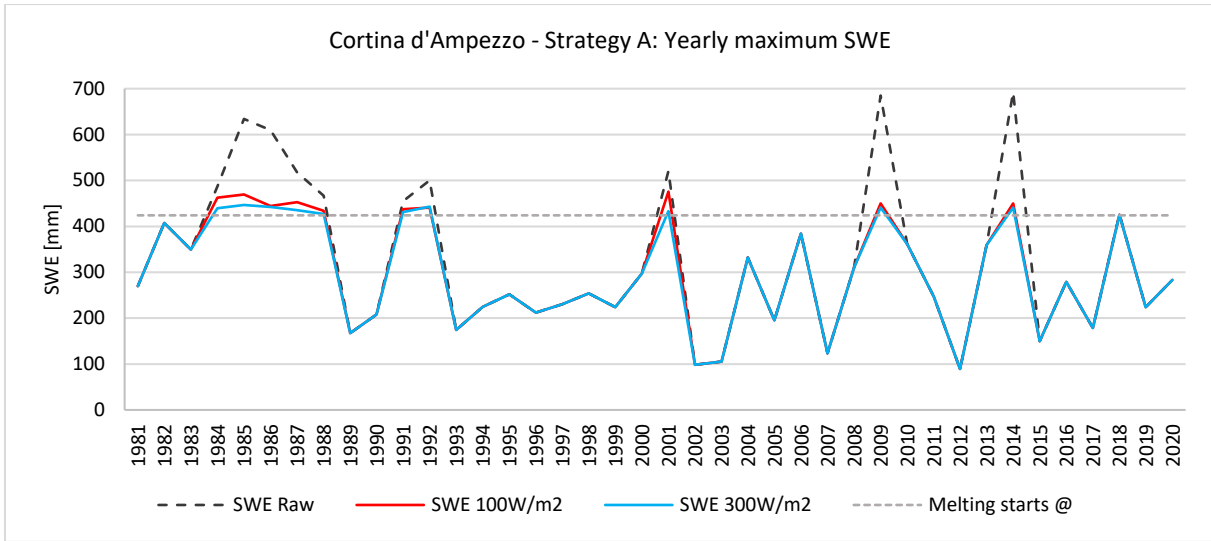
Bergen



## Copenhagen

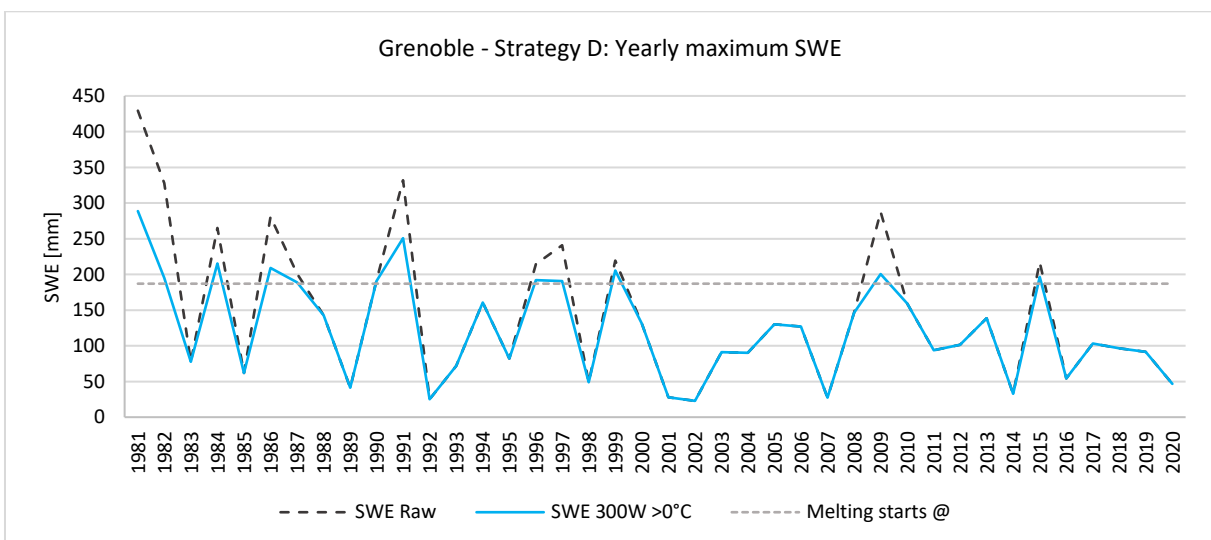
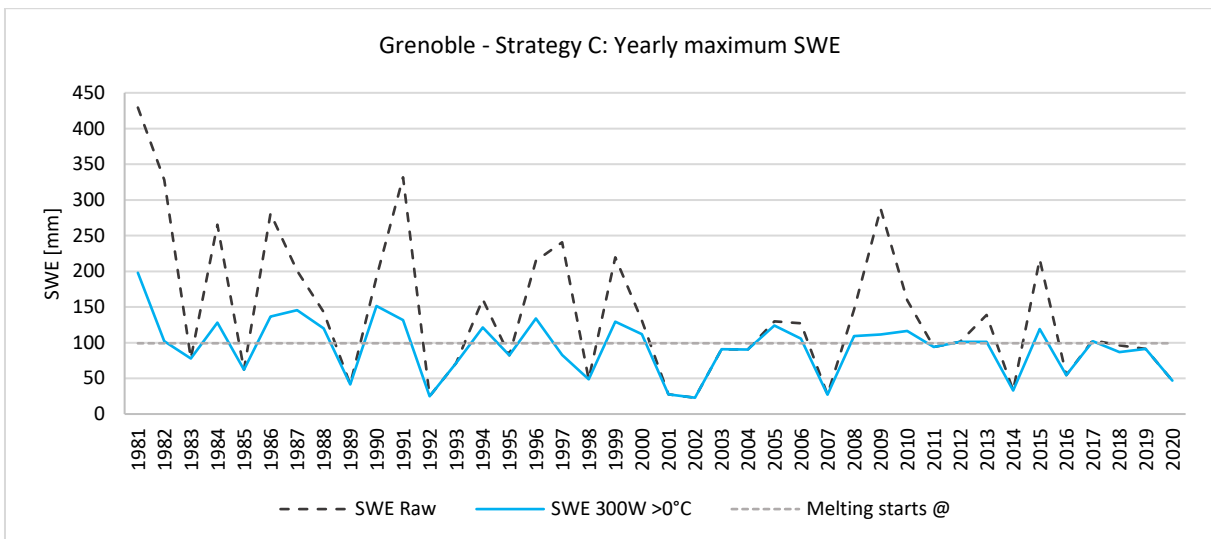
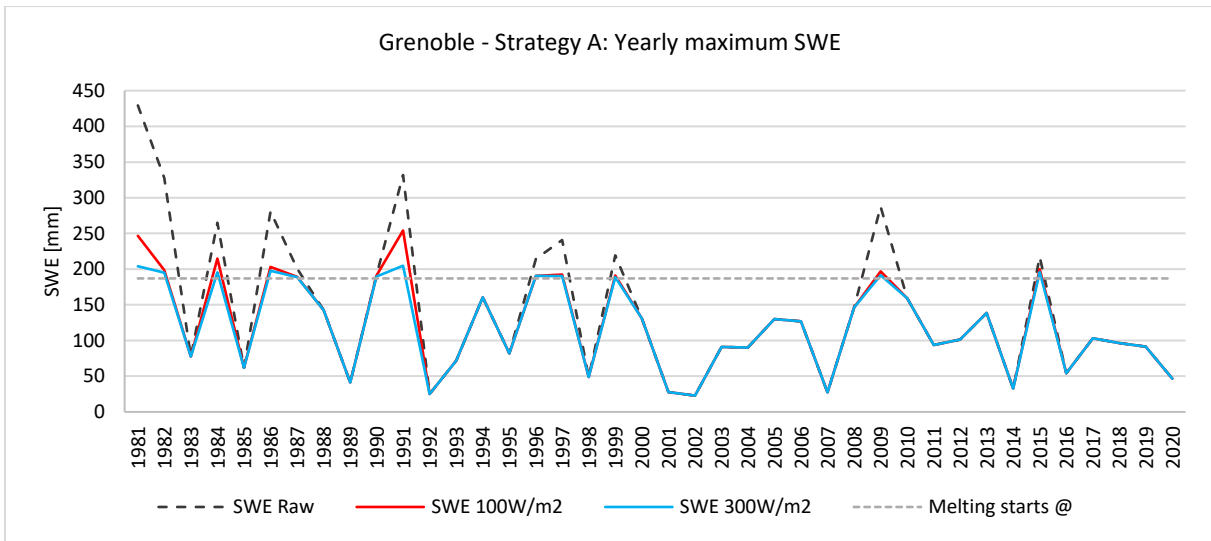


# Cortina d'Ampezzo



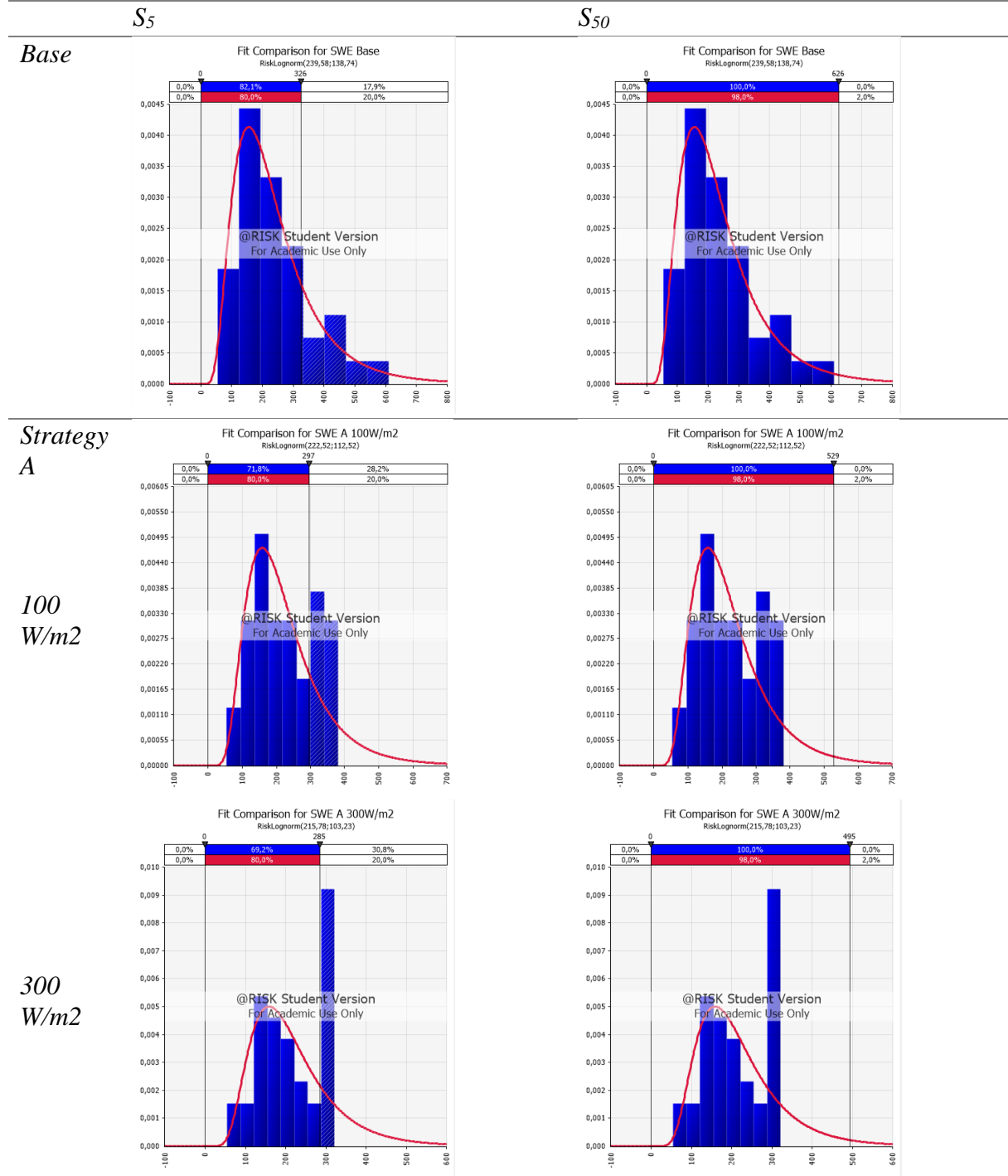


# Grenoble



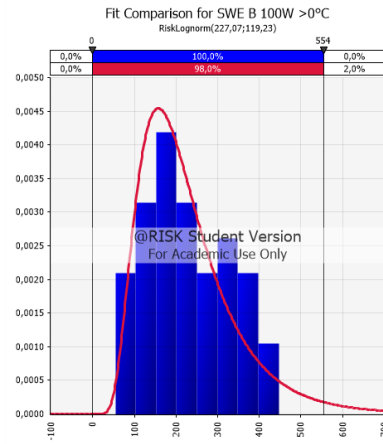
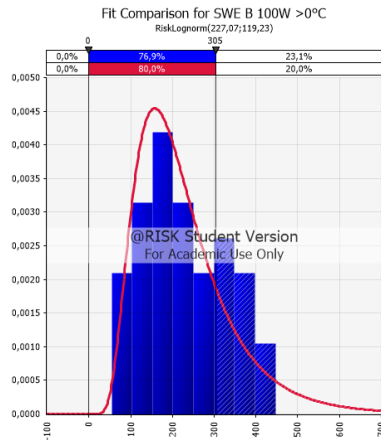
## A.2 Extreme value analysis - The 5 YRP ( $S_5$ ) and the 50 YRP ( $S_{50}$ ).

### Tromsø - Extreme value analysis

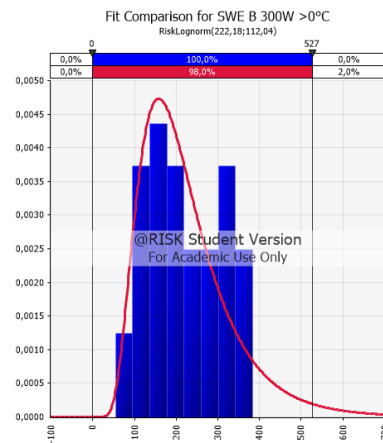
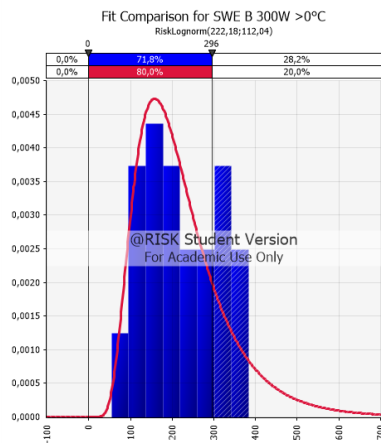


**Strategy B**

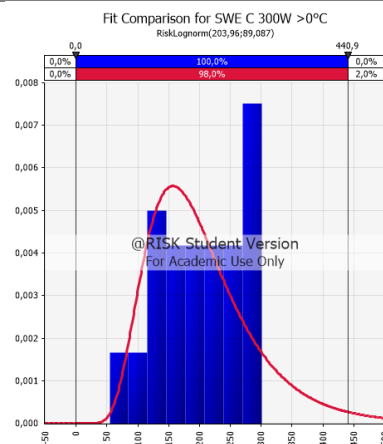
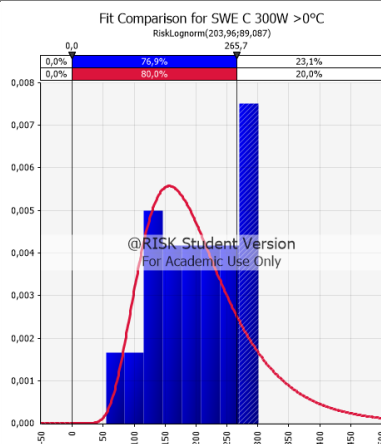
100 W/m<sup>2</sup>



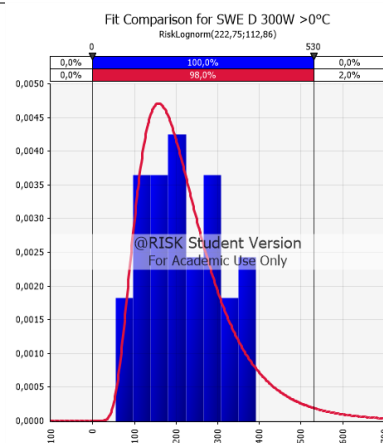
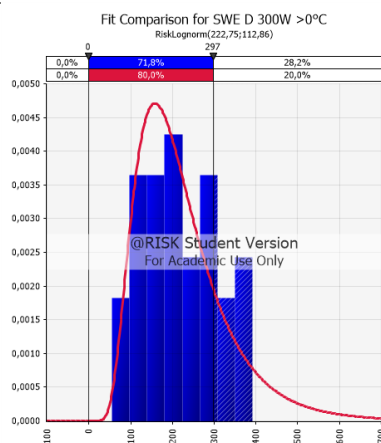
300 W/m<sup>2</sup>



**Strategy C**



**Strategy D**

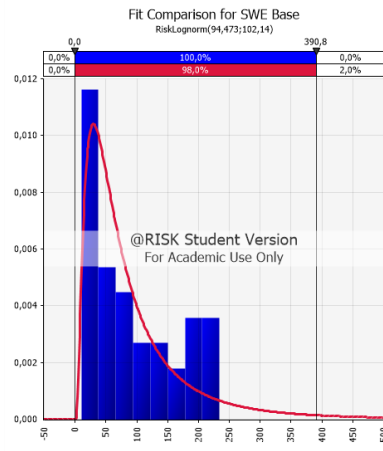
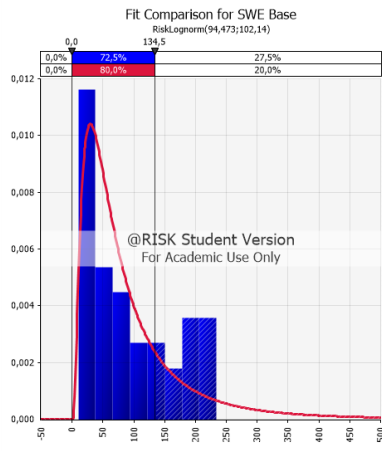


# Oslo - Extreme value analysis

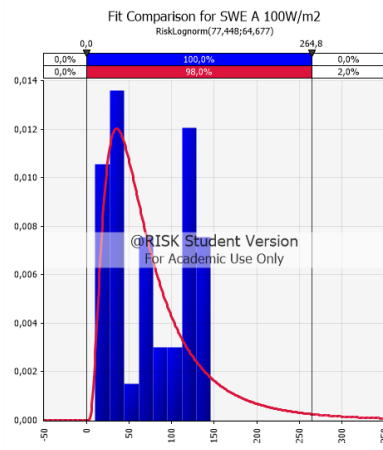
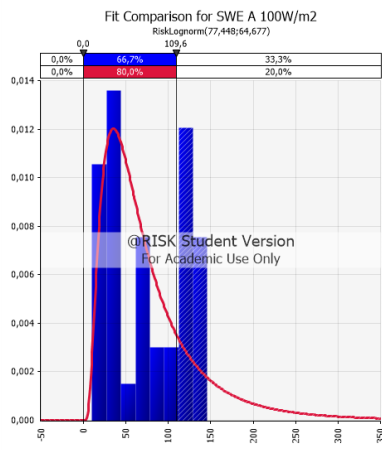
$S_5$

$S_{50}$

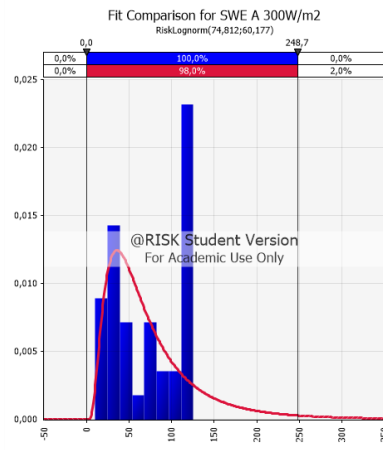
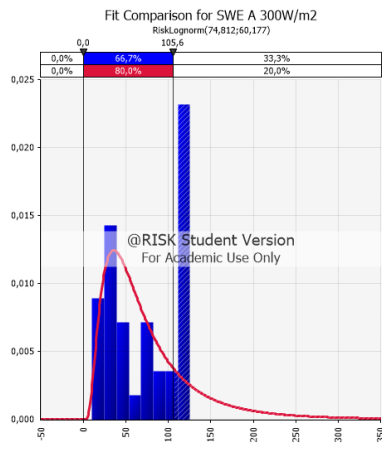
*Base*



*Strategy A*



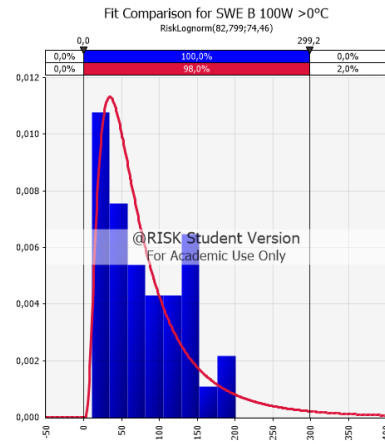
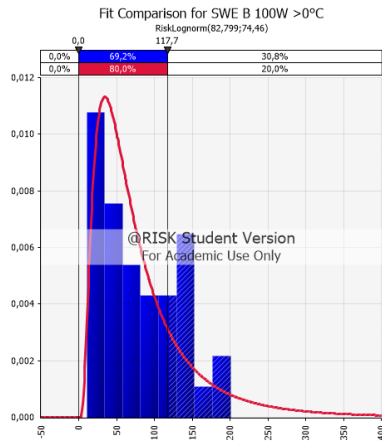
*100 W/m2*



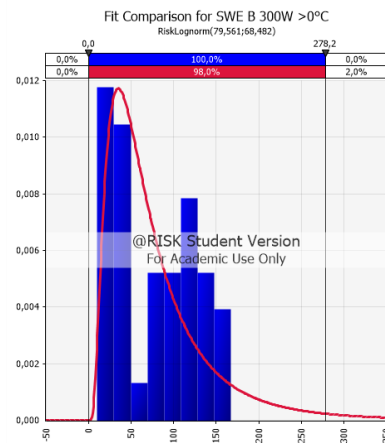
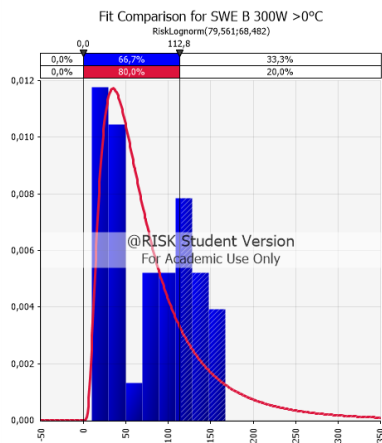
*300 W/m2*

**Strategy B**

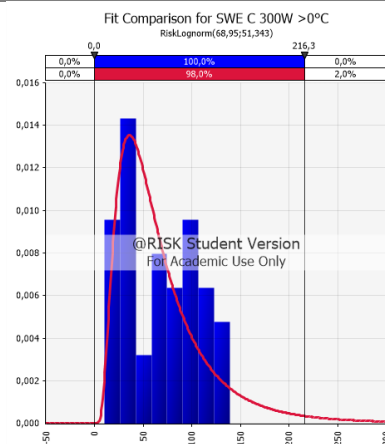
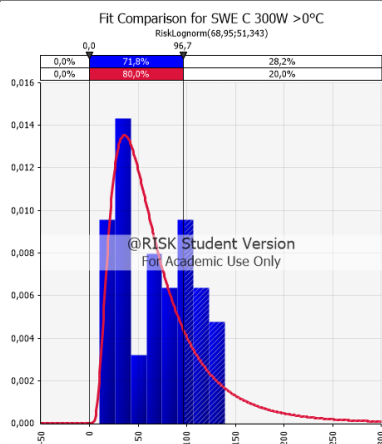
100 W/m<sup>2</sup>



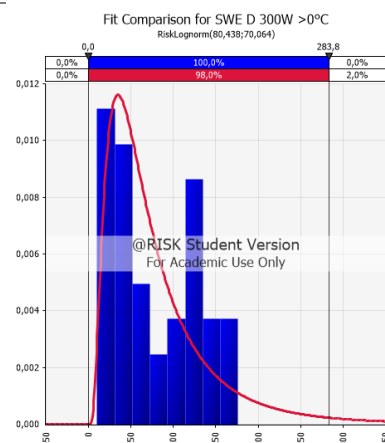
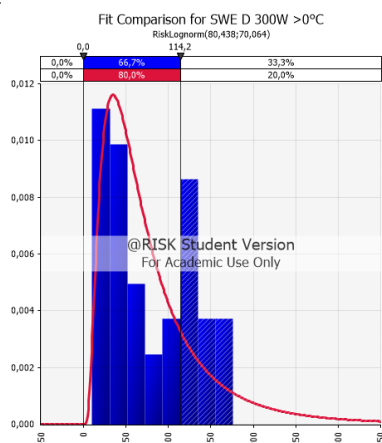
300 W/m<sup>2</sup>



**Strategy C**



**Strategy D**

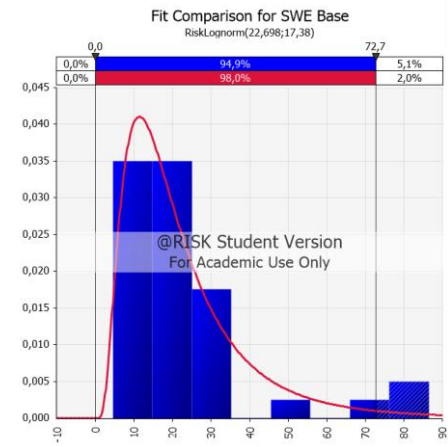
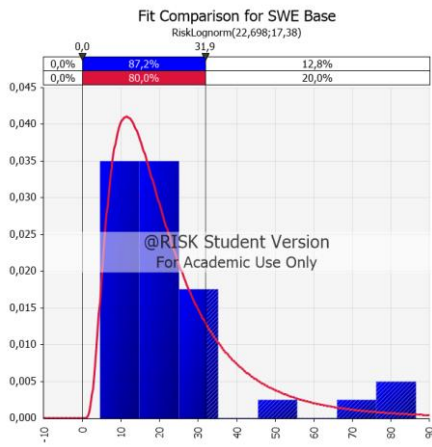


Bergen - Extreme value analysis

$S_5$

$S_{50}$

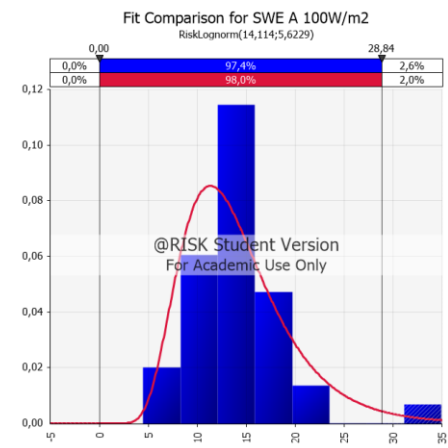
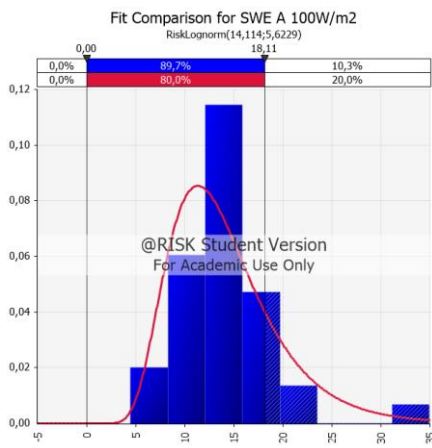
Base



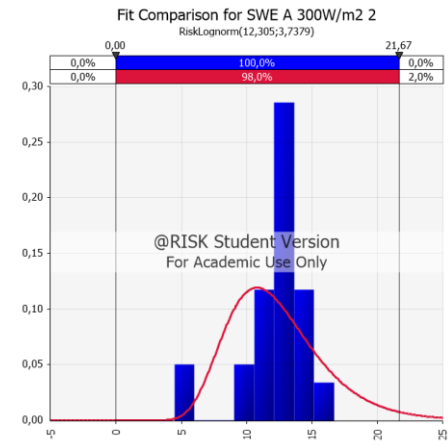
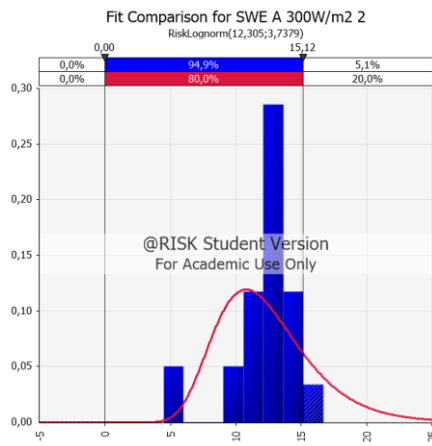
Strategy

A

100  
W/m<sup>2</sup>

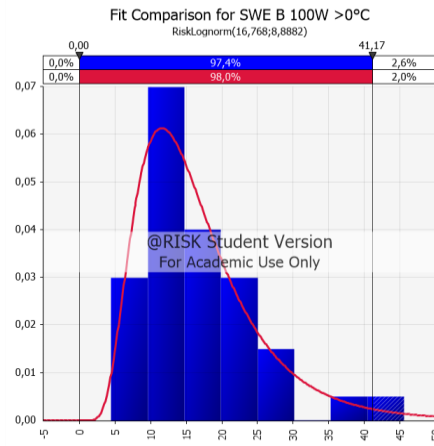
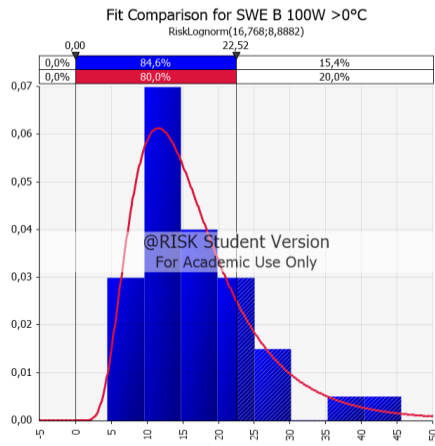


300  
W/m<sup>2</sup>

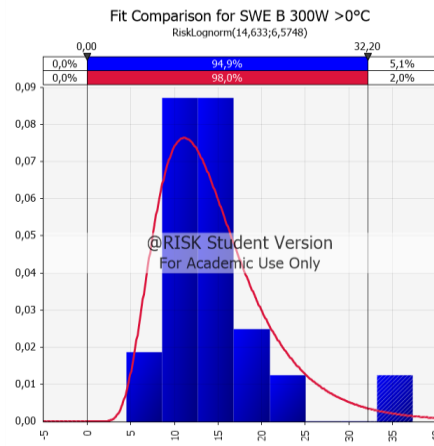
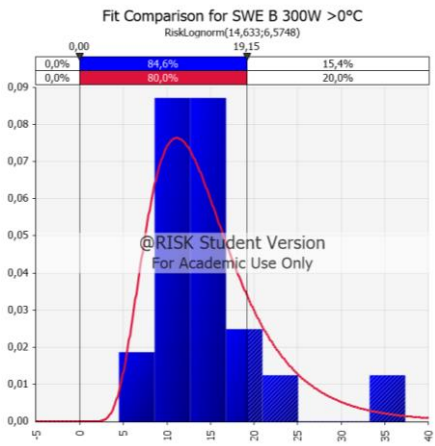


**Strategy B**

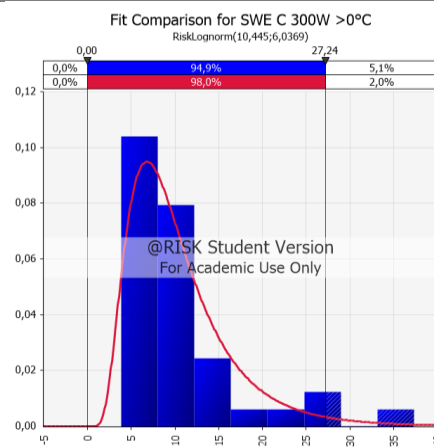
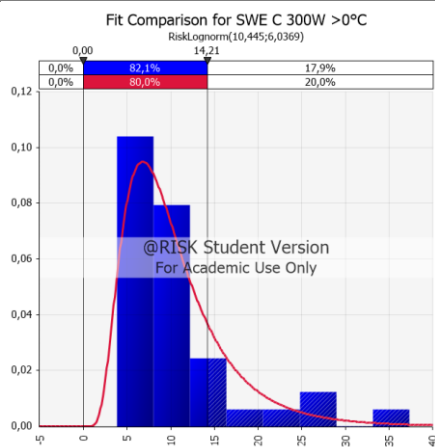
100 W/m<sup>2</sup>



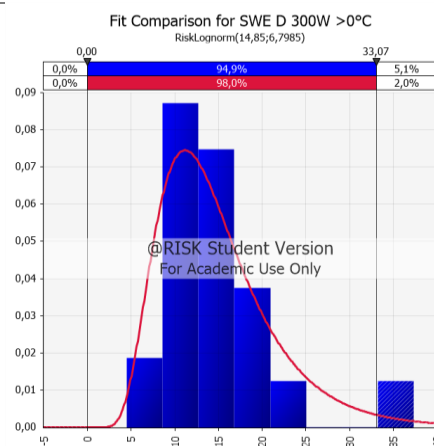
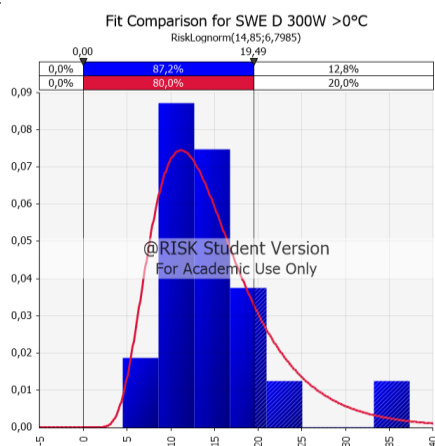
300 W/m<sup>2</sup>



**Strategy C**



**Strategy D**

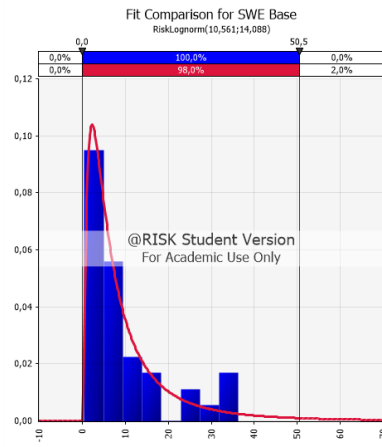
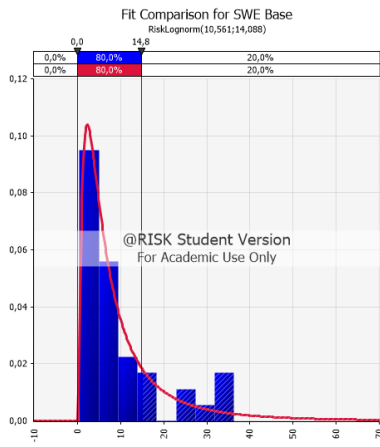


Copenhagen – Extreme value analysis

$S_5$

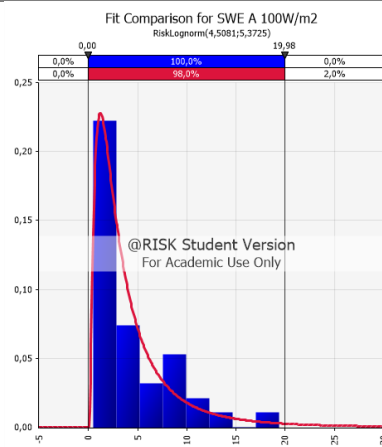
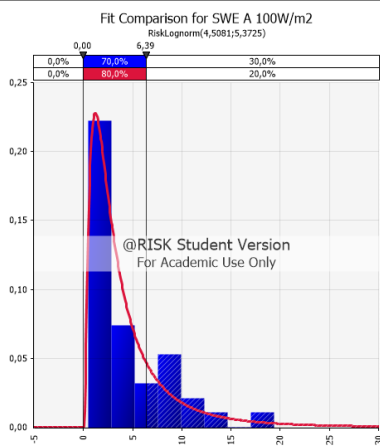
$S_{50}$

Base

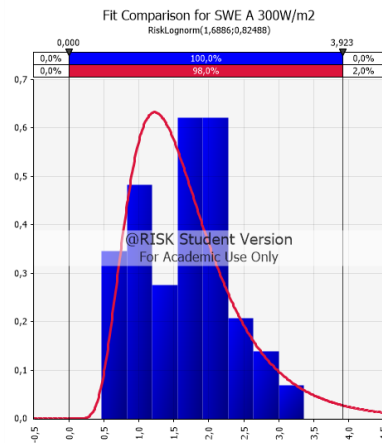
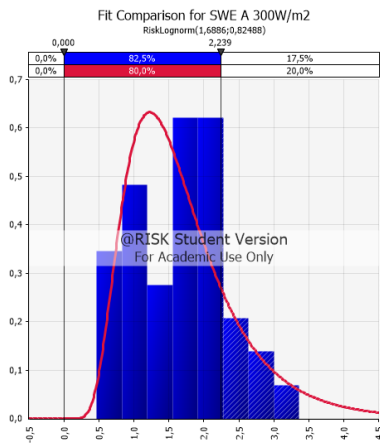


Strategy

A



100  
W/m2

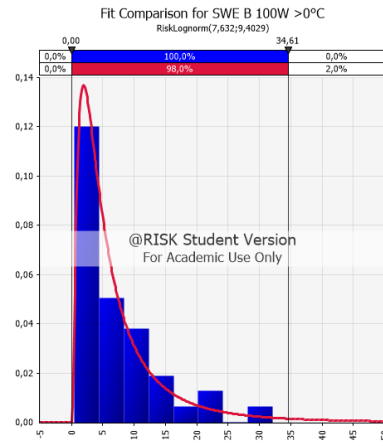
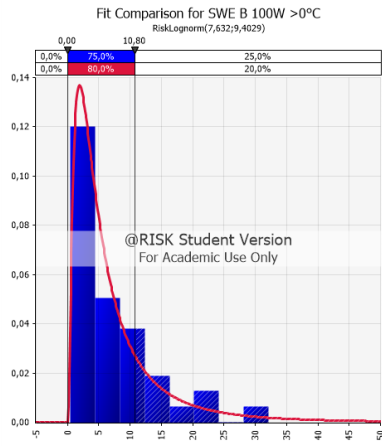


300  
W/m2

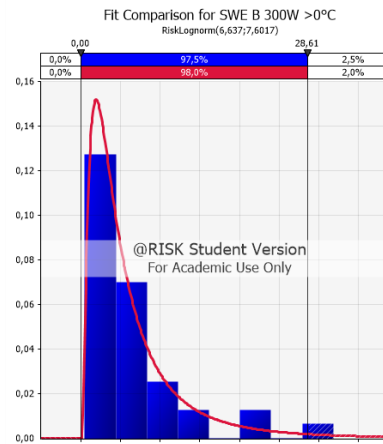
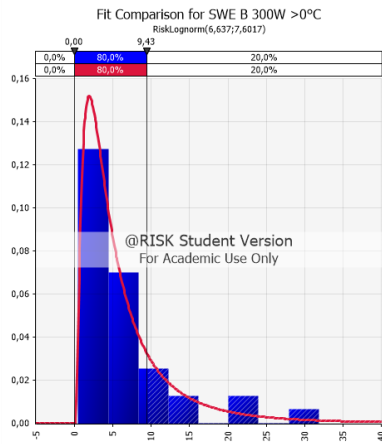


Strategy  
B

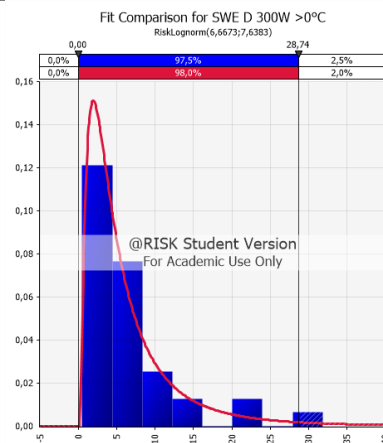
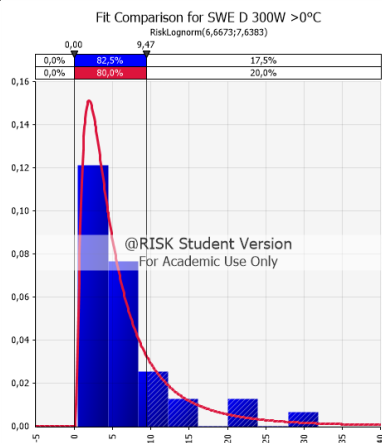
100  
W/m<sup>2</sup>



300  
W/m<sup>2</sup>



Strategy  
D

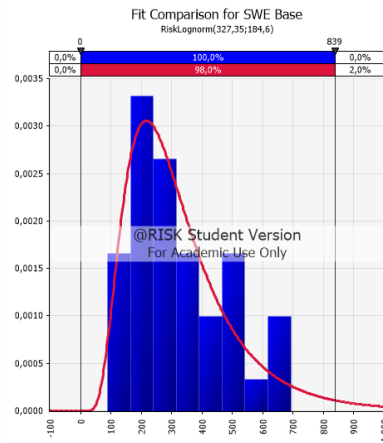
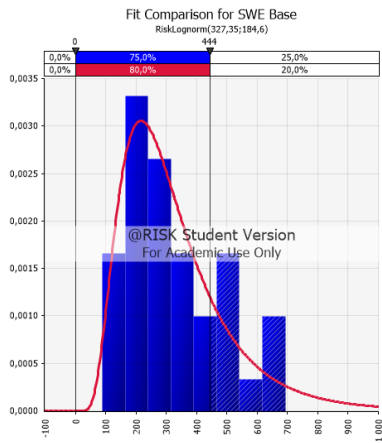


Cortina d'Ampezzo – Extreme value analysis

S<sub>5</sub>

S<sub>50</sub>

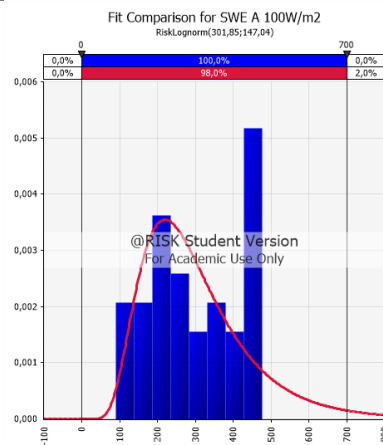
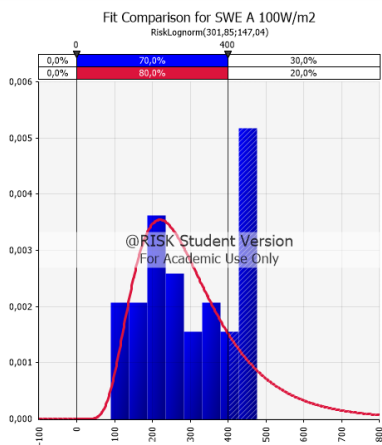
Base



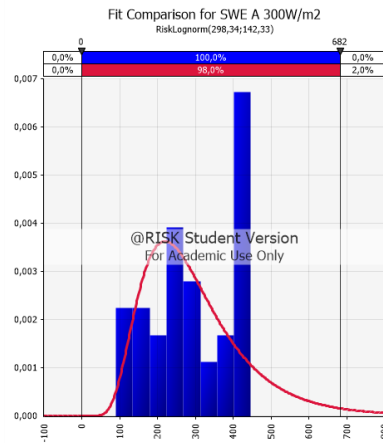
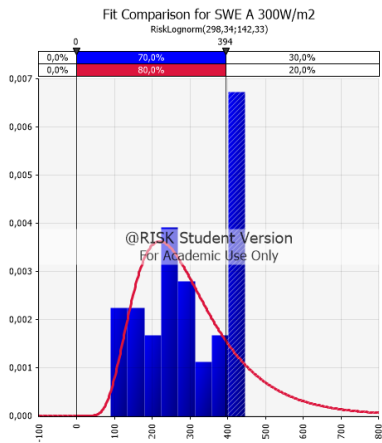
Strategy

A

100  
W/m<sup>2</sup>

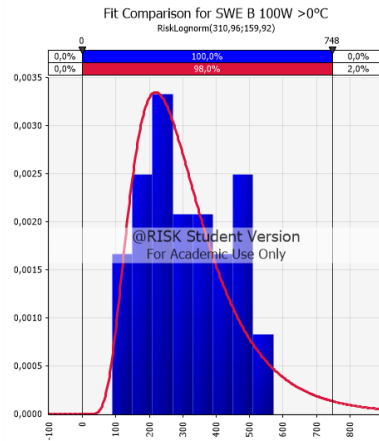
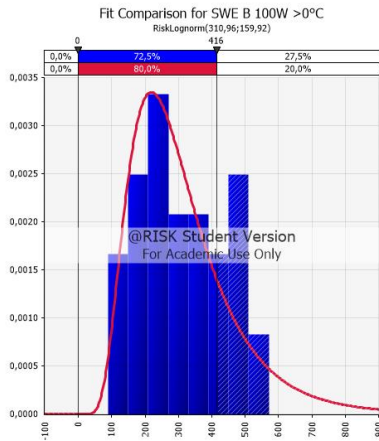


300  
W/m<sup>2</sup>

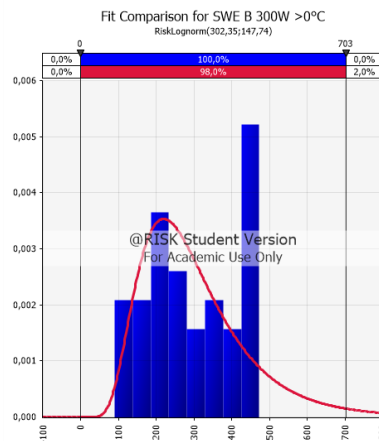
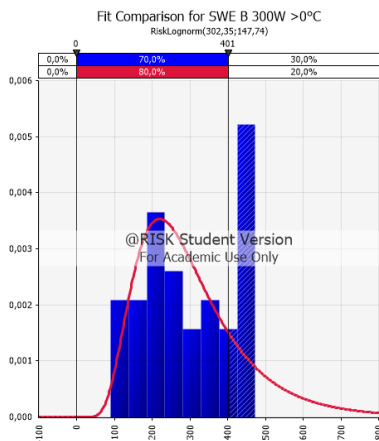


**Strategy B**

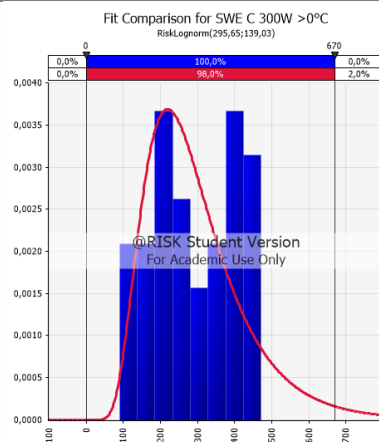
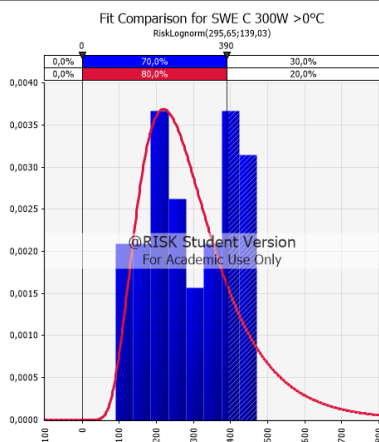
**100 W/m<sup>2</sup>**



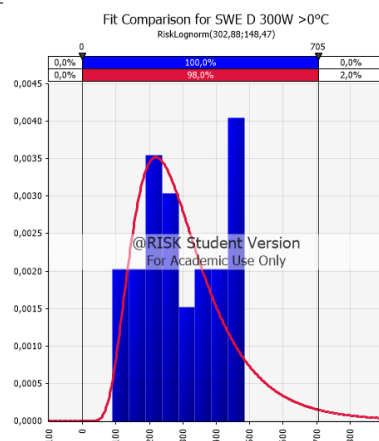
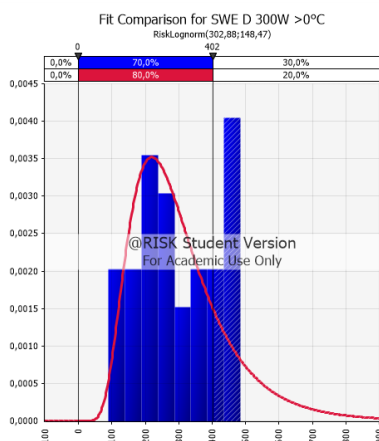
**300 W/m<sup>2</sup>**



**Strategy C**

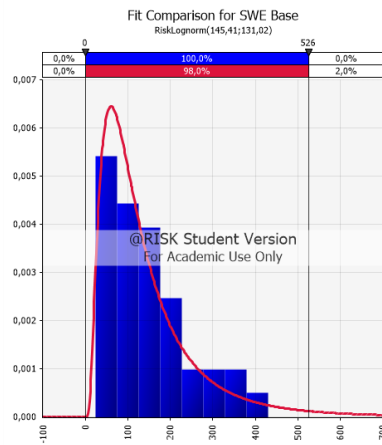
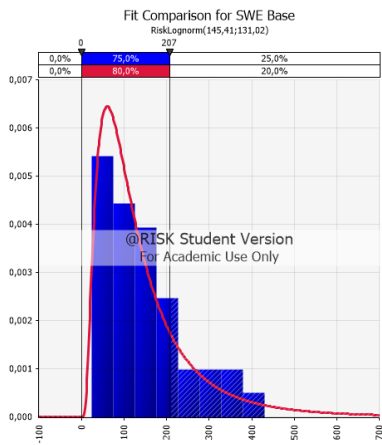


**Strategy D**



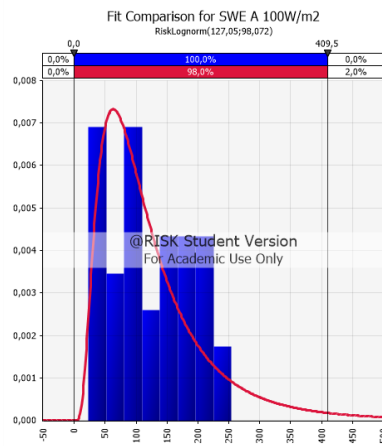
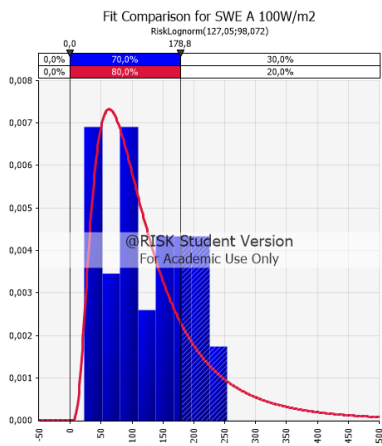
Grenoble

Base

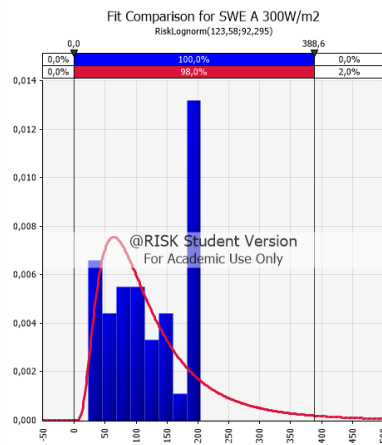
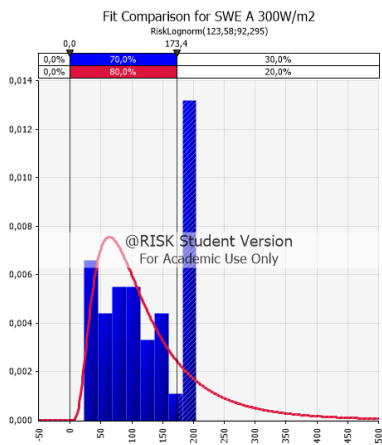


Strategy  
A

100  
W/m2

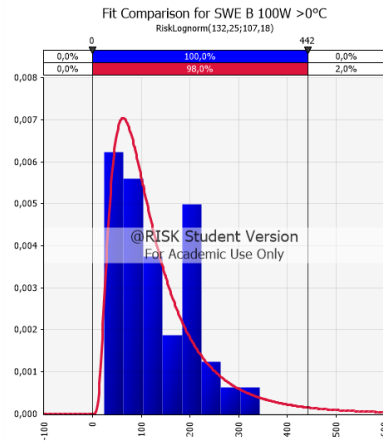
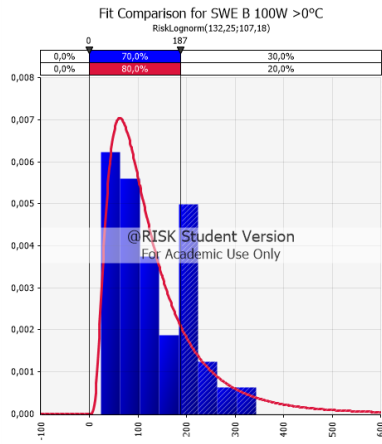


300  
W/m2

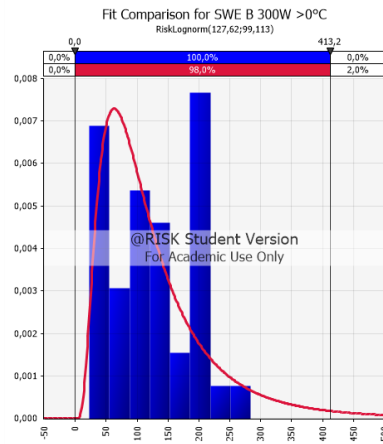
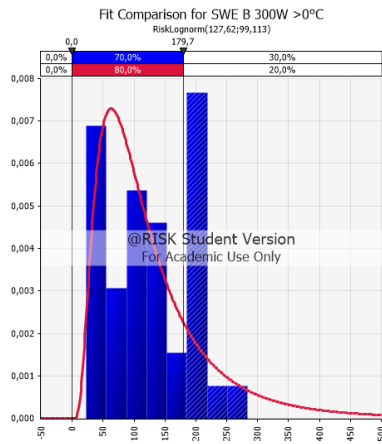


**Strategy B**

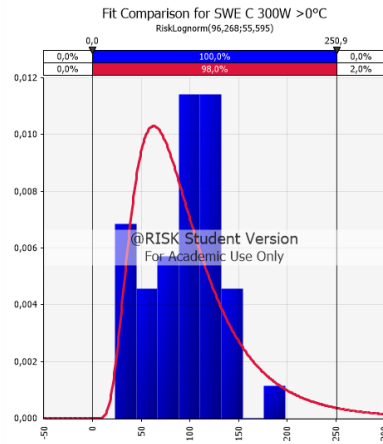
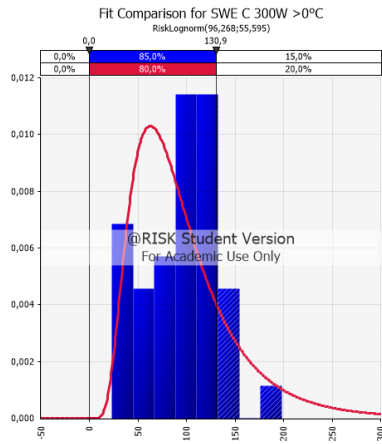
100 W/m<sup>2</sup>



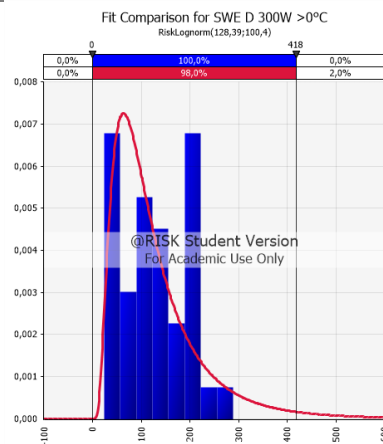
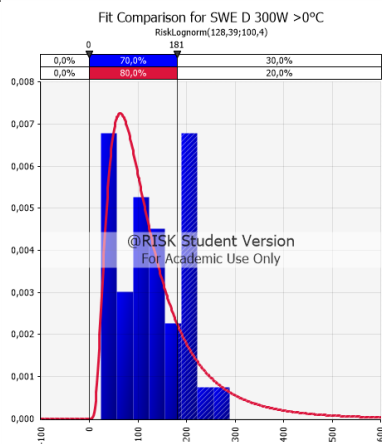
300 W/m<sup>2</sup>



**Strategy C**



**Strategy D**





**Norges miljø- og biovitenskapelige universitet**  
Noregs miljø- og biovitenskapelige universitet  
Norwegian University of Life Sciences

Postboks 5003  
NO-1432 Ås  
Norway